Journal Pre-proofs

Review

Iron-mediated activation of persulfate and peroxymonosulfate in both homogeneous and heterogeneous ways: A review

Sa Xiao, Min Cheng, Hua Zhong, Zhifeng Liu, Yang Liu, Xin Yang, Qinghua Liang

PII: S1385-8947(19)32677-4
DOI: https://doi.org/10.1016/j.cej.2019.123265
Reference: CEJ 123265

To appear in: *Chemical Engineering Journal*

Received Date: 7 July 2019
Revised Date: 22 September 2019
Accepted Date: 21 October 2019

Please cite this article as: S. Xiao, M. Cheng, H. Zhong, Z. Liu, Y. Liu, X. Yang, Q. Liang, Iron-mediated activation of persulfate and peroxymonosulfate in both homogeneous and heterogeneous ways: A review, *Chemical Engineering Journal* (2019), doi: https://doi.org/10.1016/j.cej.2019.123265

Iron-mediated activation of persulfate and peroxymonosulfate in both homogeneous and heterogeneous ways: A review

Sa Xiao [a, 1], Min Cheng [a, 1], Hua Zhong [b,*], Zhifeng Liu [a, *],Yang Liu [a] , Xin Yang [a], Qinghua Liang [a]

[a] *College of Environmental Science and Engineering, Hunan University, and Key Laboratory of Environmental Biology and Pollution Control (Hunan University), Ministry of Education, Changsha 410082, P.R. China*

[b] *State Key Laboratory of Water Resources and Hydropower Engineering Science, Wuhan University, Wuhan, Hubei 430072, China*

* Corresponding authors at:

[a] College of Environmental Science and Engineering, Hunan University and Key Laboratory of Environmental Biology and Pollution Control (Hunan University), Ministry of Education, Changsha 410082, P.R. China

[b] State Key Laboratory of Water Resources and Hydropower Engineering Science, Wuhan University, Wuhan, Hubei 430072, China

E-mail: zhifengliu@hnu.edu.cn (Z. Liu)

E-mail: zhonghua21cn@126.com (H. Zhong)

[1] The authors contribute equally to this paper.

Abstract

Various organic contaminants accumulated in the environment pose great threat to ecosystems and human health. Sulfate radical-based advanced oxidation processes (SR-AOPs) have attracted increasing attention for the removal of these contaminants in recent years. Iron species, including ferrous and ferric iron, zero-valent iron, iron oxides and oxyhydroxides, iron sulfides and various supported iron catalysts, as known to be effective in activating persulfate (PS) or peroxymonosulfate (PMS) to generate sulfate radicals. This review is dedicated to summarize the up-to-date research progresses of iron-mediated activation of PS and PMS mediated by these iron-based species in both homogeneous and heterogeneous ways. The activators are categorized based on their chemistry and the up-to-date knowledge regarding the activation mechanisms are summarized and discussed. Then, a summary of frequently-used synthesis methods of heterogeneous iron catalysts is presented. In addition, the effects of anions, solution pH, dissolved oxygen, and external energy on the activation processes are discussed. Finally, future research perspectives on the iron-based PS/PMS activation method are proposed and how to further improve such a technology for practical application are also discussed.

Keywords: Iron; Persulfate and peroxymonosulfate; Sulfate radical; Homogeneous and heterogeneous activation; Advanced oxidation processes

Contents

1 Introduction

In the past decades, an ever-increasing variety of organic contaminants have been discharged into the environment due to the industrial development and become a rising concern. Many of these organic contaminants are persistent and non-biodegradable, posing great threat to ecosystems as well as human health [1-5]. Advanced oxidation processes (AOPs) involving highly reactive oxidants, such as hydroxyl and sulfate radicals (•OH and $SO_4^{\bullet-}$), have stimulated significant interest for their ability to degrade and mineralize such refractory organic compounds [6-8]. Fenton and Fenton-like systems have prevailed for many years for the production of •OH (1.8-2.7 V vs. normal hydrogen electrode (NHE)) [9]. However, there are several critical disadvantages for these systems, such as a narrow working pH range (2-4), instability of H_2O_2 during storage and transportation, and massive consumption of H_2O_2 during application [10-12]. Sulfate radical-based AOPs (SR-AOPs) have been increasingly considered as a promising alternative to Fenton due to many advantages over •OH-based processes. Possessing a similar or even higher oxidation potential (2.5–3.1 V vs. NHE) and a longer half-life period than •OH (30–40 μs vs 20 ns), $SO_4^{\bullet-}$ can transfer long distances to target contaminants and oxidize them more thoroughly. Additionally, those reactions can take place effectively in aqueous systems on a wider pH range (2–8) [13, 14].

Peroxymonosulfate (PMS, HSO_5^-) and persulfate (PS, $S_2O_8^{2-}$) are the two major sources of $SO_4^{\bullet-}$. They display some differences in molecular structure in that PMS has an asymmetrical molecular structure, while PS is symmetric. As a result, PS is more stable than PMS and requires higher energy input to generate radicals via the homolytic

cleavage of the O-O bond. On the other hand, PS and PMS have distinct redox potential of 2.01 V and 1.82 V, respectively. Therefore, PS presents higher oxidation capacity than PMS. Despite these differences, both PS and PMS have been extensively studied and utilized for their common advantages of cost effectiveness, high aqueous solubility and environmentally friendly nature. Moreover, as relatively stable solids, they can be easily stored and transported on a large-scale and used with accurate dosage, which make them superior to liquid H_2O_2 [15, 16].

To make the best use of their oxidizing power, PS and PMS need activating to generate $SO_4^{\bullet-}$. They can be activated by various transition forms of metals in homogeneous or heterogeneous systems. These transition metals include Fe, Co, Mn, Cu, Ni, Zn, V, etc. [17-24]. Iron, a non-toxic and the second most abundant metal, has played a fundamental part in diverse processes from physiological activities to industrial manufacture [25]. It is have been known for a long time to be an effective activator for PS and PMS. Although some other transition metals, such as Co, have shown comparable ability to activate PS or PMS, they are not recognized as ideal activators due to some significant drawbacks of these metals, particularly toxicity and high cost for application [26]. The high effectiveness and benign properties of iron differentiate it from other transition metals for PS and PMS activation and thus make it the most studied and used metal species.

The recent review articles about activation of PS and PMS always try to cover all aspects of activation methods for PS or PMS in their works, such as thermal, alkaline, radiation, electrolysis, ultrasound, and various types of homogenous and heterogeneous

metal activators (Co, Mn, Cu, Ni, Fe, etc.) [27-31]. It is well known that iron is superior to other metals for PS or PMS activation and iron-based materials have been widely applied to activate PS or PMS, whereas application of activators based on other metals is scarce due to their nature or low activity. As illustrated in Fig. 1, an increasing number of works regarding iron-based PS or PMS activation have been published each year, whether focusing on homogeneous or heterogeneous ways. A specific and deep review supported by state-of-the-art information regarding how iron-based materials activate PS and PMS will add to the knowledge of advanced oxidation chemistry and help develop more effective iron-based materials or methods for catalyzing the peroxysulfate-based oxidation reaction. Therefore, it is worth reviewing exclusively on the iron-based materials for PS and PMS activation. To the best of my knowledge, no review with such a specific focus is available so far.

The topics discussed in this article mainly comprise mechanisms and recent advances of iron-mediated PS and PMS activation and some details about synthesis strategies for heterogeneous catalysts. The homogeneous and heterogeneous iron-based species for PS and PMS activation discussed include ferrous/ferric ions, zero-valent iron (ZVI), iron oxides and oxyhydroxides, iron sulfides, iron-based multimetallic catalysts and various supported iron catalysts. Synergistic approaches for enhancing the activation efficiency are presented. In addition, the influence of reaction conditions, including solution pH, anions and dissolved oxygen are discussed. Finally, the aspects for future research on iron-based activation of PS and PMS and the application of this method are proposed.

2 Homogeneous activators

Activating PS and PMS with ferrous and ferric ions in a homogeneous way has long been a common practice for its simple operation and low cost [32-34]. Compared with heterogeneous systems, homogeneous systems have low mass-transfer resistance between phases and thus enable higher reaction rates [35]. In this section, the general role and fate of ferrous and ferric ions in activating PS and PMS are presented. Some useful techniques to promote the activation efficiency are discussed, such as optimization of ratio of iron ions to oxidants, sequential addition of the iron solution, and use of chelating and/or reducing agents. For easy-reading, Fe^{2+} and Fe^{3+} as the homogeneous activators in the presence of absence of chelators for PS or PMS activation and the reaction characteristics are summarized in Table. 1.

Fe^{2+} activating PS can be described as Eq.(1) [36, 37]. As for the decomposition of PMS, there may exist two pathways as illustrated in Eqs.(2)-(3) [38]. Regardless of the type of oxidants, the cleavage of the O–O bond is the key to generating free radicals. Fe^{2+} can achieve this by transferring an electron to the oxidant, following by the formation of the oxidized Fe^{3+} [39]. Free $SO_4^{\bullet-}$ and •OH radicals can trigger the propagation via a series of chain reactions. Among them, the scavenging of free radicals can render the system inefficient for the less use of free radicals (Eq.(4)). As can be seen from the disparity of the second-order rate constants between $SO_4^{\bullet-}$ generation and scavenging, five or eight orders of magnitude clearly show that $SO_4^{\bullet-}$ can be swept out much faster than its formation, especially when surplus Fe^{2+} is available. In addition, the scavenging effect of excessive Fe^{2+} is much more notable than excessive PS or PMS

[40, 41]. Generally, there is a two-stage reaction process in both Fe^{2+}/PS and Fe^{2+}/PMS systems, comprising a fast stage at first followed by a slow stage. The initial stage is fast because of sufficient reactants and rapid generation of radicals, while along with the proceeding of reaction, the generation of radicals becomes low due to the consumption of Fe^{2+} [42-44].

$$Fe^{2+} + S_2O_8^{2-} \rightarrow Fe^{3+} + SO_4^{\bullet -} + SO_4^{2-} \quad k = 3 \times 10^1\ M^{-1}S^{-1} \tag{1}$$

$$Fe^{2+} + HSO_5^- \rightarrow Fe^{3+} + SO_4^{\bullet -} + HO^- \quad k = 3 \times 10^4\ M^{-1}S^{-1} \tag{2}$$

$$Fe^{2+} + HSO_5^- \rightarrow Fe^{3+} + SO_4^{2-} + \bullet OH \tag{3}$$

$$SO_4^{\bullet -} + Fe^{2+} \rightarrow Fe^{3+} + SO_4^{2-} \quad k = 4.6 \times 10^9\ M^{-1}S^{-1} \tag{4}$$

$$Fe^{3+} + HSO_5^- \rightarrow Fe^{2+} + SO_5^{\bullet -} + H^+ \tag{5}$$

In order to minimize the scavenging of free radicals and enhance the efficiency of the homogeneous activation process, one commonly used measure is to adopt an appropriate molar ratio of PS/PMS to Fe^{2+} [45, 46]. As frequently found in references, the ratio of 1:1 may be a suitable molar ratio for both PS/Fe^{2+} and PMS/Fe^{2+} systems [47-55]. Another useful strategy is to shift the Fe^{2+} addition policy from direct spiking to sequential addition, which plays a significant part in minimizing not-desired termination reactions [46, 56, 57]. Ayoub et al. found that when providing the same total amount of Fe^{2+}, gradual supplementation of Fe^{2+} doubled the rate for sulfamethoxazole removal after 2h of reaction compared to that obtained using one-time addition policy, although the degradation rate was lower in the first 10 min [58]. Vicente et al. also reported that higher diuron oxidation and mineralization rates were achieved when the measure of multiple times of iron addition was taken (using the same

amount of Fe^{2+}) [59]. Therefore, through one-time Fe^{2+} spiking, the degradation rate turns out to be low due to a high rate of radicals quenching, while better degradation performance can be achieved by adding Fe^{2+} sequentially.

Actually, no matter how to optimize Fe^{2+} addition, Fe^{2+} would transform to Fe^{3+} inevitably in the activation process. It is found that iron in both divalent and trivalent forms shows reactivity in activating PMS and PS [17, 47], but Fe^{3+} cannot mediate the decomposition of oxidants and generate radicals as effectively as Fe^{2+} can. On the other hand, the fate of Fe^{3+} is different when coupled with different oxidants, i.e. PMS and PS. In the Fe^{3+}/PMS system, PMS can somewhat act as a reducing reagent apart from an oxidant. It is well-documented that Fe^{3+} can spontaneously react with PMS and generate Fe^{2+}–peroxo complex, which is believed that no O-O bond cleavage occurs. Then, an electron transfers in Fe–O towards iron, and consequently Fe^{2+} and $SO_5^{\bullet-}$ radicals are generated (Eq.(5)) [47]. $SO_5^{\bullet-}$ is less reactive than $SO_4^{\bullet-}$ and not expected to participate in the oxidation of contaminants, but more importantly, this reaction can convert Fe^{3+} to Fe^{2+}, which further reacts with PMS and forms highly active $SO_4^{\bullet-}$. In the case of Fe^{3+}/PS, PS is more stable than PMS for its symmetrical structure, and so far, the reports about the role of PS in reducing Fe^{3+} are scarce. However, it has been reported that some organic compounds and/or their degradation intermediates can reduce Fe^{3+} to Fe^{2+} [60]. For example, Rodriguez et al. found that in the Fe^{3+}/ PS/orange G system, Fe^{3+} could be reduced to Fe^{2+} at low pH by quinones intermediates produced during orange G oxidation, and quinones acted as electron shuttles. The regeneration of Fe^{2+} could form a Fe^{3+}-Fe^{2+} cycle and activates PS again [61]. This role of quinones as

electron shuttles in reducing Fe^{3+} was also demonstrated in serval other works [62-64]. Accordingly, the spontaneous Fe^{2+} regeneration process depending on oxidants and organic compounds adopted in homogeneous systems is an interesting phenomenon, which may be taken advantaged of and boost the degradation efficiency in some cases.

Even though Fe^{2+} regeneration takes place, this process is rather slow as a rate-limiting process. The stead accumulation of Fe^{3+} in the system can not only lead to the decline of reaction rates, but also cause precipitation because of its lower solubility and narrower working pH range than Fe^{2+} [65]. Under these circumstances, apart from adopting appropriate oxidant-to-Fe molar ratio and Fe addition policy, the efficiency of the homogeneous iron-activated PS/PMS systems can also be improved by introducing chelating agents and/or reducing agents. To date, various types of such organic or inorganic materials are reported for such functions, including ethylene diamine tetraacetic acid (EDTA) [66, 67], (S,S)-ethylenediamine-N,N-disuccinic acid trisodium salt (EDDS) [68], citric acid (CA) [69], oxalic acid (OA) [70], gallic acid(GA) [71], hydroxylamine (HA) [72]. Some inorganic counterparts, including pyrophosphate [73] and sodium thiosulfate, are also studied [74]. These kinds of materials can play two major roles in systems: (i) regulate and maintain the concentration of Fe^{2+} to minimize the unnecessary loss, (ii) promote the Fe^{2+} regeneration to alleviate the accumulation of Fe^{3+} and to facilitate PS/PMS activation [70, 75]. For instance, Ji et al. found that the combination of Fe^{2+} and EDTA, as the most extensively used chelating agent, showed some promoting effects on PS activation for sulfamethoxazole degradation [76]. However, EDTA itself is an organic contaminants of a rising concern due to its non-

biodegradable and persistent nature [77]. EDDS, a structural isomer of EDTA, was reported as an environmentally friendly substitute for EDTA [38], and showed similar enhancement [68, 78, 79]. As a kind of naturally occurring organic chelating agent, CA is readily biodegradable. It is found that CA can not only coordinate the Fe^{2+} availability, but accelerate electron transfer [80]. Han et al. reported that CA possessed moderate chelating ability among tested CA, OA, and EDDS, and could decrease the accessibility of Fe^{2+} center through the steric hindrance effects coming from its molecule structure, which rendered it become the most suitable chelating agent for Fe^{2+} and improve the PS activation efficiency (Fig. 2) [78]. The superiority of CA was also justified by the study of Liang et al., in which CA/Fe^{2+}/PS showed better removal efficiency than EDTA/Fe^{2+}/PS system towards BTEX [81].

The use of reducing agent, e.g. hydroxylamine, can effectively promote the conversion from Fe^{3+} to Fe^{2+} [72, 82]. In a related work, Zou et al. reported that in the HA/Fe^{2+}/PMS process, a relatively low concentration of Fe^{2+} was enough to eliminate benzoic acid rapidly, thanks to the strongly accelerated Fe^{3+}/Fe^{2+} redox cycle [83]. Moreover, Wu et al. testified that when coupled with Fe^{2+}/PS, HA was most effective in the degradation of trichloroethylene among other four reducing agents, namely, sodium thiosulfate, ascorbic acid, sodium ascorbate and sodium sulfite [84]. As for inorganic chelating agents, they have some inherent advantages, e.g. like less likely to compete for radicals compared with organic chelating agents [38, 85], and not introducing total organic carbon (TOC) into the solution [38]. Pyrophosphate is the most commonly used inorganic chelating agent for iron stabilization in Fenton-like

systems [73]. Rastogi et al. reported that in the case of Fe^{2+}/PMS system, pyrophosphate was most effective to facilitate the activation of PMS for 4-chlorophenol degradation, in comparison with citrate and EDDS [38]. Moreover, it was found that sodium thiosulfate could not only serve as a chelating agent, but also a reducing agent. When coupled with Fe^{2+} to activate PS (Eqs.(6)-(8)), sodium thiosulfate showed stronger effects than EDTA-Na_2 and diethylene triamine pentaacetic acid (DTPA) in enhancing degradation of diuron [74]. Nevertheless, although the overall degradation efficiency can be enhanced, the introduction of an additional reagent to the system may otherwise bring some adverse effects. For instance, HA still can react with radicals with high rate ($k_{SO4^{\cdot-}}$= 8.5×10^8 $M^{-1}s^{-1}$, $k_{HO^{\cdot}}$= 9.5×10^9 $M^{-1}s^{-1}$), which can cause some competition for generated radicals with target contaminants [79]. At the same time, HA is toxic, although it could be degraded to NO_3^-, N_2, NO_2^- and N_2O under ambient conditions [86]. Finally, many researchers found that excessive additives could directly lead to unavailability of soluble Fe^{2+} [71, 81, 87]. Therefore, it should be cautious about the selection and addition of the chelating reagents or reducing reagents.

$$XS_2O_3^{2-} + YFe^{2+} \rightarrow \text{Complexanion} \quad (6)$$

$$\text{Complexanion} + S_2O_8^{2-} \rightarrow Fe^{3+} + SO_4^{\bullet -} + SO_4^{2-} + \text{residue} \quad (7)$$

$$S_2O_3^{2-} + Fe^{3+} \rightarrow Fe^{2+} + {}^1/_2S_4O_6^{2-} \quad (8)$$

3 Heterogeneous catalysts

As mentioned in the foregoing section, utilizing Fe^{2+} or Fe^{3+} to activate PS/PMS in a homogeneous way involves many undesired side reactions, which make the system

quite complex and hard to control. In addition, homogeneous activation of PS/PMS using Fe ions has other drawbacks, such as (i) further separation and disposal of iron sludge is required, (ii) to avoid hydrolysis and precipitation of iron ions, these systems become highly pH-dependent, (iii) the introduction of anions related to iron salts, such as SO_4^{2-}, Cl^-, is inevitable, which may have inhibitory effects on activation efficiency due to radical quenching effect of these ions [88-91]. As alternatives to avoid these drawbacks, heterogeneous iron catalysts, including zero-valent iron, iron oxides and oxyhydroxides, iron sulfides, and iron catalysts immobilized on various supports, such as oxides, molecular sieves, carbonaceous materials, and metal-organic frameworks have attracted great interest. Although homogeneous activation of PS or PMS by iron ions derived from the dissolution and corrosion of heterogeneous catalysts may still play an important role in the heterogeneous system, a great many research works confirm that the leaching ions in the solution are insufficient to activate PS or PMS to reach the degradation results, which means that activation of PS or PMS in a heterogeneous way is more dominant [92, 93]. In the cases of nZVI and sulfur modified nZVI (S-nZVI), it is true that the production of Fe^{2+} from the dissolution and corrosion of Fe^0 can occur rapidly under both aerobic and anaerobic conditions (Eqs.(9)-(10)), and subsequently activate PS or PMS in a homogeneous way (Eqs.(1)-(4)), however, the direct electron transfer from Fe0 to PS or PMS occurred on the surface is a key to activating PS or PMS (Eq.(12)) [94-98], which is illustrated in Fig. 3 [98]. In addition, some S species formed during iron sulfidation is reported to facilitate electrons transfer and regenerate Fe(II) from Fe(III) (Eq.) [90, 96]. For those iron species containing Fe(II)

and/or Fe(III) inside, including iron oxides and oxyhydroxides and natural iron sulfides, the Fe(II) on the surface contacts with aqueous solution and activates PS or PMS directly (Eqs.(17)-(20)). Fe(III), due to low reaction reactivity in activating PS/PMS, often requires one-electron reduction of surface site from Fe(III) to Fe(II) (Eqs.(21)-(23)). These two processes can form a catalytic cycle, which occurs on the surface and sustain the activation (Fig. 4) [16, 92, 99-107]. Finally, various supported iron catalysts can benefit from the interaction between iron species and supports, which can significantly retard the leaching of iron ions. Metal additives in the iron-based multimetallic catalysts may also play a similar role. Therefore, the homogeneous activation part is further diminished, and the activation reactivity mainly depends on heterogeneous part. Moreover, the supports and metal additives can directly activate PS/PMS, or facilitate the electron transfer, making the composites achieve satisfactory activation efficiency (Fig. 5 and Fig. 6) [51, 58, 108-115]. Today heterogeneous activators can be synthesized through various approaches, including borohydride reduction [116], coprecipitation [100], hydrothermal [117], impregnation [118], pyrolysis [119], plating [58], which contributes greatly to the development of heterogeneous activation method. Performance and synthesis methods of typical iron-based heterogeneous activators in activating PS and PMS are summarized in Table. 2.

3.1 Zero-valent iron

Since the use of ZVI for the remediation of groundwater contamination was first reported in 1990 [120, 121], ZVI has extensively applied in environmental fields by virtue of its high reducibility (Fe^0, E_0=−0.44 V), easy accessibility and environmental

friendliness [39].

When combined with PS/PMS, ZVI can be corroded and produce dissolved Fe^{2+} in the presence or absence of dissolved oxygen, especially under acidic conditions (Eqs.(9)-(11)) [120, 122]. More importantly, there exists another way that direct electron transfer could occur on the surface of ZVI to PS and generate $SO_4^{\bullet-}$ (Eq.(12)) [97, 123, 124]. In addition, Fe^{2+} can be regenerated from the action between ZVI and Fe^{3+} which is produced after the interaction between Fe^{2+} and PS/PMS (Eq.(13)) [98, 125, 126]. Similar to the homogeneous activation process, the Fe^{2+} released into the system from above reactions can activate PS/PMS and produce $SO_4^{\bullet-}$ and •OH radicals (Eqs.(1)-(3)) [48, 87]. What makes a difference is that ZVI serves as a controllable and slow-releasing source of Fe^{2+}, which can greatly alleviate the quenching effects [97]. As the same time, the produced Fe^{3+} can relatively easily be reduced and recycled by ZVI, and thus the hydrolysis and precipitation due to the accumulation of Fe^{3+} in the systems can be reduced.

$$2Fe + O_2 + 2H_2O \rightarrow 2Fe^{2+} + 4OH^- \quad (9)$$

$$Fe + 2H_2O \rightarrow 2Fe^{2+} + 2OH^- + H_2 \quad (10)$$

$$2Fe + 2H^+ \rightarrow Fe^{2+} + H_2 \quad (11)$$

$$Fe + 2S_2O_8^{2-} \rightarrow \equiv Fe(II) + 2SO_4^{\bullet-} + 2SO_4^{2-} \quad (12)$$

$$Fe + 2Fe^{3+} \rightarrow 3Fe^{2+} \quad (13)$$

In these ZVI/PS or ZVI/PMS systems, the production of Fe^{2+} from ZVI surface dissolution is the rate-limiting step, which varies according to the particles size of ZVI

[61]. It was confirmed that the release of Fe^{2+} from ZVI surface could be controllable by selecting the proper particle sizes [60, 127]. Song et al. made a comparison between nano-sized ZVI (nZVI) and commercial micron-sized ZVI (mZVI) coupled with PS to degrade PAHs, and found that the PAHs removal efficiencies were 82.21% and 69.14%, for nZVI and mZVI, respectively, which could be attribute to difference in particle sizes [128]. When it comes to the application cost and the Fe^{2+} release, there are also some differences depending on the particle size. Generally, the fabrication of nZVI usually requires high cost, which might hamper large-scale applications. In contrast, mZVI, with larger size and much lower price, possesses a more stable property, making it easier to handle and apply [129]. On the other hand, the release of Fe^{2+} from nZVI is not the same to granular and microscale ZVI. The smaller the particle size gives larger specific surface area will be, leading to higher surface reactivity [130]. For instance, nZVI can achieve PS activation rapidly, and this process are more likely to allow the Fe^0 to be utilized completely. For granular and microscale ZVI having relatively smaller surface area, it usually cannot be corroded quickly. It was reported that iron (oxyhydr) oxides, including magnetite, hematite and goethite could form and deposit on granular and microscale ZVI surface [131, 132]. These corrosion products could subsequently show some inhibitory effect on the PS activation, which might be because the iron (oxyhydr) oxides surface layers cannot activate PS effectively and hinder the direct contact between ZVI core and the bulky liquid [133, 134]. Kim et al. put out a ZVI core-shell structure in activating PS, in which a distinct two-stage process was observed. Fe^0 could be consumed rapidly in the first stage, while the second stage was three orders

of magnitude slower because it was governed by aqueous Fe^{3+} and iron (oxyhydr) oxides on the outer shells of Fe^0 formed during the activation process, which significantly slowed down the reaction rate (Fig. 3) [98]. The multilayered shell was also observed by Tan et al. after ZVI reacted with PMS. They reported that the FeOOH layer was generated on the surface of fresh Fe^0, and a part of them subsequently reacted with adsorbed SO_4^{2-} to form $FeSO_4$ layer (Eqs.(14)-(15)), which resulted in an increase in the average particle sizes and decrease in the degradation rate [135]. Whether ZVI exhausts rapidly or shows decline in reactivity due to the formation of corrosion products, it raises concerns about the sustainability of using ZVI. In a related work, Ghauch et al. tested the reusability of micrometric Fe^0 particles (MIPs) by performing 3 successive experiments respectively in 3 different water matrix of tap water, underground water and DI water. 90% degradation of sulfamethoxazole was observed in the MIPs/PS/DI system in the first and second cycle, while only 20% in the third cycle [136]. Hayat et al. investigated the recycling of nZVI in 5 consecutive cycles of total 60 min, finding that the degradation rate of imidacloprid decreased from 83.45% in the first cycle to 21.95% after five cycles in the nZVI/PS system [137].

$$Fe^{3+} + 2H_2O \rightarrow \equiv FeOOH + 3H^+ \quad (14)$$

$$\equiv FeOOH + SO_4^{2-} + H_2O \rightarrow FeSO_4 + 2OH^- + {}^1/_2H_2 + {}^1/_2O_2 \quad (15)$$

However, some promoting effects made by the corrosion products were also found. Cao et al. observed that in the ZVI/PMS process, the corrosion products deposited on the surface of Fe^0 could activate PMS or adsorb contaminants directly [138]. The role of iron corrosion products in adsorbing contaminants was also observed in previous

works [112, 139, 140]. Apart from the formation of oxidized layer after reaction with liquid or air medium, surface oxidation is usually unavoidable during the synthesis process of ZVI, and thereafter develops into core-shell morphology. This core-shell structure could not only allow electron transfer to activate PS/PMS, but adsorb various contaminants because of electrostatic interactions and surface complexation [141, 142]. Besides, the shell of iron (oxyhydr) oxides could protect ZVI core from rapid oxidation under neutral pH conditions [143]. Another extreme example was that the core–shell $Fe^0@Fe_3O_4$ was intentionally synthesized for PS activation, and showed better performance than pure Fe^0 [144]. It might be because that Fe2+ oct species existing in Fe_3O_4 shell was reactive in activating PS, while it could be supplied via Eq.(13) taking place on the interface between Fe^0 and Fe_3O_4 [144].

Plentiful techniques have been developed to fabricate micro/nano sized ZVI. Physical methods still have been used. Kang et al. reported a facile method to manufacture a micro/nano ZVI particles via ball-milling the industrially reduced iron powders. The ZVI produced via this method demanded much lower cost and also showed satisfactory reducibility [145]. It is more common to adopt a liquid-phase reduction method using borohydride salt as a reducing agent, and it requires simple operation and equipment. In this typical method, ZVI can be obtained through nucleation form homogeneous solution. More specific, aqueous solution of borohydride is added dropwise into the iron salt solution, and then the following reaction occurs (Eq.(16)) [116, 143]. Sometimes, for the sake of increasing the dispersion and migration performance, and improving the stability during storage and application, some additives

would be added during the synthesis procedure to modify the surface properties of ZVI, including polymers, anionic surface-active agents, and other organic coatings [146]. Wang et al. reported an ascorbic acid (H_2A) coated ZVI nanoparticles acting as an effective catalysts for PS, which could be due to both the reduction and chelating ability of H_2A [147]. In recent year, it is found that the use of $NaBH_4$ could cause secondary pollution, so greener substitutes are developed and put into use, e.g. using polyphenolic solution by heating plant extracts (oak, green tea, lemon, pomegranate, bran, grape etc.) [148-150]. For instance, Liu et al. reported that green tea extract as a reductive was adopted in the ZVI synthesis procedure, and the prepared ZVI also showed high reactivity in activating PS to simultaneously remove Cu^{2+} and bisphenol A [150].

$$Fe(H_2O)_6^{3+} + 3BH_4^- + 3H_2O \rightarrow Fe^0\downarrow + 3B(OH)_3 + 10.5H_2\uparrow \quad (16)$$

3.2 Iron oxides and oxyhydroxides

Oxides and hydroxide minerals are mostly found on the surface of earth, which includes magnetite, hematite, goethite, maghemite, akaganeite, leidocrocite, ferrrihydrite, etc. Up to now, Fe_3O_4, Fe_2O_3, FeO(OH) are the forms that are mostly investigated in activating PS/PMS. In addition, natural media containing these minerals can also activate PS or PMS. For example, Yan et al. found that the activation efficiency of PS was strongly linked to the iron components in soils and sediments [151]. For Fe_3O_4, an inverse spinel crystal, possesses octahedral sites that can stably accommodate Fe(II) and Fe(III). Also, it is a type of semiconductor with a narrow band gap of 0.1eV, which enables it to easily achieve electron transfer [152, 153]. Fe(II) in the Fe_3O_4 plays a significant role in activating PS/PMS (Eqs.(17)-(20)) [99]. Unlike homogenous Fe^{2+}

activation process, the activation of PS/PMS by Fe(II) existed in Fe_3O_4 occurs on the surface of solids and avoids full contact and fast consumption of Fe(II) [100, 101]. Moreover, by virtue of magnetic properties, Fe_3O_4 provides a possibility of being easily recycled at the end of reaction, and used in succeeding runs [154]. Several works tested the reusability of Fe_3O_4. Xue et al. reported that Fe_3O_4 exhibited good structural and catalytic stabilities in two reaction cycles [155]. However, the decrease of reactivity with varying degrees was also observed by some researchers. For instance, Liu et al. found that the ratio of Fe(III)/Fe(II) decreased from 1.8 before reaction to 0.8 after reaction, and nano-Fe_3O_4 was oxidized into r-Fe_2O_3 [102]. It is might be because the process of transformation from Fe(II) to Fe(III) is much more faster than the reverse process, the activity of Fe_3O_4 declined after excessive rounds [156].

$$\equiv \mathrm{Fe(II)} + \mathrm{HSO_5^-} \rightarrow \equiv \mathrm{Fe(III)} + \mathrm{SO_4^{\bullet -}} + \mathrm{HO^-} \quad (17)$$

$$\equiv \mathrm{Fe(II)} + \mathrm{HSO_5^-} \rightarrow \equiv \mathrm{Fe(III)} + \mathrm{SO_4^{2-}} + \bullet\mathrm{OH} \quad (18)$$

$$\equiv \mathrm{Fe(II)} - \mathrm{OH} + \mathrm{S_2O_8^{2-}} \rightarrow \equiv \mathrm{Fe(III)} - \mathrm{OH} + \mathrm{SO_4^{\bullet -}} + \mathrm{SO_4^{2-}} \quad (1.8 \pm 0.2) \times 10^{-4} \quad (19)$$

$$\equiv \mathrm{Fe(II)} - \mathrm{O^-} + \mathrm{S_2O_8^{2-}} \rightarrow \equiv \mathrm{Fe(III)} - \mathrm{O^-} + \mathrm{SO_4^{\bullet -}} + \mathrm{SO_4^{2-}} \quad (2.2 \pm 0.3) \times 10^{-5} \quad (20)$$

In the case of PS/PMS activation with Fe_2O_3 and FeO(OH) that only contains Fe(III) species, the reaction mechanism could be analogous with Fenton-like oxidation, in which Haber–Weiss reaction was significant and the first step of the catalytic cycle involves reduction of Fe(III) to Fe(II) [107, 157]. Liu et al. studied the detailed processes of naturally occurring iron minerals ($Fe(OH)_3$ and α-FeOOH) for PS decomposition [16, 103]. First, the one-electron reduction of surface site from Fe(III)

to Fe(II) by PS takes place, which could be described as Eq.(21) or (22), accompanied by the formation of $S_2O_8^{\bullet-}$. After the production of Fe(II) sites, Fe(II) could react with PS rapidly to achieve the decomposition of PS. When it comes to the combination with PMS, similar first-step reduction of Fe(III) to Fe(II) is also observed, along with the production of $SO_5^{\bullet-}$ (Eq.(23)) [104-106]. However, note that the reaction rate of this fundamental conversion of Fe(III) to Fe(II) is slow and rate-limiting [158], and this is the reason why Fe(III) bearing oxides is less effective than Fe(II)-containing oxides [159], and thus results in a weak removal efficiency of contaminants or acquired long time scales for contaminant removal. For instance, 50μM of 4-tert-butylphenol was degraded by about 60% in the presence of 1g/L ferrihydrite ($(Fe(OH)_3$) and 1mM PS after 5 h [92]. In another system comprising 50g/L goethite and 1mM PS, approximately 25% of initial 1000μM benzene was removed after the 32-day experiment [107]. Overall, the activation of PS and PMS in the presence of iron oxides and oxyhydroxides could be described in Fig. 4.

$$\equiv \mathrm{Fe(III)} - \mathrm{OH} + \mathrm{S_2O_8^{2-}} \rightarrow \equiv \mathrm{Fe(II)} - \mathrm{OH} + \mathrm{S_2O_8^{\bullet-}} \quad (6.0 \pm 0.6) \times 10^{-6} \qquad (21)$$

$$\equiv \mathrm{Fe(III)} - \mathrm{O^-} + \mathrm{S_2O_8^{2-}} \rightarrow \equiv \mathrm{Fe(II)} - \mathrm{O^-} + \mathrm{S_2O_8^{\bullet-}} \quad (2.8 \pm 0.8) \times 10^{-6} \qquad (22)$$

$$\equiv \mathrm{Fe(III)} + \mathrm{HSO_5^-} \rightarrow \equiv \mathrm{Fe(II)} + \mathrm{SO_5^{\bullet-}} + \mathrm{H^+} \qquad (23)$$

When it comes to synthesis of iron oxides and oxyhydroxides, various methods have been applied. For Fe_3O_4, co-precipitation method is a kind of facial and efficient way [100, 160, 161]. In general, solution of Fe^{3+} and Fe^{2+} are well mixed in a proper ratio, and then the mixture is added dropwise into alkaline solution, usually ammonia or sodium hydroxide solution. Fe_3O_4 particles form via reaction (Eq.(24)). During this

process, anaerobic environment is usually needed to prevent the oxidation of unstable Fe^{2+} before and after nucleation. Solvothermal method is another classic approach to synthesize Fe_3O_4. According to the Li et al., they reported a modified synthesis route for monodispersed and uniform-sized Fe_3O_4 particles, in which the addition of NaAc and polyethylene glycol was a critical measure against particle agglomeration [162]. Besides, using ultrasound might also help to disperse the Fe_3O_4 particles [163]. Hydrothermal method is also used for the fabrication of Fe_2O_3 using bivalent or trivalent iron salts as precursors [106, 164]. Through this method, Ji et al. successfully synthesized Fe_2O_3 particles, which was made up of many bread crumb-like particles and showed a rough and porous morphology, possessing much higher BET surface and catalytic activity than commercial particles [105]. It should be noted that the calcination temperature might influence crystallinity and metal coordination. For example, γ-Fe_2O_3 nanoparticles (maghemite) could be converted to α-Fe_2O_3 at a certain temperature. On the other hand, crystallinity could play a role in the PS/PMS activation. For instance, akaganeite (β-FeOOH) could effectively activate PS to degrade 4-tert-butylphenol, while both leidocrocite (γ-FeOOH) and geothite (α-FeOOH) showed little reactivity in the PS decomposition [165]. A similar example was also observed that amorphous ferrihydrite ($Fe(OH)_3$) resulted in much higher H_2O_2 decomposition rate than crystalline goethite in the Fenton system [166].

$$Fe^{2+} + 2Fe^{3+} + 8OH^- \rightarrow Fe_3O_4 + 4H_2O \quad (24)$$

3.3 Iron sulfides

Many studies have been reported the role of sulfur-bearing iron species in

reductive dechlorination of chlorinated compounds [90, 167-170]. These iron species can be divided into two broad categories. Naturally occurring iron sulfides, including amorphous FeS, makinawite ($Fe_{0.93–0.96}S$), troilite (FeS), greigite (Fe_3S_4), pyrite (FeS_2), pyrrhotite ($Fe_{1-x}S$), and marcasite (FeS_2), contain Fe(II) and are ubiquitous in subsurface soils or easily available in the sulfuric acid market [171, 172]. Another form that has been extensively studied is sulfur modified zero-valent iron [167, 169]. It was found that sulfidized nZVI showed higher dechlorination effects than nZVI because iron sulfidation enables depassivation of iron surface [173, 174], provides catalytic pathways, or promotes electron transfer [90, 96, 175, 176]. Other properties derived from sulfidation compared with nZVI involve lower magnetic performance, higher surface area, and a better adaptability in pH variation [167, 169, 175, 177]. Therefore, they are proposed as a promising electron donor to activate PS or PMS for contaminants degradation.

3.3.1 Natural iron sulfides

Sulfur-containing iron minerals, such as mackinawite (FeS), pyrite (FeS_2) and pyrrhotite (Fe1-xS), have been recognized as effective in activating oxidants (PS/PMS, H_2O_2 and O_3) [171, 178, 179]. When combined with PS or PMS to remove contaminants, mackinawite was sometimes found more effective than ZVI. Yuan et al. used 1.41 g/L mackinawite ore particles (70.0% purity, particle size 0.30 mm) to activate PS, and achieved 99% degradation of 0.2 mM p-chloroaniline within 30 min. By contrast, only 20% of p-chloroaniline was degraded in the Fe^{2+}/PS system and 88% in the ZVI/PS system after 100 min with equimolar theoretical Fe contents [180].

Owing to good solubility under acidic condition, Fe^{2+} is found continuously released from mackinawite participates (Eq. (25)), which can participate in the activation of PS or PMS subsequently (Eqs. (1)-(4)) [171, 180]. Besides, the Fe(II) and S(II) and surface bound Fe(II) on the surface was observed to experience independent oxidations. Surface bound Fe(II) can activate PS or PMS directly, while S(II) can play a role in regenerating Fe(II) from Fe(III) (Eq.(26)) [13].

$$FeS + H^+ \rightarrow Fe^{2+} + HS^- \quad k_{eq} = [Fe^{2+}][HS^-]/[H^+] = 10^{-2.96} \tag{25}$$

$$8 \equiv Fe(III) + \equiv S(II) + 4H_2O \rightarrow 8 \equiv Fe(III) + SO_4^{2-} + 8H^+ \tag{26}$$

By virtue of magnetic properties, mackinawite can be easily recycled, but its reusability is relatively poor [13, 181]. Chen et al. used the modified Butler' method to synthesize FeS for PS activation [168], and found that the removal rate of 2,4-dichlorophenoxyacetic acid decreased rapidly from 100% in the first 2-hour run to only 24.7% in the fifth run [181].

Mackinawite is a metastable mineral, which may age and finally transform to more stable iron sulfides, such as greigite and pyrite [182]. Pyrite is the most common metal sulfide on the Earth's surface[183]. Although pyrite was reported less effective in activating agent for 2,4-dinitrotoluene than mackinawite, which was presumably its insufficient release of Fe^{2+} [171], it still can activate PS in both homogeneous and heterogeneous ways (Eqs.(27)–(30)) [184].

$$2FeS_2 + 7O_2 + 2H_2O \rightarrow 2Fe^{2+} + 4SO_4^{2-} + 4H^+ \tag{27}$$

$$FeS_2 + 8H_2O \rightarrow Fe^{2+} + 2SO_4^{2-} + 16H^+ + 14e^- \tag{28}$$

$$2FeS_2 + 15S_2O_8^{2-} + 16H_2O \rightarrow 2 \equiv Fe(III) + 34SO_4^{2-} + 32H^+ \tag{29}$$

$$FeS_2 + 2S_2O_8^{2-} \rightarrow \equiv Fe(II) + 2SO_4^{\bullet -} + 2SO_4^{2-} + 2S \quad (30)$$

Zhou et al. developed an effective FeS_2/PMS system for diethyl phthalate degradation, and suggested S_2^{2-} was more significant electron donor than Fe(II) on the FeS_2 surface and played a key role in reducing Fe(III), more eminent than that of Fe(II) regenerated by PMS. In addition, different sulfur species, including S_5^{2-}, S_8^0, $S_2O_3^{2-}$ and SO_3^{2-} were testified during the reaction. Among them, $S_2O_3^{2-}$ directly engaged in activating PMS or regenerating Fe(II) to initiate the sequent radical chain reaction (Eqs.(31)-(33))[185].

$$\equiv Fe(III) + SO_3^{2-} \rightarrow \equiv Fe(II) + SO_3^{\bullet -} \quad (31)$$

$$SO_3^{\bullet -} + O_2 \rightarrow SO_5^{\bullet -} \quad (32)$$

$$SO_3^{2-} + SO_5^{\bullet -} \rightarrow SO_4^{2-} + SO_4^{\bullet -} \quad (33)$$

Pyrrhotite has specific ferromagnetic properties, and is the second most common iron sulfide minerals after pyrite in nature [186]. Xia et al. utilized 1.25 g/ L pyrrhotite to activate PS and H_2O_2 (0.5 mM) for phenol degradation respectively, and found that almost 100% of the phenol (2 μM) was degraded in 20 min, while only 59% phenol removal was observed after 30 min in the pyrrhotite /H_2O_2 system [187]. They also demonstrated that dissolved Fe^{2+} in solution and Fe(II) of pyrrhotite collectively contributed to activate PS and generate $SO_4^{\bullet -}$ and HO• radicals [187, 188]. Additionally, the reductive S(II) from pyrrhotite could also reduce Fe(III) to Fe(II) [186].

3.3.2 Sulfur modified iron

Apart from natural iron sulfides, sulfur modified zero-valent iron (S-nZVI) has

attracted great attention, and many desired properties as mentioned before have been discovered during the synthesis and utilization. In a related work, Rayaroth et al. made a comparative study using S-nZVI and nZVI to activate persulfate for benzoic acid, and found that the efficient pH range in the nZVI/PS system was confined to 3-5, while the S-nZVI/PS system was less pH dependent and proven efficient on a broader pH range of 3-9 [94]. This was also observed by Dong et al. in the S-nZVI/PS/ sulfamethazine system [95].

Kim et al. observed that the type of sulfidation reagents, namely, dithionite, sodium sulfide, and thiosulfate, and the adding sequence of reagents for S-nZVI synthesis procedure have little influence on the reactivity of S-nZVI, while the sulfur to iron ratio was crucial [175]. It was also demonstrated by Dong et al., who reported that the particle size of S-nZVI increased and a flake-like shell was more obvious along with the decreasing of Fe/S ratio [167]. This flake-like shell structure was reported to play a role in increasing surface to volume ratio, and decreasing magnetic properties between particles [167, 189]. The shell might be mainly composed of FeS and FeSn [95]. The existence of FeS could facilitate electrons transfer from the iron core to the surface, which would form surface bound ferrous continuously and then activate PS [90, 96]. However, an excessively low Fe/S ratio would lead to the redundant accumulation of FeSn on S-nZVI surface, which was considered to have a much lower reactivity than FeS and decrease particles reactivity [190]. Finally, an optimum Fe/S ratio (25–30) was utilized in the S-nZVI/PS/trichloroethylene, achieving about 90% degradation within 30min [90].

3.4 Iron-based multimetallic catalysts

For the purpose of achieving higher reactivity, iron-based bimetallics or trimetallics materials have been extensively studied and used in the degradation of persistent pollutants [111, 112, 191]. The superiority of a bimetallic or trimetallics system could be explained based on four theories or mechanisms, including (i) the metal additives directly serve as a catalyst [112, 192, 193], (ii) the difference between iron and metal additives leads to the formation of galvanic cells, accelerating an electrochemical corrosion of iron [112, 194-196], (iii) the non-uniform deposition of metal additives on the surface of iron base improve the surface roughness, which can enhance the catalytic performance of the newly formed particles [39], (iv) the metal additives may retard the precipitation of corrosion products on the surface, and sustain the catalytic ability [58, 111].

Ghauch et al. used to introduce metallic atoms to Fe for fabricating bimetallic and trimetallic systems through plating or metal displacement reaction [58, 111, 112]. They also tested a series of activators, including Fe^{2+}, Fe^{0}, AgFe and CoFe, AgCoFe and CoAgFe on activating PS for sulfamethoxazole degradation. Results showed that non-plated iron particles/PS system displayed better sulfamethoxazole removal efficiency largely because of smooth corrosion. However, the Fe corrosion speed decreased and higher reaction stoichiometric efficiency maintained with acceptable sulfamethoxazole degradation rate in the plated systems [58].

To avoid the complicated preparation procedure and control solid waste, many iron wastes, such as steel slag [197], boring scrap [51], steel converter slag [12, 198-

200], basic oxygen furnace slag [113, 201, 202] and drinking water treatment residuals [114, 115, 203, 204] have been utilized as cheap and easily available iron-based activators for PS/PMS activation. These materials usually contains elements other than iron, which can render the whole system similar to other bimetallic or trimetallics iron-based catalysts. In a related work, Naim et al. made a comparison between the boring scrap (iFe) collected from a car shop and commercial iron (cFe) coupled with PS for ranitidine abatement. They found that iFe not only showed sustainable PS activation ability superior to cFe, but released fewer soluable Fe and therefore less iron sludge than cFe, because of the existence of trace elements in its composition such as C, Si, Mn, Ti and Cu. In addition, iFe could achieve a great RSE (reaction stoichiometric efficiency) at 72% by using a low load of iFe [51].

BOF slag is one of the main byproducts during steel making process in the basic oxygen furnace, which has complex and iron abundant components [201, 202]. Some researchers utilized this kind of industrial waste in activation PS or PMS. For example, Matthaiou et al. prepared a series of BOF slags through an oxidative digestion in acid media. These treated BOF slags with magnetite in its composition could activate PS effectively, while the ones with goethite and/or hematite unable to achieve this purpose. In this sense, the best results obtained in experiments was about 90% degradation of propylparaben (0.4 mg/L) in the presence of 1 g/L of PS and 50 mg/L catalysts within 90 min. In addition, negligible iron leaching was observed [113].

WTRs, an inevitable and safe byproducts of drinking water treatment, comprises precipitated Fe and Al oxyhydroxides and organic compounds removed from water by

coagulation [203]. Qi et al. modified WTRs through reduction calcination method and utilized them to activate PS for sulfamethoxazole degradation. The results showed that 80% of sulfamethoxazole (50 μM) was degraded by 2.0mM PS and 0.2 g/L modified WTRs at pH 5.3 in 60 min. Iron species detected in modified WTRs, including iron and magnetite, accounted for the heterogeneous activation of PS [114]. In addition, the RSE at the final stage of degradation reached at 9.5%, in comparison to maximum 5.2% in the ZVI/PS/sulfamethoxazole system (sulfamethoxazole= 39.5μM, micrometric Fe^0 particles=2.23 mM, PS content= 0.4 mM, pH= 5.75) [136]. Li et al. also prepared magnetic catalysts derived from WTRs through oxygen-free pyrolysis treatment. Pyrolysis temperature strongly influenced the composition and performance, and reusability of catalysts, and the highest performance was 95.6% of atrazine (10 μM) in the presence of 0.05 g/L modified WTRs and 0.2 mM PMS [115].

3.5 Supported iron catalysts

Although the aforementioned iron-based heterogeneous PS and PMS activators possess some advantages over the homogeneous PS or PMS activators, they still suffer some drawbacks, which are (i) prone to aggregate due to high surface energy and inherent magnetic forces (particularly true for nanoparticles), (ii) easy to be oxidized in air, (iii) leaching of the iron ions. To overcome these disadvantages, catalysts can be distributed on various supports. The interaction between iron species and supports could exhibit novel physicochemical properties, which could further improve the stability, dispersivity, and reactivity [205-208].

3.5.1 Oxides supports

Many metal oxides, such as CuO, ZrO, CeO and ZnO, can act as catalysts on their own for PS or PMS activation. They can also be used as the supports for iron species [209-211]. As a matrix base, metal oxides (Al_2O_3 for instance) could provide larger contact surface area and serves as a charged particle carrier [212]. Especially for Mn oxides, their almost none-toxic and various valences (+2, +3 and +4) could not only make themselves catalysts for PS or PMS activation, but provide variable forms as they functioned as a kind of support [164]. Kong et al. immobilized iron on MnO and MnO_2 respectively using $FeSO_4$ as iron source, and the formed iron oxides (mainly Fe_3O_4 and/or Fe_2O_3) immobilized on the surface of MnO or MnO_2 improved the activation reactivity towards PS [118, 213]. Moreover, it was observed that lattice matched support-active phase combinations can formed in the intimate interactions between iron species and the supports. These formed linkages, such as Fe-Mn and Fe–Si, can enhance stability and durability of the catalysts, even superior catalytic performance [118, 213, 214].

TiO_2 is a well-known catalyst for both oxidation and reduction. As a highly effective photocatalysts, it strongly corresponds to ultraviolet (UV) light (Eq.(34)) [215]. Iron species immobilized on the surface of TiO_2 can not only function as catalysts for the activation of PS or PMS, but as electron acceptors for transmitting band electrons as well as reducing the recombination of electrons and holes [216-218]. The photogenerated electrons could promote the regeneration of Fe(II) by reducing Fe(III) (Eq.(35)) [218-220], which could facilitate the continuous decomposition of oxidants.

In addition, it may also directly activate oxidants to produce reactive radicals (Eqs.(36)-(38)). On the other hand, the holes on valence band that migrates to the TiO_2 surface have oxidation capacity toward adsorbed organic compounds under UV irradiation [221]. Similar mechanism was observed in analogous Fenton-like systems [220, 222]. Therefore, Fe immobilized on TiO_2 could be considered as a multi-functional catalyst for PS and PMS activation.

$$TiO_2 \xrightarrow{hv} h_{VB}^{+} + e_{CB}^{-} \quad (34)$$

$$\equiv Fe(III) + e_{CB}^{-} \rightarrow \equiv Fe(II) \quad (35)$$

$$S_2O_8^{2-} + e_{CB}^{-} \rightarrow 2SO_4^{\bullet -} \quad (36)$$

$$HSO_5^{-} + e_{CB}^{-} \rightarrow SO_4^{\bullet -} + OH^{-} \quad (37)$$

$$HSO_5^{-} + e_{CB}^{-} \rightarrow \bullet OH + SO_4^{2-} \quad (38)$$

3.5.2 Molecular sieve supports

Since the first synthesis of zeolite as a molecular sieve in 1940s, 245 types of open-framework molecular sieves have been developed up to date [223]. Due to their unique characteristics, e.g., excellent hydrothermal stability, tunable size and morphology, and abundant channel system, they have been popular for catalysis, adsorption and ion-exchange [224].

Among all the zeolites, ZSM-5 (Zeolite Socony Mobile) is a typical molecular sieve with MFI (Mobil fifth) structure [223, 225], and is one of the most important catalysts in petrochemistry [226]. When it comes to iron anchored onto zeolite, Fe/ZSM-5 has been successfully fabricated by Zhao et al. using liquid impregnation and boron hydride reduction method. The formation of Fe_3O_4/Fe^0 was found partly

dispersed on the surface, and partly incorporated into the framework of ZSM-5. These iron-containing active sites could achieve effective PS activation. In addition, Al in the ZSM-5 could play a synergistic role in two aspects to enhance the activation, which are (i) favoring the dispersion and preventing the aggregation of iron, (ii) as a Lewis acid, Al could attract electron density from iron and promote the regeneration of Fe(II) from Fe(III), which then benefits the catalytic activation [227].

MCM-41 (Mobile Composite Material) and SBA-15 (Santa Barbara Amorphous) are two representative highly ordered large-pore mesoporous silica with highly and uniformly ordered hexagonal array of channels [228, 229]. SBA-15 possesses a higher thermal and hydrothermal stability by virtue of its thick wall [230], while MCM-41 enjoys a larger specific surface area (>1000 m^2/g) due to its thinner wall [231]. These tributes make them promising as catalysts supports. Actually, in the direct application of activating PS or PMS, both SBA-15 and MCM-41 generally show little reactivity due to their electrically neutral frameworks and lack of Brønsted acidity [232-234]. Redox active centers could be created by incorporating transition metal ions into the hexagonally arranged framework. The coordination and stabilization of iron and other metallic elements by the silica lattice could significantly improve the catalytic capability and enable them to possess new and often improved properties [235]. For instance, Cai et al. co-incorporated bimetal (Fe and Co) into the mesostructured SBA-15 silica using in situ auto combustion method, which was used to activate PS for the degradation of orange II. With the assistance of electrolysis, 95.6% decolorization efficiency was achieved in 60 min, slight higher than 91.1% for Co/SBA-15 and

Fe/SBA-15. Besides, these bimetallic Fe-Co/SBA-15 catalysts presented less leaching concentration, showing higher stability than monometallic catalyst [236]. Mazilu et al. demonstrated co-incorporation of Fe and Al into the SBA-15 could allow the formation of highly dispersed and/or isolated Fe active sites, which played an important role in PS or PMS activating reactions [237]. Moreover, Vinu fabricated a series of Fe and Al co-incorporated mesoporous molecular sieves (FeAlMCM-41) with different ratios of Si to metal ions (Fe and Al) from 20 to 80, and found that the catalytic activity increased along with the fraction of Fe and Al, which could be attributed to the increase of Brønsted acidity [238]. However, the over-increase of metal ions content may in turn lead to some opposite effects [239]. It was observed that higher iron content (2 wt%) could lead to the decline in both pore volume and surface area of MCM-41, which could be attributed to channels blockage by iron oxides located in the pores [240].

There are two mainstream approaches, namely, direct synthesis and post-synthesis, used for metal ions incorporation, e.g., iron ions. In the direct synthesis, including ionothermal method [241], hydrothermal synthesis [242] and auto-combustion method [243], the surfactant solution is mixed with the prepared precursors of both metal ions and silica, and then metallic elements are in-situ incorporated into the framework of silicate. As for post-synthesis, the surfactant-free matrix is firstly synthesized, and then metal ions could be boned to the silica surface by chemical interactions with silanol groups, such as ion exchange methods and impregnation [235, 244, 245]. The second approach is capable of incorporating a large number of iron species, but it may lead to the aggregation of metal oxides in the mesopores and then the reduction of the surface

area and pore volume of catalysts. For the direct synthesis, it has a simple procedure, but the strong acidic synthesis conditions could inhabit the formation of metal-O-Si bonds, which may cause the instability of loaded metal ions [241]. Liu et al. reported a facile method, in which Fenton's reagent (Fe^{2+}-H_2O_2) was used, it achieved simultaneous detemplation without high-temperature calcination and controlled incorporation of a higher amount of iron oxide species into the mesoporous silica of as-synthesized parent SBA-15 [246].

3.5.3 Carbonaceous materials supports

Carbonaceous materials, such as biochar, activated carbon, carbon black, graphene and its derived materials (graphene oxide, and reduced graphene oxide), have attracted great interest as promising catalysts and catalysts supports for PS/PMS activation, thanks to their superior biocompatibility, large surface area, highly acid and base stability, and controllable electronic and physicochemical features.

When it comes to the role that carbonaceous materials alone play in the PS/PMS aqueous solution for contaminants degradation, an insightful understanding would be obtained from the low-dimensional carbon structures in the carbonaceous materials. As a matter of fact, they are capable of adsorbing organic compounds, due to large porosity and specific surface area, π–π interactions and electrostatic force, and also the chemisorption via chemical bonding [247, 248]. In addition, it is revealed that carbonaceous materials can also directly activate PMS and produce radicals, while PS activated by carbon was considered as not involving the generation of free radicals.

This is related to the oxygen-containing functional groups and exposed edge sites and vacancies on the carbon [8, 249].

Granular activated carbon (GAC), as a type of environmental friendly and economical carbonaceous materials, is one of the most used adsorbents in the removal of contaminants. When GAC is combined with iron species through facial impregnation or co-precipitation approaches [250, 251], this iron-based catalysts can exhibit benign property in activating PS or PMS. Wang et al. simultaneously immobilized Fe and Ag on GAC using two-step impregnation method and found that the formed Fe_3O_4 played a major role in activating PS to degrade acid red 73, while the doping Ag could accelerate the rate of electron transfer and thus achieved efficient regeneration of Fe(II). Additionally, the interaction of between Fe-Ag and GAC, can not only retard the metal leaching, but also enhance the degradation efficiency of acid red 73 [251]. Carbon black (CB) is the product of incomplete combustion or thermal decomposition of hydrocarbons, and this material's primary particle possesses the diameter of nanometric range [252]. When Fe_3O_4 was supported on CB, it was observed that 100% BTEX (10mg/L) and 69% MTBE (10mg/L) could be degraded within 24 h under the optimal conditions (PS= 15mg/L, Fe_3O_4-CB=1g/L, pH=3), with their degradation products presenting low cytotoxicity *in vitro*. This promising performance was attributed to the special interphase surface between Fe_3O_4 and CB, which could facilitate efficient electron conduct to initiate the radical generation process [253]. Graphene (GP) has two dimensional single layer honeycomb structure made up of sp^2 hybridized carbon atoms,

which allows it to possess outstanding properties, such as high specific surface area, fantastic electro-conductibility and strong mechanical strength [254, 255]. When combined with nZVI, the nZVI/GP composite, was demonstrated to be capable of activating PS to effectively remove 92.1% atrazine within 21 min, in comparison of 66.1% in nZVI/PS system and 36.7% in GP/PS system after 60 min. Additionally, the degradation efficiency remained 84.7% in the third cycles, showing superior stability and recyclability [256]. Graphene oxide (GO) and reduced graphene oxide (rGO) are derived from graphene, comprising both sp^2- and sp^3-bonded carbon atoms. The interaction between GO or rGO and metals could contribute to the fine dispersion of nanoparticles and facilitate an interface electron transfer [257], which may in turn enhance activation of PS or PMS by these nanoparticles. Gu et al. successfully prepared nZVI-rGO, which was able to effectively activate PS, PMS and H_2O_2 and achieved similar degradation rate towards trichloroethylene [258]. Park et al. fabricated rGO-Ag^0/Fe_3O_4 nanocomposites by incorporating rGO with individual Ag^0 and Fe_3O_4 to activate PS for phenol degradation. The deposited active sites of Ag^0 and Fe_3O_4 in rGO nanosheet achieved catalytic heterogeneous activation of PS, while rGO could play a role in adsorbing phenol and facilitating an electron transfer from phenol to PS [259].

Recently, biochar, which can be obtained from the pyrolysis of various lignocellulosic biomass such as bamboo [260], sawdust [119], rice hull [261],pine needles [262], banana peels [117], and kenaf bar [150] has attracted great attention as promising supports because of their low cost and wide availability, as well as other

merits, such as porous structure, superior biocompatibility, large specific surface area and abundant oxygen functionality. Correspondingly, biochar supported iron catalysts can be prepared through various methods, including impregnation [119], co-precipitation [262], liquid-phase reduction [263], and a hydrothermal method [117], which is dependent on the iron sources aimed to be loaded on the biochar. Yu et al. prepared a series of magnetic nitrogen-doped biochar catalysts using a one-pot synthesis method. The catalysts were derived from sludge processed by polyacrylamide and polyferricsulfate, which then functioned as nitrogen and iron sources respectively. In addition, these catalysts presented better degradation efficiency towards tetracycline than many other representative carbon materials (GP, GO, wood biochar, etc.), which could be attributed to the collaborative work of carbon, nitrogen species and iron oxides where carbon acted as electron transport intermediary (Fig. 5) [110].

3.5.4 Metal-organic frameworks

Metal-organic frameworks (MOFs), fabricated from metal ions (or clusters) and organic ligands, are a group of crystalline inorganic-organic hybrid [264, 265]. MOFs not only benefit from characteristics of both organic and organic components, but often present some unexpected properties, such as chemical tenability, tailorable molecular structure, and large specific surface areas, making them a desirable substance applied in separation [266], sensing [267], gas storage [268], and catalysis [269].

To date, Fe-based MILs (Materials of Institute Lavoisier) series have been used in activating PS or PMS. Li et al. prepared a series of Fe-based MILs by hydrothermal treatment to activate PS, including MIL-101(Fe), MIL-100(Fe), MIL-53(Fe), and MIL-

88B(Fe). These MILs was found to possess high surface areas and abundant active metal sites, and showed good acid orange 7 removal efficiency via adsorption and radicals generation. MIL-101(Fe) presented the best performance and possible mechanism was proposed (Fig. 6A) [108]. Pu et al. investigated the influence of synthesis conditions on the crystallinity, morphology and activation performance of MIL-53(Fe) prepared by solvothermal method. The superior activation capacity could be attributed to coordinatively unsaturated Fe(II)/Fe(III) sites existing in the framework of MIL-53(Fe), which could be converted to each other continuously and activate PS for orange G degradation [93, 270]. Yue et al. fabricated a core-shell Fe_3O_4@MIL-101(Fe) composites to activate PS for acid orange 7 degradation, and suggested that due to the catalytic activity of metal clusters in MOFs and the favorable recycling of Fe(II) and Fe(III) in the interaction between MIL-101(Fe) and Fe_3O_4, the activation of PS was significantly promoted. In addition, these nanocomposites could be recycled easily and rapidly from the reaction system, and exhibited high stability at least three cycles [271].

The efficiency of the MOF-catalyzed PS or PMS activation process can be further promoted by modifying with additional catalytic sites. For instance, Zhang et al. utilized ferrocene (Fc) to be grafted on MIL-101(Fe) to form Fc-modified MIL-101(Fe), which equipped MIL-101(Fe) with additional Fe(II) sites coming from Fc and outperformed MIL-101(Fe) in activation PMS for amaranth removal [272]. Li et al. synthesized the novel quinone-modified NH_2-MIL-101(Fe) composite as PS catalyst for the removal of bisphenol A. The introduction of 2-anthraquinone sulfonate (AQS) was believed to

establish two redox cycles in the oxidation process, involving a quinone/hydroquinones cycle and a Fe(II)/Fe(III) cycle, which significantly facilitated the generation of reactive radicals. Besides, it was found that the semiquinones produced in the process could directly active PS (Fig. 6B). The overall removal rate of bisphenol A was 97.7% in 120 minutes, showing much better efficiency than NH_2-MIL-101(Fe) or the simple combination of NH_2-MIL-101(Fe) and free AQS [109].

Iron-based MOFs composites used as precursors to synthesize hierarchical carbonaceous materials have also been studied in activating PS or PMS. In a related work, Lin et al. synthesized magnetic iron/carbon nanorod (MICN) nanocomposites derived from one-step carbonization of MIL-88A. These MICN composites, retaining hexagonal rod-like morphology and exhibiting magnetic and porous characteristics, could activate both H_2O_2 and PS to decolorize rhodamine B dye, while adsorption was not observed [273]. On the other hand, the carbonization of MOFs modified with additional active sites is also a promising strategy to further improve the PS activation efficiency. Nitrogen-containing-group-decorated MOFs, including NH_2-MIL-53(Fe) and NH_2-MIL-88B(Fe) was prepared and used as precursors to fabricate N-doped porous carbon hybrid through simple pyrolysis method [274, 275]. In these pyrolysis products, graphite-like layer was both observed, which could play an important role in electron transfer. Besides, N-doped carbon not only provided abundant active sites, but improved the structure and chemical properties, which might be favorable for the enhancement of the adsorption and catalytic activity. Liu et al. reported a newly synthesized Fe@N-doped graphene-like carbon derived from a combination of g-C_3N_4

and NH_2-MIL-53(Fe) through direct pyrolysis under N_2, showing great improved PMS activation performance. They pointed out that the addition of nitrogen precursors (g-C_3N_4 and NH_2 groups) could not only help the stabilization of phase composition and framework morphology during MOF pyrolysis, but increase the surface area. The high reactivity could be attribute to the iron nanoparticles, N species and carbonyl (C=O) groups in the support [276]. However, in some cases, the role of iron species in the prepared catalysts was controversial. Zeng et al. demonstrated the ability of Fe-based nanoparticles with variable chemical valences in activating PMS [275], while Liu et al. found that in some cases, iron species just acted as a magnetic core, and made no contribution to the activation of PMS, which probably resulted from the strong capsulation by porous carbon [274].

4 Enhancement by external energy

The combination of external energy, including ultrasound, magnetic field, electric field and photo irradiation, with the homogeneous or heterogeneous iron species has been found to show synergistic enhancement in the activation of PS or PMS.

4.1 Ultrasound

When ultrasound is applied to an aqueous solution, microbubbles can form, grow and violently collapse. The acoustic cavitation can result in sonoluminescence and hot spots, where extreme conditions of high temperature and pressures are generated [277]. Some volatile organic compounds could be directly decomposed under the ultrasonic irradiation [278]. In addition, S_2O_8•− and •OH radicals can be produced simultaneously

via the direct activation of PS or PMS, and •OH can additionally form via the decomposition of water [279-282]. Zhou et al. reported that when Fe_3O_4 was employed for PMS activation to degrade acid orange 7, which removal efficiency was 90% within 30 min under the optimal conditions (Fe_3O_4=0.4g/L, PMS=3mM, AO7=0.06mM, ultrasound power=200W), in contrast to 39.6% without ultrasound [283]. Pang et al. reported that the degradation rate of rhodamine-B (40 mg/L) increased from 35% to 99.76% within 12 min in the presence of 1g/L ZVI, 1mM PMS and 50W ultrasound power. In addition, this remarkable degradation efficiency could sustain five cycles without decline, while it decreased to 75% in the sixth cycle. It was attributed to the exhaustion of ZVI instead of the precipitation of passive film on the ZVI surface [284]. Actually, the additionally promoting effects that ultrasound exerts on heterogeneous catalysts include (i) ultrasound can enhance the dispersion of nanoparticles in the system, as well as the mass transfer in the solid-liquid interface [285, 286], and (ii) ultrasound can clean the oxidized surface layer and facilitate the contact between fresh catalysts and PS or PMS [286, 287]. However, too intensive ultrasound input could lead to inhibition effect on the activation processes, which may be due to the over-sized cavitation bubbles shielding the shockwave transmission under the intensive ultrasonic power [283, 288].

4.2 Electric field

The activation efficiency of PS and PMS can also be significantly enhanced by the introduction of an electric field. One of the major advantages of electrolysis is that Fe^{2+} can be electro-generated from the sacrificial iron anode to the aqueous solution [289].

Moreover, electrolysis can directly provide electrons, which favorably supports the continuous conversion of Fe(III) to Fe(II), and then retains high PS or PMS activation efficiency [243, 290]. Furthermore, electrochemical process can provide electron directly to activate PS or PMS in the aqueous solution [236, 291, 292]. Zhang et al. combined Fe^3/PS with bioelectricity provided by microbial fuel cell to remove bisphenol A. The introduction of electric field could overcome the limit of pH and facilitate the reaction process under near-neutral pH regime. While the Fe^{3+} precipitated, the iron species in the precipitate could be reduced on the cathode and eventually played a major role in activating PS [293]. Arellano et al. tested pyrite, goethite and magnetite as catalyst to activate PMS for 1-butyl-1-methylpyrrolidinium chloride degradation under electric field, and found that over 80% TOC decay was achieved in the pyrite/PMS/electro system within 300 min [294]. Lin et al. reported the electro-enhanced α-FeOOH activation of PS to degrade orange II, in which the decolorization efficiency of orange II and the decomposition rate of PS are 91.3% and 66.3%, respectively, in comparison with that of 0 and 6.1% in α-FeOOH/PS system [158].

4.3 Magnetic field

Owing to the magnetic property, researchers have found that the combination of magnetic field with ZVI/PS or ZVI/PMS is another way to promote the activation efficiency. When a uniform magnetic field applied, the reaction mechanism remains the corrosion of ZVI to release Fe^{2+} to the solution and then activate oxidants. However, an additional convective transfer of paramagnetic Fe^{2+} could be exerted by the Lorentz force and magnetic field gradient force. This could not only accelerate the

transportation of the released Fe^{2+}, but also reduce the formed precipitation of iron oxides on the surface of ZVI [295]. Therefore, the fresh surface of ZVI can be exposed to the solution, which enhances the corrosion of ZVI to release Fe^{2+}. Xiong et al. found that the application of weak magnetic field to Fe^0/PS system achieved a 28.2 fold enhancement in the degradation rate of orange G under optimal experiment conditions compared with its counterpart without the magnetic field [296].

The acceleration of ZVI corrosion rate and promotion of Fe^{2+} release were even observed in pre-magnetized Fe^0/PS system, where the external magnetic field was absent during the experiment. According to Zhou et al., pre-magnetized Fe^0 could significantly promote the activation of PS and then the removal of various selected organic contaminants, such as p-nitrophenol, fulvic acid, phenol, tartrazine, 2,4-dichlorophenol. In this pre-magnetized Fe^0/PS system, the Fe^0 and PS could be greatly saved compared with conventional Fe^0/PS process [125, 126, 297]. These series of promoting effects might be due to the magnetic property of Fe^0 which enables Fe^0 to maintain magnetization without magnetic field after exposure to magnetic field of certain intensity [298]. However, unsuitable magnetic field intensity may inhibit or not promote the activity of Fe^0. Pan et al. examined the influence of magnetic field and pre-magnetization time on rate constants in the pre-magnetized Fe^0/PS/orange anthraquinone dye system, finding that the rate constants reached the highest when the magnetic field and time were 30 mT and 3 min, respectively [125].

4.4 Photo irradiation

As an important energy input method, UV-Vis irradiation can also enhance the

activation efficiency. In the first place, PS and PMS are proven to be photosensitive and the introduction of UV can directly lead to the photolysis of oxidants to generate radicals through Eqs.(39)-(40) [299-302]. In addition, radiation absorption by them is associated with a ligand-to-metal charge transfer, and then promotes Fe(III) reduction to Fe(II) (Eq.(41)) [106, 250, 302, 303]. This enhancement can be applied in both homogeneous and heterogeneous systems. In homogeneous systems, Wang et al. made a comparison of activation efficiencies between Fe^{3+}/EDDS/H_2O_2 and Fe^{3+}/EDDS under UVA irradiation at same conditions, achieving good degradation rate of p-hydroxyphenylacetic acid, although it was lower than H_2O_2 system whatever the solution pH's. The reduction of Fe^{3+} to Fe^{2+} under irradiation was considered as a crucial step in activating oxidants [304]. In heterogeneous systems, Fe(III) species, including magnetite, hematite and hydroxocomplexes, are often photochemically active. As observed by Jaafarzadeh et al., 90.2% of 2,4-dichlorophenoxyacetic acid was degraded in 60 mins in a UV/PMS/hematite nanoparticle system compared with 79.8% degradation in the absence of UV [106]. It should be noted that the radiation wavelength may have influence on the activation process. In a related work, UVC irradiation (wavelength between 200 and 280 nm) and UVA (wavelength ranged from 315 nm to 400 nm) [305] was employed as radiation source by Kaur et al. to activate PS for ceftriaxone oxidation, 72% degradation and 4% mineralization of ceftriaxone in UVA-induced systems after 2h, while complete ceftriaxone degradation and 74% TOC removal was observed in the UVC-activated PS system during the 15 min of oxidation [306].

Owing to the development of photocatalytic technology, solar light and LED light as applicable light sources are also being combined with PS or PMS for the decontamination process of organic compounds [307-309]. Ahmed et al. utilized Xenon lamp (1500 W) as simulated solar light and Fe^{2+} to activate PS, and achieved 100% removal of carbamazepine in 30min, in contrast to less than 30% removal in the absence of light [310]. Miralles-Cuevas et al. designed a pilot plant study to compare removal of five microcontaminants (antipyrine, carbamazepine, caffeine, ciprofloxacin and sulfamethoxazole at 100 μg/L) in both solar/Fe:EDDS/H_2O_2 and solar/Fe:EDDS/PS systems. In the presence of equal concentration of Fe^{2+} and EDDS (0.1mM) and 1mM PS, five microcontaminants at 100 μg/L achieved highest 90% degradation rate with a solar energy of 2 kJ/L [311]. The visible LED is now a type of promising light sources due to a series of advantages, such as high efficiency and compactness [312, 313], but it cannot directly activate PS or PMS. By contrast, some target organic compounds could be excited by visible LED light, and then involved in a chain of reactions [310]. For example, Gao et al. found that rhodamine B could absorb visible LED light to an excited state, and subsequently transfer electrons to PS and Fe(III) species, leading to the generation of $SO_4^{\bullet-}$ and catalytic cycle of Fe(III)/Fe(II) [314]. On the other hand, visible LED light can stimulate some iron catalysts to show promoting activation performance. As observed by Gao et al., MIL-53(Fe), with a band gap energy at 2.62 eV, could be excited under visible LED light and produced photo induced electrons, which could be trapped by PS and facilitate the generation of $SO_4^{\bullet-}$ for acid orange 7 degradation. [315]. Hu et al. demonstrated that MIL-101(Fe), with a band gap energy

of 2.41 eV, could be firstly excited by visible LED light and then the reduction of Fe(III) to Fe(II) occurred, which subsequently activated PS to degrade tris(2-chloroethyl) phosphate adsorbed onto MIL-101(Fe) crystals [316]. Iron species directly immobilized on some photocatalysts supports can also enhance the performance of activating PS or PMS. Apart from TiO_2 as supports mentioned in Section 3.3.1, Zhang et al. reported a FeOOH/C_3N_4-based photoactuated self-healing system. Under irradiation, charges were excited from valence band in C_3N_4, and subsequently injected into conduction band of FeOOH. This type of interfacial photoexcited electron transport facilitated the reduction of Fe(III) and optimized the Fe(II)/Fe(III) ratio on FeOOH surface during PS activation [317]. In another related work by Yan et al., the excellent heterostructure of the fabricated g-C_3N_4/Fe_2O_3 (CNFe) could significantly accelerate the transfer of charge carrier under the visible LED light, and exhibited superior activity over pure g-C_3N_4 and Fe_2O_3 in activating PS for bisphenol A degradation [318].

$$S_2O_8^{2-} \xrightarrow{hv} 2SO_4^{\bullet -} \quad (39)$$

$$HSO_5^- \xrightarrow{hv} SO_4^{\bullet -} + \bullet OH \quad (40)$$

$$\equiv Fe(III) \xrightarrow{hv} \equiv Fe(II) \quad (41)$$

5 Influences of reaction conditions on the performance of activators

Reaction conditions, including temperature, pH, anions, dissolved oxygen, dosage of catalysts and oxidants, can exert influence on the activation of oxidants and the degradation of contaminants. It was well documented that increasing the dosage of catalysts and oxidants can increase the removal rate, although excessive oxidants may

result in the quenching effect on reactive radicals. Temperature rise in the solution, as another kind of energy input, can also boost the overall reaction rate and even directly activate oxidants [87, 184, 319, 320]. On the other hand, pH value, dissolved oxygen, and anionic composition in solution can affect the activation efficiency in a complex way. Therefore, it is worth discussing the influence of pH and anions in iron-mediated activation of PS and PMS systems.

5.1 pH

The solution pH is considered as a critical parameter in iron-based activation systems, since it affects the decomposition of oxidants (PS and PMS) and speciation of radicals. In addition, it also influences the structural form of iron species and target contaminants [116, 321, 322]. It is generally accepted that low pH is needed in the homogeneous oxidation process when Fe^{2+} or Fe^{3+} is present. In fact, Fe^{2+} is readily soluble in pH value ranging from 2 to 9, while Fe^{3+} starts to precipitate in the form of ferric hydroxides when pH is higher than 3 [47, 323]. The formation of ferrous and ferric complexes, including $FeOH^{+}$, $Fe(OH)_2$, $FeOH^{2+}$, $Fe_2(OH)_2^{4+}$, $Fe(OH)_2^{+}$, $Fe(OH)_3$ and $Fe(OH)_4^{-}$, cannot activate PS or PMS as effectively as free Fe^{2+} does [66, 324]. In addition, extremely acidic condition would result in formation of $(Fe(H_2O))^{2+}$ (pH < 2.5) and $Fe(OH)^{2+}$ (pH < 3), which can also reduce the availability of Fe^{2+} and subsequently hinder the activation performance [289]. On the other hand, solution pH exerts relatively weak influence on heterogeneous catalysts, which can operate under the conditions of wide pH range. Under acidic conditions, the corrosion of iron species would be favored, along with producing more soluble Fe^{2+}, which is favorable for the

activation of PS or PMS [184, 188, 280, 325]. Notably, it also means that the stability of iron-based catalysts can be affected under acidic conditions [251, 326]. Evidence shows that a high amount of iron leaching from Fe_3O_4 takes place at low pH conditions, which hampers the reusability of these heterogeneous catalysts [260]. However, when the pH value is too high, a layer of iron oxides or oxyhydroxides complexes would attach on the surface of catalysts due to hydrolysis, which can prevent further corrosion followed by the decrease of degradation rate (Fig. 7) [129, 181, 327].

In addition to the effects on catalysts, pH also influences the distribution of oxidants and generation of radical species [137, 328, 329]. It is found that the pKa1 and pKa2 of PMS are 0 and 9.4, respectively. Therefore, the dominant specie of PMS is HSO_5^- when solution pH is below 9.4, while SO_5^{2-} when pH above 9.4 [283]. On the other hand, evidence has shown that $SO_4^{\bullet-}$ predominates under acidic conditions, while •OH is more prominent under basic conditions. •OH has a shorter life span than $SO_4^{\bullet-}$. Besides, it was reported that •OH existed a lower standard reduction potential of 1.8 V in neutral and basic solutions than that of 2.7 V in acidic solutions [276]. Therefore, under neutral or basic pH solutions, the dominant •OH exhibits a relatively weaker oxidation capability and a shorter life span than $SO_4^{\bullet-}$, which might cause the decline of degradation efficiency at basic pH [244, 330, 331]. However, it should also be noted that when further increasing the solution pH, PS and PMS can be decomposed to $SO_4^{\bullet-}$, known as alkaline activation [116, 332].

The solution pH can additionally affect the surface charge of catalysts and the existing form of organic compounds, which can further influence the interaction

between catalysts, oxidants and target contaminants [333, 334]. For example, the pHzpc (the pH at zero point of charge (ZPC)) of Fe_3O_4 was reported to be 7.1, resulting in the negative charge when solution pH was higher than 7.1, and positive charge at pH lower than 7.1 [283]. The pHzpc of $CuFe_2O_4$ was about 7.9, suggesting that the surface of $CuFe_2O_4$ presented positive charge when pH of the solution was below 7.9 [335]. Therefore, when the solution pH is on a proper range, the electrical interaction between oxidants and catalysts could benefit the contact between them, which could facilitate the activation [306]. On the other hand, the existing form of organic compounds can also be influenced by pH. For instance, the pKa of acetaminophen was examined to be 9.5, which meant that it would be protonated when pH exceeded 9.5 [336]. Wang et al. found that acetaminophen mainly existed in protonated form at pH≤7.0, while it was deprotonated by 25% at pH 9.0 [43]. Besides, SMZ was found to possessed three different forms at different pH in the aqueous solution, namely, predominantly protonated at pH < 2.3 (pKa1), neutral at pH 2.3–7.3 (pKa2), and deprotonated at pH > 7.3, and showed differences in the reactivity with radicals [123]. In a comprehensive view, Jiang et al. found that the pHzpc of catalysts (Fe functionalized biochar composites) is about 3–5, and that of biphenol A was 9.73. Under the condition of pH 9, the surface charge of catalyst was negative, and could quickly adsorb the cationic form of biphenol A, leading to the promotion of reaction rate [119].

5.2 Anions

Various anions, including Cl^-, HCO_3^-, CO_3^{2-}, NO_3^-, SO_4^{2-}, and $H_2PO_4^-$, ubiquitously exist in natural waters and industrial wastewaters. These anions would

react with reactive radicals and affect the iron-based activation efficiency towards PS and PMS [337].

It has been reported that chloride ion (Cl^-) would react with the activation products, namely, $SO_4^{\bullet-}$ and •OH, to form chlorine containing radicals, such as Cl•, Cl_2•−, and HOCl•-, through a series of chain reactions (Eqs.(42)-(54)) [212, 334, 338]. These radicals possess lower redox potential ($E_{(Cl2•/Cl-)}$=2.0V, $E_{(Cl•/Cl-)}$=2.4V and $E_{(HOCl•-/Cl-)}$=1.48V) than ordinary $SO_4^{\bullet-}$ and •OH, and prefer to react with substituted aromatics [286, 338]. As a result, it is observed that the presence of Cl^- exerted an inhibitory effect on oxidation systems. As Zhou et al. observed, 100 mM Cl^- would strongly decrease the sulfadiazine degradation rate in the neutral sonochemical Fe^0-catalyzed PS system for the annihilation of highly reactive radicals [339]. On the other hand, the promoting role of Cl^- in systems was also reported [290, 326, 327]. Li et al. found that the degradation rate of three pharmaceuticals and personal care products (PPCP) could be enhanced in the presence of Cl^- due to the increase of ionic strength [327]. Rao et al. also observed that the increase of Cl^- concentration from 0 to 10mM would simply promote the degradation rate of carbamazepine [340]. More researchers reported the dual role of Cl^-, and whether Cl^- exhibits inhibition or enhancement depends on the concentration [43, 52, 54, 114, 341]. It might be because the reaction between Cl^- and $SO_4^{\bullet-}$ or •OH is reversible (Eqs. (42)-(43)). The forward pathway is scavenging, but the formed chlorine containing species can also degrade contaminants. On the other hand, the backward way can regenerate highly reactive $SO_4^{\bullet-}$ or •OH, and maintain the oxidation efficiency [51].

Initiation:

$SO_4^{\bullet -} + Cl^- \leftrightarrow Cl^{\bullet} + SO_4^{2-}$ $k_{forward} = 2.47\text{-}6.6 \times 10^8\ M^{-1}S^{-1}$ $k_{backward} = 2.5 \times 10^8\ M^{-1}S^{-1}$ (42)

$\bullet OH + Cl^- \leftrightarrow HOCl^{\bullet -}$ $k_f = 4.3 \times 10^9\ M^{-1}S^{-1}$ $k_b = 6.1 \times 10^9\ M^{-1}S^{-1}$ (43)

Propagation:

$Cl^{\bullet} + H_2O \leftrightarrow HOCl^{\bullet -} + H^+$ $k_f = 1.3\text{-}4.5 \times 10^3\ M^{-1}S^{-1}$ $k_b = 2.1 \times 10^{10}\ M^{-1}S^{-1}$

(44)

$Cl^{\bullet} + Cl^- \leftrightarrow Cl_2^{\bullet -}$ $k_f = 8.0 \times 10^9\ M^{-1}S^{-1}$ $k_b = 4.7 \times 10^4\ M^{-1}S^{-1}$ (45)

$Cl^{\bullet} + OH^- \rightarrow ClOH^{\bullet -}$ $k = 1.8 \times 10^{10}\ M^{-1}S^{-1}$ (46)

$Cl_2^{\bullet -} + OH^- \rightarrow HOCl^{\bullet -} + Cl^-$ $k = 4.0 \times 10^6\ M^{-1}S^{-1}$ (47)

$OCl^- + \bullet OH \rightarrow ClO^{\bullet} + OH^-$ $k = 9.0 \times 10^9\ M^{-1}S^{-1}$ (48)

$2ClO^{\bullet} + H_2O \rightarrow ClO^- + ClO_2^- + 2H^+$ $k = 2.5 \times 10^9\ M^{-1}S^{-1}$ (49)

$ClO_2^- + \bullet OH \rightarrow ClO_2^{\bullet} + OH^-$ $k = 4.2 \times 10^9\ M^{-1}S^{-1}$ (50)

Termination:

$Cl_2^{\bullet -} + Cl_2^{\bullet -} \rightarrow Cl_2 + 2Cl^-$ $k = 2.1 \times 10^9\ M^{-1}S^{-1}$ (51)

$Cl_2^{\bullet -} + \bullet OH \rightarrow HOCl + Cl^-$ $k = 1.0 \times 10^9\ M^{-1}S^{-1}$ (52)

$ClO_2^{\bullet} + \bullet OH \rightarrow ClO_3^- + H^+$ $k = 4.0 \times 10^9\ M^{-1}S^{-1}$ (53)

$\bullet OH + \bullet OH \rightarrow H_2O_2$ $k = 5.5 \times 10^9\ M^{-1}S^{-1}$ (54)

Different from a debatable role of chloride in the oxidation systems, HCO_3^-, CO_3^{2-}, NO_3^-, SO_4^{2-}, and $H_2PO_4^-$ are generally reported to have negative effects on reactive species generated by iron-mediated activation of PS and PMS (Eqs.(55)-(62)) [129, 331, 342]. Bicarbonate/carbonate (HCO_3^-/CO_3^{2-}) and phosphate ions ($H_2PO_4^-$) are well

known scavengers of $SO_4^{\bullet-}$ or •OH, and then less reactive species form, e.g. $E_{CO3^{\bullet-}}$=1.78V [123, 135, 324, 343]. Cao et al. tested the effect of $H_2PO_4^-$ from 1mM to 10Mm in the Fe^0/PMS/tetracycline system, and found that the inhabitation effects increased along with the increasing concentration of $H_2PO_4^-$ [138]. Besides, both bicarbonate and phosphate ions have strong buffer capability. This may lead to a series of negative effects through increasing the solution pH, suppressing the corrosion of iron species or decreasing oxidation potentials of radical species [90, 95, 250, 305]. Moreover, $H_2PO_4^-$ was observed to impose negative influence by complexing with iron species or occupying active sites of catalysts in homogeneous or heterogeneous systems [136, 339, 344]. As for SO_4^{2-} it was reported that concentrated SO_4^{2-} could reduce the oxidation reduction potential (ORP) of $SO_4^{\bullet-}/SO_4^{2-}$, resulting in low activation efficiency of PS or PMS [51, 94, 297]. NO_3^- also has negative influence of NO_3^- on PS/PMS activation, which mainly comes from the reaction with $SO_4^{\bullet-}$ or •OH to produce a less reactive species (NO_3•, 2–2.2 V) [345]. In addition, the passivating effect of NO_3^- on iron surface was also reported, which could then retard the further corrosion of Fe^0 [120, 137].

$$HCO_3^- + SO_4^{\bullet-} \rightarrow SO_4^{2-} + HCO_3^{\bullet} \quad k = 9.1 \times 10^6\ M^{-1}S^{-1} \tag{55}$$

$$HCO_3^- + \bullet OH \rightarrow OH^- + HCO_3^{\bullet-} \quad k = 8.5 \times 10^8\ M^{-1}S^{-1} \tag{56}$$

$$CO_3^{2-} + SO_4^{\bullet-} \rightarrow SO_4^{\bullet-} + CO_3^{\bullet-} \quad k = 6.1 \times 10^6\ M^{-1}S^{-1} \tag{57}$$

$$CO_3^{2-} + \bullet OH \rightarrow OH^- + CO_3^{\bullet-} \quad k = 3.9 \times 10^8\ M^{-1}S^{-1} \tag{58}$$

$$H_2PO_4^- + SO_4^{\bullet-} \rightarrow SO_4^{2-} + H_2PO_4^{\bullet} \quad k < 7.0 \times 10^4\ M^{-1}S^{-1} \tag{59}$$

$$H_2PO_4^- + \bullet OH \rightarrow OH^- + H_2PO_4^{\bullet} \quad k = (1-2) \times 10^4\ M^{-1}S^{-1} \tag{60}$$

$$NO_3^- + SO_4^{\bullet -} \rightarrow NO_3^{\bullet} + SO_4^{2-} \quad k = 5.5 \times 10^5\ M^{-1}S^{-1} \tag{61}$$

$$NO_3^- + \bullet OH \rightarrow NO_3^{\bullet} + OH^- \quad k < 5.0 \times 10^5\ M^{-1}S^{-1} \tag{62}$$

5.3 Dissolved oxygen

Many researchers scrutinized the role of dissolved oxygen (DO) in the aqueous solution [100]. It is found that DO can participant in the radical chain reactions so that affects the degradation of contaminants [112, 327]. To be specific, as an electron acceptor, DO can acquire one electron donated from ferrous species to generate superoxide radicals ($\bullet O_2^-$, $E(O_2/\bullet O_2^-) = -0.046$ eV vs. NHE) (Eq.(63))[112, 188, 346], which can react with PS or PMS to generate $SO_4^{\bullet -}$ (Eq.(64)) In addition, when two protons get involved in the one-electron reduction [347], $\bullet O_2^-$ can also be further reduced to H_2O_2 that undergoes Fenton's reaction (Eq.(65)) [184, 339, 348].

In this regard, the existence of DO can facilitate the decomposition of oxidants (PS or PMS) and radicals' formation. Lei et al. found that 100% degradation of phenol was achieved within 10 min with air purging and it prolonged to 20 min without air purging, while 80% removal rate with argon purging after 30 min [349]. This phenomenon that degradation efficiency was enhanced under aerobic conditions in comparison with anaerobic conditions was also reported in other researchers' works [336, 337, 350]. However, out of the same reason, excessive DO may serve as an electron quencher to hamper activation process [114, 185].

$$Fe^{2+} + O_2 \rightarrow Fe^{3+} + \bullet O_2^- \tag{63}$$

$$\bullet O_2^- + S_2O_8^{2-} \rightarrow SO_4^{\bullet -} + SO_4^{2-} + O_2 \tag{64}$$

$$\bullet O_2^- + Fe^{2+} + 2H^+ \rightarrow Fe^{3+} + H_2O_2 \tag{65}$$

6 Conclusion and prospects

Persulfate and peroxymonosulfate are considered as superior advanced oxidants for degrading ever-increasing organic contaminants by virtue of high redox potential, modest cost and environmentally friendly property, especially when they are activated to generate highly reactive radicals by all sorts of transition metals. Iron, the second most abundant and non-toxic metal, comes out on top from various transition metals and can effectively activate PS/PMS in both homogeneous and heterogeneous ways. Generating sulfate radicals by ferrous or ferric iron in a homogeneous way has become a common practice in various environmental areas, while iron-based heterogeneous activators, including zero-valent iron, iron oxides and oxyhydroxides, iron sulfides, iron-based multimetallic activators, and immobilized iron catalysts on different supports have also be fabricated and utilized. As a matter of fact, these two types of activation share some similarities and differences in activation processes. When combined with common external energy, including ultrasound, electric field and photo irradiation, activation efficiency can be significantly enhanced. In particular, magnetic field can exert positive influence on the magnetic iron species. On the other hand, because of their inherent attributes, homogeneous iron/oxidants systems are more sensitive to operation conditions, in particular the pH of the system, which is the main limitation in the practical application. In comparison, heterogeneous systems could be operated over a broad pH range, although it generally achieves higher efficiency at acidic and circumneutral pH. As for anions and dissolved oxygen that are ubiquitous in

systems, they can both participant in the radical chain reactions, and their positive or negative impacts are quite dependent on the concentrations.

In the future study the following four aspects deserve extra research efforts for further improvement of the iron-based PS/PMS activation technology.

1. Most studies to date have been performed in batch-reactor systems and aim for the decontamination of wastewater, usually simulated wastewater. Few studies have been conducted to target at actual wastewater or other application scenarios except wastewater treatment. It raises two concerns. One is the huge difference between the composition of simulated wastewater and actual wastewater, which makes the removal efficiency obtained in simulated wastewater less persuasive. Besides, the batch reactors cannot represent the authentic environment of wastewater. A good example is a recent study made by Brusseau and his team workers, in which experiments were conducted with column systems to mimic real flow field environment of underground water [151]. The other is that the application of this advanced oxidation technology should not be confined in such a narrow application scenario of wastewater treatment. For instance, combined with ultrafiltration to play a role in suppressing membrane fouling, are currently emerging and appealing. New practical application fields that iron-activated radicals oxidation may be faced with in the future should be developed.
2. Novel organic compounds with complex molecular structures are ever-emerging, and some of them may pose threat to our environment. Besides, the oxidation mechanism of existing various contaminants requires further in-depth study.

However, current research works largely rely on an empirical "trial-and-error" method. Theoretical calculation based on first-principles density functional (DFT), for instance, might provide an approach to uncover the most preferentially attacked sites and potential degradation products of target contaminants, which could be favorable for the rational analysis for the reaction mechanism. Crystalline phases of iron oxides and oxyhydroxides play a role in their magnetic property, which is critical for the recyclability of these heterogeneous catalysts. Additionally, iron species with different morphologies and crystalline phases can exhibit different catalytic efficiencies in the activation of PS or PMS. However, few studies have made a comparison and analyzed the mechanism behind these phenomenon. In this regard, further research works are needed which may be important for properly selecting iron catalysts.

3. For one thing, homogeneous activation of PS/PMS has successfully applied in the in-situ remediation of contaminated soil or underground water. For another, heterogeneous iron catalysts have suffered the problem that metal leaching cannot be completely tackled so far, although they can be separated or recovered from environmental systems. In these cases, the production of iron sludge is inevitable in real applications, so how to limit the loss of initial iron species and make full use of the residual reactivity of iron sludge left in the environmental systems are worth investigating.
4. The integration of external energy with either homogeneous or heterogeneous system generally proves advantageous. In this respect, further research works are

required on process optimization, operating costs control and proper selection of external energy type and strength according to matrices contaminated by pollutants. Besides, hybrid utilization of different external energies has been seldom studied, which might be a prospective research line and a promising way for environmental remediation.

Acknowledgements

The study was financially supported by the National Natural Science Foundation of China (51979203, 51679085, 51909084, 51909085), the Distinguished Young Scholar Fund of Hubei Province of China (2017CFA058), the Program for Changjiang Scholars and Innovative Research Team in University (IRT-13R17), the Fundamental Research Funds for the Central Universities of China (531118010055), the Funds of Hunan Science and Technology Innovation Project (2018RS3115).

Reference

[1] B. Petrie, R. Barden, B. Kasprzyk-Hordern, A review on emerging contaminants in wastewaters and the environment: Current knowledge, understudied areas and recommendations for future monitoring, Water Res. 72 (2015) 3-27.

[2] N.H. Tran, M. Reinhard, K.Y.-H. Gin, Occurrence and fate of emerging contaminants in municipal wastewater treatment plants from different geographical regions-a review, Water Res. 133 (2018) 182-207.

[3] Y. Deng, C.M. Ezyske, Sulfate radical-advanced oxidation process (SR-AOP) for simultaneous removal of refractory organic contaminants and ammonia in landfill leachate, Water Res. 45 (2011) 6189-6194.

[4] Y. Liu, Z. Liu, G. Zeng, M. Chen, Y. Jiang, B. Shao, Z. Li, Y. Liu, Effect of surfactants on the interaction of phenol with laccase: Molecular docking and molecular dynamics simulation studies, J. Hazard. Mater. 357 (2018) 10-18.

[5] Z. Liu, B. Shao, G. Zeng, M. Chen, Z. Li, Y. Liu, Y. Jiang, H. Zhong, Y. Liu, M. Yan, Effects of rhamnolipids on the removal of 2,4,2,4-tetrabrominated biphenyl ether (BDE-47) by Phanerochaete chrysosporium analyzed with a combined approach of experiments and molecular docking, Chemosphere 210 (2018) 922-930.

[6] I. Oller, S. Malato, J.A. Sanchez-Perez, Combination of Advanced Oxidation Processes and biological treatments for wastewater decontamination-A review, Sci. Total Environ. 409 (2011) 4141-4166.

[7] M. Klavarioti, D. Mantzavinos, D. Kassinos, Removal of residual pharmaceuticals from aqueous systems by advanced oxidation processes, Environ. Int. 35 (2009) 402-417.

[8] X.G. Duan, H.Q. Sun, S.B. Wang, Metal-Free Carbocatalysis in Advanced Oxidation Reactions, Acc. Chem. Res. 51 (2018) 678-687.

[9] J. Herney-Ramirez, M.A. Vicente, L.M. Madeira, Heterogeneous photo-Fenton oxidation with pillared clay-based catalysts for wastewater treatment: A review, Appl. Catal. B-Environ. 98 (2010) 10-26.

[10] F.C. Moreira, R.A.R. Boaventura, E. Brillas, V.J.P. Vilar, Electrochemical advanced oxidation processes: A review on their application to synthetic and real wastewaters, Appl. Catal. B-Environ. 202 (2017) 217-261.

[11] A. Babuponnusami, K. Muthukumar, Advanced oxidation of phenol: A comparison between Fenton, electro-Fenton, sono-electro-Fenton and photo-electro-Fenton processes, Chem. Eng. J. 183 (2012) 1-9.

[12] M. Cheng, G. Zeng, D. Huang, C. Lai, Y. Liu, P. Xu, C. Zhang, J. Wan, L. Hu, W. Xiong, C. Zhou, Salicylic acid–methanol modified steel converter slag as heterogeneous Fenton-like catalyst for enhanced degradation of alachlor, Chem. Eng. J. 327 (2017) 686-693.

[13] J. Fan, L. Gu, D. Wu, Z. Liu, Mackinawite (FeS) activation of persulfate for the degradation of p-

chloroaniline: Surface reaction mechanism and sulfur-mediated cycling of iron species, Chem. Eng. J. 333 (2018) 657-664.

[14] Q.Q. Jin, S. Zhang, T. Wen, J. Wang, P.C. Gu, G.X. Zhao, X.X. Wang, Z.S. Chen, T. Hayat, X.K. Wang, Simultaneous adsorption and oxidative degradation of Bisphenol A by zero-valent iron/iron carbide nanoparticles encapsulated in N-doped carbon matrix, Environ. Pollut. 243 (2018) 218-227.

[15] G.Z. Liu, Y.C. Dong, P. Wang, L.R. Bian, Activation of Na2S2O8 for dye degradation by Fe complexes fixed on polycarboxylic acids modified waste cotton, Carbohydr. Polym. 181 (2018) 103-110.

[16] H.Z. Liu, T.A. Bruton, F.M. Doyle, D.L. Sedlak, In Situ Chemical Oxidation of Contaminated Groundwater by Persulfate: Decomposition by Fe(III)- and Mn(IV)-Containing Oxides and Aquifer Materials,Environ. Sci. Technol. 48 (2014) 10330-10336.

[17] G.P. Anipsitakis, D.D. Dionysiou, Radical generation by the interaction of transition metals with common oxidants,Environ. Sci. Technol. 38 (2004) 3705-3712.

[18] E. Saputra, S. Muhammad, H. Sun, H.-M. Ang, M.O. Tadé, S. Wang, Manganese oxides at different oxidation states for heterogeneous activation of peroxymonosulfate for phenol degradation in aqueous solutions, Appl. Catal. B, Environ. 142-143 (2013) 729-735.

[19] X.D. Du, Y.Q. Zhang, I. Hussain, S.B. Huang, W.L. Huang, Insight into reactive oxygen species in persulfate activation with copper oxide: Activated persulfate and trace radicals, Chem. Eng. J. 313 (2017) 1023-1032.

[20] Y.J. Yao, J. Zhang, M.X. Gao, M.J. Yu, Y. Hu, Z.R. Cheng, S.B. Wang, Activation of persulfates by catalytic nickel nanoparticles supported on N-doped carbon nanofibers for degradation of organic pollutants in water, J. Colloid Interface Sci. 529 (2018) 100-110.

[21] D.T. Yue, X.F. Qian, M. Ren, M.Y. Fang, J.P. Jia, Y.X. Zhao, Secondary battery inspired alpha-nickel hydroxide as an efficient Ni-based heterogeneous catalyst for sulfate radical activation, Science Bulletin 63 (2018) 278-281.

[22] G.D. Fang, W.H. Wu, Y.M. Deng, D.M. Zhou, Homogenous activation of persulfate by different species of vanadium ions for PCBs degradation, Chem. Eng. J. 323 (2017) 84-95.

[23] Y.Q. Chen, Y.P. Liu, L. Zhang, P.C. Xie, Z.P. Wang, A.J. Zhou, Z. Fang, J. Ma, Efficient degradation of imipramine by iron oxychloride-activated peroxymonosulfate process, J. Hazard. Mater. 353 (2018) 18-25.

[24] Q.H. Yi, L.J. Bu, Z. Shi, S.Q. Zhou, Epigallocatechin-3-gallate-coated Fe3O4 as a novel heterogeneous catalyst of peroxymonosulfate for diuron degradation: Performance and mechanism, Chem. Eng. J. 302 (2016) 417-425.

[25] C. Bolm, A new iron age, Nature Chemistry 1 (2009) 420-420.

[26] L.O. Simonsen, H. Harbak, P. Bennekou, Cobalt metabolism and toxicology—A brief update, Sci. Total Environ. 432 (2012) 210-215.

[27] J.L. Wang, S.Z. Wang, Activation of persulfate (PS) and peroxymonosulfate (PMS) and application for the degradation of emerging contaminants, Chem. Eng. J. 334 (2018) 1502-1517.

[28] F. Ghanbari, M. Moradi, Application of peroxymonosulfate and its activation methods for degradation of environmental organic pollutants: Review, Chem. Eng. J. 310 (2017) 41-62.

[29] I.A. Ike, K.G. Linden, J.D. Orbell, M. Duke, Critical review of the science and sustainability of persulphate advanced oxidation processes, Chem. Eng. J. 338 (2018) 651-669.

[30] C.G. Liu, B. Wu, X. Chen, Sulfate radical-based oxidation for sludge treatment: A review, Chem. Eng. J. 335 (2018) 865-875.

[31] Z. Zhou, X.T. Liu, K. Sun, C.Y. Lin, J. Ma, M.C. He, W. Ouyang, Persulfate-based advanced oxidation processes (AOPs) for organic-contaminated soil remediation: A review, Chem. Eng. J. 372 (2019) 836-851.

[32] Y.F. Shi, J.K. Yang, W.B. Yu, S.N. Zhang, S. Liang, J. Song, Q. Xu, N. Ye, S. He, C.Z. Yang, J.P. Hu, Synergetic conditioning of sewage sludge via Fe2+/persulfate and skeleton builder: Effect on sludge characteristics and dewaterability, Chem. Eng. J. 270 (2015) 572-581.

[33] G.Y. Zhen, X.Q. Lu, B.Y. Wang, Y.C. Zhao, X.L. Chai, D.J. Niu, A.H. Zhao, Y.Y. Li, Y. Song, X.Y. Cao, Synergetic pretreatment of waste activated sludge by Fe(II)-activated persulfate oxidation under mild temperature for enhanced dewaterability, Bioresour. Technol. 124 (2012) 29-36.

[34] P. Nfodzo, H. Choi, Triclosan decomposition by sulfate radicals: Effects of oxidant and metal doses, Chem. Eng. J. 174 (2011) 629-634.

[35] V. Kavitha, K. Palanivelu, The role of ferrous ion in Fenton and photo-Fenton processes for the degradation of phenol, Chemosphere 55 (2004) 1235-1243.

[36] C.Y. Zhu, G.D. Fang, D.D. Dionysiou, C. Liu, J. Gao, W.X. Qin, D.M. Zhou, Efficient transformation of DDTs with Persulfate Activation by Zero-valent Iron Nanoparticles: A Mechanistic Study, J. Hazard. Mater. 316 (2016) 232-241.

[37] I. M. Kolthoff, A. I. Medalia, H. Parks, The Reaction between Ferrous Iron and Peroxides. IV. Reaction with Potassium Persulfate1a, 1951.

[38] A. Rastogi, S.R. Al-Abed, D.D. Dionysiou, Effect of inorganic, synthetic and naturally occurring chelating agents on Fe(II) mediated advanced oxidation of chlorophenols, Water Res. 43 (2009) 684-694.

[39] M.A. Al-Shamsi, N.R. Thomson, S.P. Forsey, Iron based bimetallic nanoparticles to activate peroxygens, Chem. Eng. J. 232 (2013) 555-563.

[40] X.R. Xu, X.Z. Li, Degradation of azo dye Orange G in aqueous solutions by persulfate with ferrous ion, Sep. Purif. Technol. 72 (2010) 105-111.

[41] H. Yang, S. Zhuang, Q. Hu, L.T. Hu, L.P. Yang, C.T. Au, B. Yi, Competitive reactions of hydroxyl and sulfate radicals with sulfonamides in Fe2+/S2O82- system: Reaction kinetics, degradation mechanism and acute toxicity, Chem. Eng. J. 339 (2018) 32-41.

[42] X.L. Wu, X.G. Gu, S.G. Lu, M.H. Xu, X.K. Zang, Z.W. Miao, Z.F. Qiu, Q. Sui, Degradation of trichloroethylene in aqueous solution by persulfate activated with citric acid chelated ferrous ion, Chem. Eng. J. 255 (2014) 585-592.

[43] S.L. Wang, J.F. Wu, X.Q. Lu, W.X. Xu, Q. Gong, J.Q. Ding, B.S. Dan, P.C. Xie, Removal of acetaminophen in the Fe2+/persulfate system: Kinetic model and degradation pathways, Chem. Eng. J. 358 (2019) 1091-1100.

[44] L.J. Bu, Z. Shi, S.Q. Zhou, Modeling of Fe(II)-activated persulfate oxidation using atrazine as a target contaminant, Sep. Purif. Technol. 169 (2016) 59-65.

[45] B. Liu, F.S. Qu, H.R. Yu, J.Y. Tian, W. Chen, H. Liang, G.B. Li, B. Van der Bruggen, Membrane Fouling and Rejection of Organics during Algae-Laden Water Treatment Using Ultrafiltration: A Comparison between in Situ Pretreatment with Fe(II)/Persulfate and Ozone,Environ. Sci. Technol. 52 (2018) 765-774.

[46] B. Liu, F.S. Qu, W. Chen, H. Liang, T.Y. Wang, X.X. Cheng, H.R. Yu, G.B. Li, B. Van der Bruggen, Microcystis aeruginosa-laden water treatment using enhanced coagulation by persulfate/Fe(II), ozone and permanganate: Comparison of the simultaneous and successive oxidant dosing strategy, Water Res. 125 (2017) 72-80.

[47] A. Rastogi, S.R. Ai-Abed, D.D. Dionysiou, Sulfate radical-based ferrous-peroxymonosulfate oxidative system for PCBs degradation in aqueous and sediment systems, Appl. Catal. B-Environ. 85 (2009) 171-179.

[48] S.Y. Oh, H.W. Kim, J.M. Park, H.S. Park, C. Yoon, Oxidation of polyvinyl alcohol by persulfate activated with heat, Fe2+, and zero-valent iron, J. Hazard. Mater. 168 (2009) 346-351.

[49] S.Z. Wang, J.L. Wang, Trimethoprim degradation by Fenton and Fe(II)-activated persulfate processes, Chemosphere 191 (2018) 97-105.

[50] S.Z. Wang, J.L. Wang, Comparative study on sulfamethoxazole degradation by Fenton and Fe(II)-activated persulfate process, Rsc Advances 7 (2017) 48670-48677.

[51] S. Naim, A. Ghauch, Ranitidine abatement in chemically activated persulfate systems: Assessment of industrial iron waste for sustainable applications, Chem. Eng. J. 288 (2016) 276-288.

[52] M. Amasha, A. Baalbaki, A. Ghauch, A comparative study of the common persulfate activation techniques for the complete degradation of an NSAID: The case of ketoprofen, Chem. Eng. J. 350 (2018) 395-410.

[53] L.W. Matzek, K.E. Carter, Activated persulfate for organic chemical degradation: A review, Chemosphere 151 (2016) 178-188.

[54] J.P. Zhu, Y.L. Lin, T.Y. Zhang, T.C. Cao, B. Xu, Y. Pan, X.T. Zhang, N.Y. Gao, Modelling of iohexol degradation in a Fe(II)-activated persulfate system, Chem. Eng. J. 367 (2019) 86-93.

[55] S. Al Hakim, S. Jaber, N. Zein Eddine, A. Baalbaki, A. Ghauch, Degradation of theophylline in a UV254/PS system: Matrix effect and application to a factory effluent, Chem. Eng. J. 380 (2020) 122478.

[56] S. Rodriguez, A. Santos, A. Romero, F. Vicente, Kinetic of oxidation and mineralization of priority and emerging pollutants by activated persulfate, Chem. Eng. J. 213 (2012) 225-234.

[57] A. Romero, A. Santos, F. Vicente, C. González, Diuron abatement using activated persulphate: Effect of pH, Fe(II) and oxidant dosage, Chem. Eng. J. 162 (2010) 257-265.

[58] G. Ayoub, A. Ghauch, Assessment of bimetallic and trimetallic iron-based systems for persulfate activation: Application to sulfamethoxazole degradation, Chem. Eng. J. 256 (2014) 280-292.

[59] F. Vicente, A. Santos, A. Romero, S. Rodriguez, Kinetic study of diuron oxidation and mineralization by persulphate: Effects of temperature, oxidant concentration and iron dosage method, Chem. Eng. J. 170 (2011) 127-135.

[60] S. Rodriguez, A. Santos, A. Romero, Oxidation of priority and emerging pollutants with persulfate activated by iron: Effect of iron valence and particle size, Chem. Eng. J. 318 (2017) 197-205.

[61] S. Rodriguez, L. Vasquez, D. Costa, A. Romero, A. Santos, Oxidation of Orange G by persulfate activated by Fe(II), Fe(III) and zero valent iron (ZVI), Chemosphere 101 (2014) 86-92.

[62] C.K. Duesterberg, W.J. Cooper, T.D. Waite, Fenton-Mediated Oxidation in the Presence and Absence of Oxygen,Environ. Sci. Technol. 39 (2005) 5052-5058.

[63] R. Chen, J.J. Pignatello, Role of Quinone Intermediates as Electron Shuttles in Fenton and Photoassisted Fenton Oxidations of Aromatic Compounds,Environ. Sci. Technol. 31 (1997) 2399-2406.

[64] G. Fang, J. Gao, D.D. Dionysiou, C. Liu, D. Zhou, Activation of Persulfate by Quinones: Free Radical Reactions and Implication for the Degradation of PCBs,Environ. Sci. Technol. 47 (2013) 4605-4611.

[65] L. Chen, J. Ma, X. Li, J. Zhang, J. Fang, Y. Guan, P. Xie, Strong enhancement on fenton oxidation by addition of hydroxylamine to accelerate the ferric and ferrous iron cycles,Environ. Sci. Technol. 45 (2011) 3925-3930.

[66] C.J. Liang, C.P. Liang, C.C. Chen, pH dependence of persulfate activation by EDTA/Fe(III) for degradation of trichloroethylene, J. Contam. Hydrol. 106 (2009) 173-182.

[67] C.G. Niu, Y. Wang, X.G. Zhang, G.M. Zeng, D.W. Huang, M. Ruan, X.W. Li, Decolorization of an azo dye Orange G in microbial fuel cells using Fe(II)-EDTA catalyzed persulfate, Bioresour. Technol. 126 (2012) 101-106.

[68] Y.F. Ji, L. Wang, M.D. Jiang, Y. Yang, P.Z. Yang, J.H. Lu, C. Ferronato, J.M. Chovelon, Ferrous-activated peroxymonosulfate oxidation of antimicrobial agent sulfaquinoxaline and structurally related compounds in aqueous solution: kinetics, products, and transformation pathways, Environ. Sci. Pollut. Res. 24 (2017) 19535-19545.

[69] C.J. Liang, C.J. Bruell, M.C. Marley, K.L. Sperry, Persulfate oxidation for in situ remediation of TCE. II. Activated by chelated ferrous ion, Chemosphere 55 (2004) 1225-1233.

[70] K.J. Zhang, X.Y. Zhou, T.Q. Zhang, L. Yu, Z.M. Qian, W.C. Liao, C. Li, Degradation of the earthy and musty odorant 2,4,6-tricholoroanisole by persulfate activated with iron of different valences, Environ.

Sci. Pollut. Res. 25 (2018) 3435-3445.

[71] H.Y. Dong, Z.M. Qiang, J. Hu, C. Sans, Accelerated degradation of iopamidol in iron activated persulfate systems: Roles of complexing agents, Chem. Eng. J. 316 (2017) 288-295.

[72] H.J. Peng, W. Zhang, L. Liu, K.F. Lin, Degradation performance and mechanism of decabromodiphenyl ether (BDE209) by ferrous-activated persulfate in spiked soil, Chem. Eng. J. 307 (2017) 750-755.

[73] L.R. Bennedsen, A. Krischker, T.H. Jørgensen, E.G. Søgaard, Mobilization of metals during treatment of contaminated soils by modified Fenton's reagent using different chelating agents, J. Hazard. Mater. 199-200 (2012) 128-134.

[74] L. Zhou, W. Zheng, Y.F. Ji, J.F. Zhang, C. Zeng, Y. Zhang, Q. Wang, X. Yang, Ferrous-activated persulfate oxidation of arsenic(III) and diuron in aquatic system, J. Hazard. Mater. 263 (2013) 422-430.

[75] D.Y. Deng, L.B. Peng, M.Y. Guan, Y. Kang, Impact of activation methods on persulfate oxidation of methyl tert-butyl ether, J. Hazard. Mater. 264 (2014) 521-528.

[76] Y.F. Ji, C. Ferronato, A. Salvador, X. Yang, J.M. Chovelon, Degradation of ciprofloxacin and sulfamethoxazole by ferrous-activated persulfate: Implications for remediation of groundwater contaminated by antibiotics, Sci. Total Environ. 472 (2014) 800-808.

[77] C.E. Noradoun, I.F. Cheng, EDTA degradation induced by oxygen activation in a zerovalent iron/air/water system,Environ. Sci. Technol. 39 (2005) 7158-7163.

[78] D.H. Han, J.Q. Wan, Y.W. Ma, Y. Wang, Y. Li, D.Y. Li, Z.Y. Guan, New insights into the role of organic chelating agents in Fe(II) activated persulfate processes, Chem. Eng. J. 269 (2015) 425-433.

[79] D.H. Han, J.Q. Wan, Y.W. Ma, Y. Wang, M.Z. Huang, Y.M. Chen, D.Y. Li, Z.Y. Guan, Y. Li, Enhanced decolorization of Orange G in a Fe(II)-EDDS activated persulfate process by accelerating the regeneration of ferrous iron with hydroxylamine, Chem. Eng. J. 256 (2014) 316-323.

[80] S.X. Yu, X.G. Gu, S.G. Lu, Y.F. Xue, X. Zhang, M.H. Xu, Z.F. Qiu, Q. Sui, Degradation of phenanthrene in aqueous solution by a persulfate/percarbonate system activated with CA chelated-Fe(II), Chem. Eng. J. 333 (2018) 122-131.

[81] C.J. Liang, C.F. Huang, Y.J. Chen, Potential for activated persulfate degradation of BTEX contamination, Water Res. 42 (2008) 4091-4100.

[82] Y.Y. Jin, S.P. Sun, X.Y. Yang, X.D. Chen, Degradation of ibuprofen in water by Fe-II-NTA complex-activated persulfate with hydroxylamine at neutral pH, Chem. Eng. J. 337 (2018) 152-160.

[83] J. Zou, J. Ma, L.W. Chen, X.C. Li, Y.H. Guan, P.C. Xie, C. Pan, Rapid Acceleration of Ferrous Iron/Peroxymonosulfate Oxidation of Organic Pollutants by Promoting Fe(III)/Fe(II) Cycle with Hydroxylamine,Environ. Sci. Technol. 47 (2013) 11685-11691.

[84] X.L. Wu, X.G. Gu, S.G. Lu, Z.F. Qiu, Q. Sui, X.K. Zang, Z.W. Miao, M.H. Xu, Strong enhancement of trichloroethylene degradation in ferrous ion activated persulfate system by promoting ferric and ferrous ion cycles with hydroxylamine, Sep. Purif. Technol. 147 (2015) 186-193.

[85] X. Wang, M. L. Brusseau, Effect of pyrophosphate on the dechlorination of tetrachloroethene by the Fenton reaction, 1998.

[86] G.F. Liu, X.C. Li, B.J. Han, L.W. Chen, L.N. Zhu, L.C. Campos, Efficient degradation of sulfamethoxazole by the Fe(II)/HSO5- process enhanced by hydroxylamine: Efficiency and mechanism, J. Hazard. Mater. 322 (2017) 461-468.

[87] F. Gao, Y.J. Li, B. Xiang, Degradation of bisphenol A through transition metals activating persulfate process, Ecotox. Environ. Safe. 158 (2018) 239-247.

[88] Y. Huang, C. Han, Y.Q. Liu, M.N. Nadagouda, L. Machala, K.E. O'Shea, V.K. Sharma, D.D. Dionysiou, Degradation of atrazine by ZnxCu1 (-) xFe2O4 nanomaterial-catalyzed sulfite under UV-vis light irradiation: Green strategy to generate SO4 center dot(-), Appl. Catal. B-Environ. 221 (2018) 380-392.

[89] R. Pulicharla, R. Drouinaud, S.K. Brar, P. Drogui, F. Proulx, M. Verma, R.Y. Surampalli, Activation of persulfate by homogeneous and heterogeneous iron catalyst to degrade chlortetracycline in aqueous solution, Chemosphere 207 (2018) 543-551.

[90] H.R. Dong, K.J. Hou, W.W. Qiao, Y.J. Cheng, L.H. Zhang, B. Wang, L. Li, Y.Y. Wang, Q. Ning, G.M. Zeng, Insights into enhanced removal of TCE utilizing sulfide-modified nanoscale zero-valent iron activated persulfate, Chem. Eng. J. 359 (2019) 1046-1055.

[91] Y.F. Li, X.Z. Yuan, D.B. Wang, H. Wang, Z.B. Wu, L.B. Jiang, D. Mo, G.J. Yang, R.P. Guan, G.M. Zeng, Recyclable zero-valent iron activating peroxymonosulfate synchronously combined with thermal treatment enhances sludge dewaterability by altering physicochemical and biological properties, Bioresour. Technol. 262 (2018) 294-301.

[92] Y.L. Wu, R. Prulho, M. Brigante, W. Dong, K. Hanna, G. Mailhot, Activation of persulfate by Fe(III) species: Implications for 4-tert-butylphenol degradation, J. Hazard. Mater. 322 (2017) 380-386.

[93] M.J. Pu, Y.W. Ma, J.Q. Wan, Y. Wang, J.M. Wang, M.L. Brusseau, Activation performance and mechanism of a novel heterogeneous persulfate catalyst: metal-organic frameworkMIL-53(Fe) with Fe-II/Fe-III mixed-valence coordinatively unsaturated iron center, Catal. Sci. Technol. 7 (2017) 1129-1140.

[94] M.P. Rayaroth, C.S. Lee, U.K. Aravind, C.T. Aravindakumar, Y.S. Chang, Oxidative degradation of benzoic acid using Fe-0 - and sulfidized Fe-0-activated persulfate: A comparative study, Chem. Eng. J. 315 (2017) 426-436.

[95] H.R. Dong, B. Wang, L. Li, Y.Y. Wang, Q. Ning, R. Tian, R. Li, J. Chen, Q.Q. Xie, Activation of persulfate and hydrogen peroxide by using sulfide-modified nanoscale zero-valent iron for oxidative degradation of sulfamethazine: A comparative study, Sep. Purif. Technol. 218 (2019) 113-119.

[96] J.K. Du, J.G. Bao, X.Y. Fu, C.H. Lu, S.H. Kim, Facile preparation of S/Fe composites as an effective peroxydisulfate activator for RhB degradation, Sep. Purif. Technol. 163 (2016) 145-152.

[97] H. Zhong, M.L. Brusseau, Y. Wang, N. Yan, L. Quig, G.R. Johnson, In-situ activation of persulfate by iron filings and degradation of 1,4-dioxane, Water Res. 83 (2015) 104-111.

[98] C. Kim, J.Y. Ahn, T.Y. Kim, W.S. Shin, I. Hwang, Activation of Persulfate by Nanosized Zero-

Valent Iron (NZVI): Mechanisms and Transformation Products of NZVI,Environ. Sci. Technol. 52 (2018) 3625-3633.

[99] M. Usman, P. Faure, C. Ruby, K. Hanna, Application of magnetite-activated persulfate oxidation for the degradation of PAHs in contaminated soils, Chemosphere 87 (2012) 234-240.

[100] G.D. Fang, D.D. Dionysiou, S.R. Al-Abed, D.M. Zhou, Superoxide radical driving the activation of persulfate by magnetite nanoparticles: Implications for the degradation of PCBs, Appl. Catal. B-Environ. 129 (2013) 325-332.

[101] L.W. Chen, X. Zuo, L. Zhou, Y. Huang, S.J. Yang, T.M. Cai, D.H. Ding, Efficient heterogeneous activation of peroxymonosulfate by facilely prepared Co/Fe bimetallic oxides: Kinetics and mechanism, Chem. Eng. J. 345 (2018) 364-374.

[102] Z. Liu, X. Li, Z. Rao, F. Hu, Treatment of landfill leachate biochemical effluent using the nano-Fe3O4/Na2S2O8 system: Oxidation performance, wastewater spectral analysis, and activator characterization, J. Environ. Manage. 208 (2018) 159-168.

[103] W. Li, R. Orozco, N. Camargos, H.Z. Liu, Mechanisms on the Impacts of Alkalinity, pH, and Chloride on Persulfate-Based Groundwater Remediation,Environ. Sci. Technol. 51 (2017) 3948-3959.

[104] W.-D. Oh, S.-K. Lua, Z. Dong, T.-T. Lim, Performance of magnetic activated carbon composite as peroxymonosulfate activator and regenerable adsorbent via sulfate radical-mediated oxidation processes, J. Hazard. Mater. 284 (2015) 1-9.

[105] F. Ji, C.L. Li, X.Y. Wei, J. Yu, Efficient performance of porous Fe2O3 in heterogeneous activation of peroxymonosulfate for decolorization of Rhodamine B, Chem. Eng. J. 231 (2013) 434-440.

[106] N. Jaafarzadeh, F. Ghanbari, M. Ahmadi, Catalytic degradation of 2,4-dichlorophenoxyacetic acid (2,4-D) by nano-Fe2O3 activated peroxymonosulfate: Influential factors and mechanism determination, Chemosphere 169 (2017) 568-576.

[107] H.Z. Liu, T.A. Bruton, W. Li, J. Van Buren, C. Prasse, F.M. Doyle, D.L. Sedlak, Oxidation of Benzene by Persulfate in the Presence of Fe(III)- and Mn(IV)-Containing Oxides: Stoichiometric Efficiency and Transformation Products,Environ. Sci. Technol. 50 (2016) 890-898.

[108] X.H. Li, W.L. Guo, Z.H. Liu, R.Q. Wang, H. Liu, Fe-based MOFs for efficient adsorption and degradation of acid orange 7 in aqueous solution via persulfate activation, Appl. Surf. Sci. 369 (2016) 130-136.

[109] X.H. Li, W.L. Guo, Z.H. Liu, R.Q. Wang, H. Liu, Quinone-modified NH2-MIL-101(Fe) composite as a redox mediator for improved degradation of bisphenol A, J. Hazard. Mater. 324 (2017) 665-672.

[110] J.F. Yu, L. Tang, Y. Pang, G.M. Zeng, J.J. Wang, Y.C. Deng, Y.N. Liu, H.P. Feng, S. Chen, X.Y. Ren, Magnetic nitrogen-doped sludge-derived biochar catalysts for persulfate activation: Internal electron transfer mechanism, Chem. Eng. J. 364 (2019) 146-159.

[111] A. Ghauch, H. Abou Assi, H. Baydoun, A.M. Tuqan, A. Bejjani, Fe-0-based trimetallic systems for the removal of aqueous diclofenac: Mechanism and kinetics, Chem. Eng. J. 172 (2011) 1033-1044.

[112] A. Ghauch, H. Abou Assi, S. Bdeir, Aqueous removal of diclofenac by plated elemental iron: Bimetallic systems, J. Hazard. Mater. 182 (2010) 64-74.

[113] V. Matthaiou, P. Oulego, Z. Frontistis, S. Collado, D. Hela, I.K. Konstantinou, M. Diaz, D. Mantzavinos, Valorization of steel slag towards a Fenton-like catalyst for the degradation of paraben by activated persulfate, Chem. Eng. J. 360 (2019) 728-739.

[114] C.D. Qi, G. Yu, J. Huang, B. Wang, Y.J. Wang, S.B. Deng, Activation of persulfate by modified drinking water treatment residuals for sulfamethoxazole degradation, Chem. Eng. J. 353 (2018) 490-498.

[115] X.W. Li, X.T. Liu, C.Y. Lin, H.J. Zhang, Z. Zhou, G.X. Fan, M.C. He, W. Ouyang, Activation of peroxymonosulfate by magnetic catalysts derived from drinking water treatment residuals for the degradation of atrazine, J. Hazard. Mater. 366 (2019) 402-412.

[116] Y. Wang, S.Y. Chen, X. Yang, X.F. Huang, Y.H. Yang, E.K. He, S.Q. Wang, R.L. Qiu, Degradation of 2,2 ',4,4 '-tetrabromodiphenyl ether (BDE-47) by a nano zerovalent iron-activated persulfate process: The effect of metal ions, Chem. Eng. J. 317 (2017) 613-622.

[117] X. Rong, M. Xie, L.S. Kong, V. Natarajan, L. Ma, J.H. Zhan, The magnetic biochar derived from banana peels as a persulfate activator for organic contaminants degradation, Chem. Eng. J. 372 (2019) 294-303.

[118] Y.H. Jo, S.H. Do, S.H. Kong, Persulfate activation by iron oxide-immobilized MnO2 composite: Identification of iron oxide and the optimum pH for degradations, Chemosphere 95 (2014) 550-555.

[119] S.F. Jiang, L.L. Ling, W.J. Chen, W.J. Liu, D.C. Li, H. Jiang, High efficient removal of bisphenol A in a peroxymonosulfate/iron functionalized biochar system: Mechanistic elucidation and quantification of the contributors, Chem. Eng. J. 359 (2019) 572-583.

[120] Y. Zhang, X. Xu, Y.W. Pan, L.T. Xu, M.H. Zhou, Pre-magnetized Fe-0 activated persulphate for the degradation of nitrobenzene in groundwater, Sep. Purif. Technol. 212 (2019) 555-562.

[121] M. Farhadian, C. Vachelard, D. Duchez, C. Larroche, In situ bioremediation of monoaromatic pollutants in groundwater: A review, Bioresour. Technol. 99 (2008) 5296-5308.

[122] G.Y. Zhen, X.Q. Lu, L.H. Su, T. Kobayashi, G. Kumar, T. Zhou, K.Q. Xu, Y.Y. Li, X.F. Zhu, Y.C. Zhao, Unraveling the catalyzing behaviors of different iron species (Fe2+ vs. Fe) in activating persulfate-based oxidation process with implications to waste activated sludge dewaterability, Water Res. 134 (2018) 101-114.

[123] J.X. Wu, B. Wang, L. Blaney, G.L. Peng, P. Chen, Y.Z. Cui, S.B. Deng, Y.J. Wang, J. Huang, G. Yu, Degradation of sulfamethazine by persulfate activated with organo-montmorillonite supported nano-zero valent iron, Chem. Eng. J. 361 (2019) 99-108.

[124] S.Y. Oh, S.G. Kang, P.C. Chiu, Degradation of 2,4-dinitrotoluene by persulfate activated with zero-valent iron, Sci. Total Environ. 408 (2010) 3464-3468.

[125] Y.W. Pan, M.H. Zhou, X. Li, L.T. Xu, Z.X. Tang, X.J. Sheng, B. Li, Highly efficient persulfate oxidation process activated with pre-magnetization Fe-0, Chem. Eng. J. 318 (2017) 50-56.

[126] X. Li, M.H. Zhou, Y.W. Pan, L.T. Xu, Pre-magnetized Fe-0/persulfate for notably enhanced degradation and dechlorination of 2,4-dichlorophenol, Chem. Eng. J. 307 (2017) 1092-1104.

[127] S. Rodriguez, L. Vasquez, A. Romero, A. Santos, Dye Oxidation in Aqueous Phase by Using Zero-Valent Iron as Persulfate Activator: Kinetic Model and Effect of Particle Size, Ind. Eng. Chem. Res. 53 (2014) 12288-12294.

[128] Y. Song, G.D. Fang, C.Y. Zhu, F.X. Zhu, S. Wu, N. Chen, T.L. Wu, Y.J. Wang, J. Gao, D.M. Zhou, Zero-valent iron activated persulfate remediation of polycyclic aromatic hydrocarbon-contaminated soils: An in situ pilot-scale study, Chem. Eng. J. 355 (2019) 65-75.

[129] N. Liu, F. Ding, C.H. Weng, C.C. Hwang, Y.T. Lin, Effective degradation of primary color direct azo dyes using Fe-0 aggregates-activated persulfate process, J. Environ. Manage. 206 (2018) 565-576.

[130] R.C. Li, X.Y. Jin, M. Megharaj, R. Naidu, Z.L. Chen, Heterogeneous Fenton oxidation of 2,4-dichlorophenol using iron-based nanoparticles and persulfate system, Chem. Eng. J. 264 (2015) 587-594.

[131] M.A.V. Ramos, W. Yan, X.-q. Li, B.E. Koel, W.-x. Zhang, Simultaneous Oxidation and Reduction of Arsenic by Zero-Valent Iron Nanoparticles: Understanding the Significance of the Core−Shell Structure, The Journal of Physical Chemistry C 113 (2009) 14591-14594.

[132] Y. Liu, S.A. Majetich, R.D. Tilton, D.S. Sholl, G.V. Lowry, TCE Dechlorination Rates, Pathways, and Efficiency of Nanoscale Iron Particles with Different Properties,Environ. Sci. Technol. 39 (2005) 1338-1345.

[133] H. Li, J. Wan, Y. Ma, M. Huang, Y. Wang, Y. Chen, New insights into the role of zero-valent iron surface oxidation layers in persulfate oxidation of dibutyl phthalate solutions, Chem. Eng. J. 250 (2014) 137-147.

[134] P. Drzewicz, L. Perez-Estrada, A. Alpatova, J.W. Martin, M. Gamal El-Din, Impact of Peroxydisulfate in the Presence of Zero Valent Iron on the Oxidation of Cyclohexanoic Acid and Naphthenic Acids from Oil Sands Process-Affected Water,Environ. Sci. Technol. 46 (2012) 8984-8991.

[135] C.Q. Tan, Y.J. Dong, D.F. Fu, N.Y. Gao, J.X. Ma, X.Y. Liu, Chloramphenicol removal by zero valent iron activated peroxymonosulfate system: Kinetics and mechanism of radical generation, Chem. Eng. J. 334 (2018) 1006-1015.

[136] A. Ghauch, G. Ayoub, S. Naim, Degradation of sulfamethoxazole by persulfate assisted micrometric Fe0 in aqueous solution, Chem. Eng. J. 228 (2013) 1168-1181.

[137] W. Hayat, Y.Q. Zhang, I. Hussain, X.D. Du, M.M. Du, C.H. Yao, S.B. Huang, F. Si, Efficient degradation of imidacloprid in water through iron activated sodium persulfate, Chem. Eng. J. 370 (2019) 1169-1180.

[138] J.Y. Cao, L.D. Lai, B. Lai, G. Yao, X. Chen, L.P. Song, Degradation of tetracycline by peroxymonosulfate activated with zero-valent iron: Performance, intermediates, toxicity and mechanism, Chem. Eng. J. 364 (2019) 45-56.

[139] A. Ghauch, H. Abou Assi, A. Tuqan, Investigating the mechanism of clofibric acid removal in Fe0/H2O systems, J. Hazard. Mater. 176 (2010) 48-55.

[140] A. Ghauch, A. Tuqan, H.A. Assi, Antibiotic removal from water: Elimination of amoxicillin and ampicillin by microscale and nanoscale iron particles, Environ. Pollut. 157 (2009) 1626-1635.

[141] D. O'Carroll, B. Sleep, M. Krol, H. Boparai, C. Kocur, Nanoscale zero valent iron and bimetallic particles for contaminated site remediation, Adv. Water Resour. 51 (2013) 104-122.

[142] W. Yan, A.A. Herzing, C.J. Kiely, W.-x. Zhang, Nanoscale zero-valent iron (nZVI): Aspects of the core-shell structure and reactions with inorganic species in water, J. Contam. Hydrol. 118 (2010) 96-104.

[143] B.D. Yirsaw, M. Megharaj, Z. Chen, R. Naidu, Environmental application and ecological significance of nano-zero valent iron, J. Environ. Sci. 44 (2016) 88-98.

[144] H.X. Li, J.Q. Wan, Y.W. Ma, Y. Wang, Synthesis of novel core-shell Fe-0@Fe3O4 as heterogeneous activator of persulfate for oxidation of dibutyl phthalate under neutral conditions, Chem. Eng. J. 301 (2016) 315-324.

[145] S. Kang, S. Liu, H. Wang, W. Cai, Enhanced degradation performances of plate-like micro/nanostructured zero valent iron to DDT, J. Hazard. Mater. 307 (2016) 145-153.

[146] M. Stefaniuk, P. Oleszczuk, Y.S. Ok, Review on nano zerovalent iron (nZVI): From synthesis to environmental applications, Chem. Eng. J. 287 (2016) 618-632.

[147] X.Y. Wang, Y. Du, H.L. Liu, J. Ma, Ascorbic acid/Fe-0 composites as an effective persulfate activator for improving the degradation of rhodamine B, Rsc Advances 8 (2018) 12791-12798.

[148] S. Machado, S.L. Pinto, J.P. Grosso, H.P.A. Nouws, J.T. Albergaria, C. Delerue-Matos, Green production of zero-valent iron nanoparticles using tree leaf extracts, Sci. Total Environ. 445-446 (2013) 1-8.

[149] C.P. Devatha, A.K. Thalla, S.Y. Katte, Green synthesis of iron nanoparticles using different leaf extracts for treatment of domestic waste water, J. Clean Prod. 139 (2016) 1425-1435.

[150] C.M. Liu, Z.H. Diao, W.Y. Huo, L.J. Kong, J.J. Du, Simultaneous removal of Cu2+ and bisphenol A by a novel biochar-supported zero valent iron from aqueous solution: Synthesis, reactivity and mechanism, Environ. Pollut. 239 (2018) 698-705.

[151] N. Yan, H. Zhong, M.L. Brusseau, The natural activation ability of subsurface media to promote in-situ chemical oxidation of 1,4-dioxane, Water Res. 149 (2019) 386-393.

[152] F. Sepyani, R.D.C. Soltani, S. Jorfi, H. Godini, M. Safari, Implementation of continuously electro-generated Fe3O4 nanoparticles for activation of persulfate to decompose amoxicillin antibiotic in aquatic media: UV254 and ultrasound intensification, J. Environ. Manage. 224 (2018) 315-326.

[153] J. Wang, C. Wang, S. Tong, A novel composite Fe-N/O catalyst for the effective enhancement of oxidative capacity of persulfate at ambient temperature, Catal. Commun. 103 (2018) 105-109.

[154] Y.S. Zhao, C. Sun, J.Q. Sun, R. Zhou, Kinetic modeling and efficiency of sulfate radical-based oxidation to remove p-nitroaniline from wastewater by persulfate/Fe3O4 nanoparticles process, Sep. Purif. Technol. 142 (2015) 182-188.

[155] X. Xue, K. Hanna, M. Abdelmoula, N. Deng, Adsorption and oxidation of PCP on the surface of magnetite: Kinetic experiments and spectroscopic investigations, Appl. Catal. B, Environ. 89 (2009) 432-440.

[156] R. Yin, J.L. Sun, Y.Y. Xiang, C.I. Shang, Recycling and reuse of rusted iron particles containing core-shell Fe-FeOOH for ibuprofen removal: Adsorption and persulfate-based advanced oxidation, J. Clean Prod. 178 (2018) 441-448.

[157] J. Weiss, The Free Radical Mechanism in the Reactions of Hydrogen peroxide, in: W.G. Frankenburg, V.I. Komarewsky, E.K. Rideal (Eds.) Advances in Catalysis, Academic Press1952, pp. 343-365.

[158] H. Lin, Y.T. Li, X.Y. Mao, H. Zhang, Electro-enhanced goethite activation of peroxydisulfate for the decolorization of Orange II at neutral pH: Efficiency, stability and mechanism, J. Taiwan Inst. Chem. Eng. 65 (2016) 390-398.

[159] R. Matta, K. Hanna, S. Chiron, Fenton-like oxidation of 2,4,6-trinitrotoluene using different iron minerals, Sci. Total Environ. 385 (2007) 242-251.

[160] Y.Q. Leng, W.L. Guo, X. Shi, Y.Y. Li, A.Q. Wang, F.F. Hao, L.T. Xing, Degradation of Rhodamine B by persulfate activated with Fe3O4: Effect of polyhydroquinone serving as an electron shuttle, Chem. Eng. J. 240 (2014) 338-343.

[161] H.L. Xie, Activation of persulfate by MMIOC for highly efficient degradation of rhodamine B, Rsc Advances 7 (2017) 45624-45633.

[162] H. Deng, X. Li, Q. Peng, X. Wang, J. Chen, Y. Li, Monodisperse magnetic single-crystal ferrite microspheres, Angewandte Chemie (International ed. in English) 44 (2005) 2782-2785.

[163] J.C. Yan, M. Lei, L.H. Zhu, M.N. Anjum, J. Zou, H.Q. Tang, Degradation of sulfamonomethoxine with Fe3O4 magnetic nanoparticles as heterogeneous activator of persulfate, J. Hazard. Mater. 186 (2011) 1398-1404.

[164] Q.L. Ma, X.Y. Zhang, R.N. Guo, H.X. Zhang, Q.F. Cheng, M.Z. Xie, X.W. Cheng, Persulfate activation by magnetic gamma-Fe2O3/Mn3O4 nanocomposites for degradation of organic pollutants, Sep. Purif. Technol. 210 (2019) 335-342.

[165] Y. Wu, R. Prulho, M. Brigante, W. Dong, K. Hanna, G. Mailhot, Activation of persulfate by Fe(III) species: Implications for 4-tert-butylphenol degradation, J. Hazard. Mater. 322 (2017) 380-386.

[166] W.P. Kwan, B.M. Voelker, Rates of Hydroxyl Radical Generation and Organic Compound Oxidation in Mineral-Catalyzed Fenton-like Systems,Environ. Sci. Technol. 37 (2003) 1150-1158.

[167] H. Dong, C. Zhang, J. Deng, Z. Jiang, L. Zhang, Y. Cheng, K. Hou, L. Tang, G. Zeng, Factors influencing degradation of trichloroethylene by sulfide-modified nanoscale zero-valent iron in aqueous solution, Water Res. 135 (2018) 1-10.

[168] E.C. Butler, K.F. Hayes, Factors influencing rates and products in the transformation of trichloroethylene by iron sulfide and iron metal, Environ. Sci. Technol. 35 (2001) 3884-3891.

[169] Y. Han, W. Yan, Reductive Dechlorination of Trichloroethene by Zero-valent Iron Nanoparticles: Reactivity Enhancement through Sulfidation Treatment,Environ. Sci. Technol. 50 (2016) 12992-13001.

[170] H.Y. Jeong, K. Anantharaman, Y.-S. Han, K.F. Hayes, Abiotic Reductive Dechlorination of cis-Dichloroethylene by Fe Species Formed during Iron- or Sulfate-Reduction,Environ. Sci. Technol. 45 (2011) 5186-5194.

[171] S.Y. Oh, S.G. Kang, D.W. Kim, P.C. Chiu, Degradation of 2,4-dinitrotoluene by persulfate activated with iron sulfides, Chem. Eng. J. 172 (2011) 641-646.

[172] Z. Yang, M. Kang, B. Ma, J. Xie, F. Chen, L. Charlet, C. Liu, Inhibition of U(VI) Reduction by Synthetic and Natural Pyrite,Environ. Sci. Technol. 48 (2014) 10716-10724.

[173] E.B. Hansson, M.S. Odziemkowski, R.W. Gillham, Formation of poorly crystalline iron monosulfides: Surface redox reactions on high purity iron, spectroelectrochemical studies, Corros. Sci. 48 (2006) 3767-3783.

[174] Y. Xie, D.M. Cwiertny, Use of Dithionite to Extend the Reactive Lifetime of Nanoscale Zero-Valent Iron Treatment Systems,Environ. Sci. Technol. 44 (2010) 8649-8655.

[175] E.-J. Kim, J.-H. Kim, A.-M. Azad, Y.-S. Chang, Facile Synthesis and Characterization of Fe/FeS Nanoparticles for Environmental Applications, ACS Appl. Mater. Interfaces 3 (2011) 1457-1462.

[176] D. Turcio-Ortega, D. Fan, P.G. Tratnyek, E.-J. Kim, Y.-S. Chang, Reactivity of Fe/FeS Nanoparticles: Electrolyte Composition Effects on Corrosion Electrochemistry,Environ. Sci. Technol. 46 (2012) 12484-12492.

[177] J. Li, X. Zhang, Y. Sun, L. Liang, B. Pan, W. Zhang, X. Guan, Advances in Sulfidation of Zerovalent Iron for Water Decontamination,Environ. Sci. Technol. 51 (2017) 13533-13544.

[178] H. Chen, Z. Zhang, Z. Yang, Q. Yang, B. Li, Z. Bai, Heterogeneous fenton-like catalytic degradation of 2,4-dichlorophenoxyacetic acid in water with FeS, Chem. Eng. J. 273 (2015) 481-489.

[179] J.L. Peng, J.F. Yan, Q.X. Chen, X. Jiang, G. Yao, B. Lai, Natural mackinawite catalytic ozonation for N, N-dimethylacetamide (DMAC) degradation in aqueous solution: Kinetic, performance, biotoxicity and mechanism, Chemosphere 210 (2018) 831-842.

[180] Y.M. Yuan, H. Tao, J.H. Fan, L.M. Ma, Degradation of p-chloroaniline by persulfate activated with ferrous sulfide ore particles, Chem. Eng. J. 268 (2015) 38-46.

[181] H. Chen, Z. Zhang, M. Feng, W. Liu, W. Wang, Q. Yang, Y. Hu, Degradation of 2,4-dichlorophenoxyacetic acid in water by persulfate activated with FeS (mackinawite), Chem. Eng. J. 313 (2017) 498-507.

[182] H.Y. Jeong, J.H. Lee, K.F. Hayes, Characterization of synthetic nanocrystalline mackinawite: Crystal structure, particle size, and specific surface area, Geochim. Cosmochim. Acta 72 (2008) 493-505.

[183] C. Liang, Y.-Y. Guo, Y.-C. Chien, Y.-J. Wu, Oxidative Degradation of MTBE by Pyrite-Activated Persulfate: Proposed Reaction Pathways, Ind. Eng. Chem. Res. 49 (2010) 8858-8864.

[184] Y. Zhang, H.P. Tran, X. Du, I. Hussain, S. Huang, S. Zhou, W. Wen, Efficient pyrite activating persulfate process for degradation of p-chloroaniline in aqueous systems: A mechanistic study, Chem. Eng. J. 308 (2017) 1112-1119.

[185] Y. Zhou, X. Wang, C. Zhu, D.D. Dionysiou, G. Zhao, G. Fang, D. Zhou, New insight into the mechanism of peroxymonosulfate activation by sulfur-containing minerals: Role of sulfur conversion in sulfate radical generation, Water Res. 142 (2018) 208-216.

[186] B.C. Wu, G.H. Gu, S. Deng, D.H. Liu, X.X. Xiong, Efficient natural pyrrhotite activating persulfate for the degradation of O-isopropyl-N-ethyl thionocarbamate: Iron recycle mechanism and degradation pathway, Chemosphere 224 (2019) 120-127.

[187] D. Xia, R. Yin, J. Sun, T. An, G. Li, W. Wang, H. Zhao, P.K. Wong, Natural magnetic pyrrhotite as a high-Efficient persulfate activator for micropollutants degradation: Radicals identification and toxicity evaluation, J. Hazard. Mater. 340 (2017) 435-444.

[188] D.H. Xia, Y. Li, G.C. Huang, R. Yin, T.C. An, G.Y. Li, H.J. Zhao, A.H. Lu, P.K. Wong, Activation of persulfates by natural magnetic pyrrhotite for water disinfection: Efficiency, mechanisms, and stability, Water Res. 112 (2017) 236-247.

[189] Y. Su, A.S. Adeleye, A.A. Keller, Y. Huang, C. Dai, X. Zhou, Y. Zhang, Magnetic sulfide-modified nanoscale zerovalent iron (S-nZVI) for dissolved metal ion removal, Water Res. 74 (2015) 47-57.

[190] M.J. Pu, Y.W. Ma, J.Q. Wan, Y. Wang, M.Z. Huang, Y.M. Chen, Fe/S doped granular activated carbon as a highly active heterogeneous persulfate catalyst toward the degradation of Orange G and diethyl phthalate, J. Colloid Interface Sci. 418 (2014) 330-337.

[191] A. Ghauch, A. Tuqan, Catalytic degradation of chlorothalonil in water using bimetallic iron-based systems, Chemosphere 73 (2008) 751-759.

[192] Y.C. Zhang, Q. Zhang, Z.Y. Dong, L.Y. Wu, J.M. Hong, Degradation of acetaminophen with ferrous/copperoxide activate persulfate: Synergism of iron and copper, Water Res. 146 (2018) 232-243.

[193] B.-W. Zhu, T.-T. Lim, Catalytic Reduction of Chlorobenzenes with Pd/Fe Nanoparticles: Reactive Sites, Catalyst Stability, Particle Aging, and Regeneration,Environ. Sci. Technol. 41 (2007) 7523-7529.

[194] Q.Q. Ji, J. Li, Z.K. Xiong, B. Lai, Enhanced reactivity of microscale Fe/Cu bimetallic particles (mFe/Cu) with persulfate (PS) for p-nitrophenol (PNP) removal in aqueous solution, Chemosphere 172 (2017) 10-20.

[195] Y. Li, D.H. Han, Y.J. Arai, X. Fu, X.Q. Li, W.L. Huang, Kinetics and mechanisms of debromination of tetrabromobisphenol A by Cu coated nano zerovalent iron, Chem. Eng. J. 373 (2019) 95-103.

[196] Y. Li, X. Li, Y. Xiao, C. Wei, D. Han, W. Huang, Catalytic debromination of tetrabromobisphenol A by Ni/nZVI bimetallic particles, Chem. Eng. J. 284 (2016) 1242-1250.

[197] X.M. Xu, D. Liu, W.M. Chen, S.Y. Zong, Y. Liu, Waste control by waste: efficient removal of bisphenol A with steel slag, a novel activator of peroxydisulfate, Environ. Chem. Lett. 16 (2018) 1435-

1440.

[198] M. Cheng, G. Zeng, D. Huang, C. Lai, Y. Liu, C. Zhang, J. Wan, L. Hu, C. Zhou, W. Xiong, Efficient degradation of sulfamethazine in simulated and real wastewater at slightly basic pH values using Co-SAM-SCS /H2O2 Fenton-like system, Water Res. 138 (2018) 7-18.

[199] M. Cheng, G. Zeng, D. Huang, C. Lai, Y. Liu, C. Zhang, R. Wang, L. Qin, W. Xue, B. Song, S. Ye, H. Yi, High adsorption of methylene blue by salicylic acid–methanol modified steel converter slag and evaluation of its mechanism, J. Colloid Interface Sci. 515 (2018) 232-239.

[200] Y. Liu, M. Cheng, Z. Liu, G. Zeng, H. Zhong, M. Chen, C. Zhou, W. Xiong, B. Shao, B. Song, Heterogeneous Fenton-like catalyst for treatment of rhamnolipid-solubilized hexadecane wastewater, Chemosphere 236 (2019) 124387.

[201] T.T. Tsai, C.M. Kao, J.Y. Wang, Remediation of TCE-contaminated groundwater using acid/BOF slag enhanced chemical oxidation, Chemosphere 83 (2011) 687-692.

[202] T.T. Tsai, C.M. Kao, A. Hong, Treatment of tetrachloroethylene-contaminated groundwater by surfactant-enhanced persulfate/BOF slag oxidation-A laboratory feasibility study, J. Hazard. Mater. 171 (2009) 571-576.

[203] H.J. Zhang, X.T. Liu, J. Ma, C.Y. Lin, C.D. Qi, X.W. Li, Z. Zhou, G.X. Fan, Activation of peroxymonosulfate using drinking water treatment residuals for the degradation of atrazine, J. Hazard. Mater. 344 (2018) 1220-1228.

[204] X.W. Li, X.T. Liu, C.Y. Lin, H.J. Zhang, Z. Zhou, G.X. Fan, J. Ma, Cobalt ferrite nanoparticles supported on drinking water treatment residuals: An efficient magnetic heterogeneous catalyst to activate peroxymonosulfate for the degradation of atrazine, Chem. Eng. J. 367 (2019) 208-218.

[205] J.C. Yan, W.G. Gao, M.G. Dong, L. Han, L.B. Qian, C.P. Nathanail, M.F. Chen, Degradation of trichloroethylene by activated persulfate using a reduced graphene oxide supported magnetite nanoparticle, Chem. Eng. J. 295 (2016) 309-316.

[206] X. Dong, B. Ren, Z. Sun, C. Li, X. Zhang, M. Kong, S. Zheng, D.D. Dionysiou, Monodispersed CuFe2O4 nanoparticles anchored on natural kaolinite as highly efficient peroxymonosulfate catalyst for bisphenol A degradation, Appl. Catal. B, Environ. 253 (2019) 206-217.

[207] M.Q. Li, R. Luo, C.H. Wang, M. Zhang, W.X. Zhang, P.K. Klu, Y.B. Yan, J.W. Qi, X.Y. Sun, L.J. Wang, J.S. Li, Iron-tannic modified cotton derived Fe-0/graphitized carbon with enhanced catalytic activity for bisphenol A degradation, Chem. Eng. J. 372 (2019) 774-784.

[208] Y.W. Wu, X.T. Chen, Y. Han, D.T. Yue, X.D. Cao, Y.X. Zhao, X.F. Qian, Highly Efficient Utilization of Nano-Fe(0) Embedded in Mesoporous Carbon for Activation of Peroxydisulfate,Environ. Sci. Technol. 53 (2019) 9081-9090.

[209] A. Nadar, A.M. Banerjee, M.R. Pai, R.V. Pai, S.S. Meena, R. Tewari, A.K. Tripathi, Catalytic properties of dispersed iron oxides Fe2O3/MO2 (M = Zr, Ce, Ti and Si) for sulfuric acid decomposition reaction: Role of support, Int. J. Hydrogen Energy 43 (2018) 37-52.

[210] P. Sathishkumar, N. Pugazhenthiran, R.V. Mangalaraja, A.M. Asiri, S. Anandan, ZnO supported

CoFe2O4 nanophotocatalysts for the mineralization of Direct Blue 71 in aqueous environments, J. Hazard. Mater. 252-253 (2013) 171-179.

[211] C.X. Wang, J.Q. Wan, Y.W. Ma, Y. Wang, Insights into the synergy of zero-valent iron and copper oxide in persulfate oxidation of Orange G solutions, Res. Chem. Intermed. 42 (2016) 481-497.

[212] Q. Wang, Y. Shao, N. Gao, W. Chu, J. Chen, X. Lu, Y. Zhu, N. An, Activation of peroxymonosulfate by Al 2 O 3 -based CoFe 2 O 4 for the degradation of sulfachloropyridazine sodium: Kinetics and mechanism, Sep. Purif. Technol. 189 (2017) 176-185.

[213] S.H. Do, Y.J. Kwon, S.J. Bang, S.H. Kong, Persulfate reactivity enhanced by Fe2O3-MnO and CaO-Fe2O3-MnO composite: Identification of composite and degradation of CCl4 at various levels of pH, Chem. Eng. J. 221 (2013) 72-80.

[214] A. Nadar, A.M. Banerjee, M.R. Pai, S.S. Meena, R.V. Pai, R. Tewari, S.M. Yusuf, A.K. Tripathi, S.R. Bharadwaj, Nanostructured Fe2O3 dispersed on SiO2 as catalyst for high temperature sulfuric acid decomposition—Structural and morphological modifications on catalytic use and relevance of Fe2O3-SiO2 interactions, Appl. Catal. B, Environ. 217 (2017) 154-168.

[215] R. Djellabi, M.F. Ghorab, T. Sehili, Simultaneous Removal of Methylene Blue and Hexavalent Chromium From Water Using TiO2/Fe(III)/H2O2/Sunlight, CLEAN – Soil, Air, Water 45 (2017) 1500379.

[216] A. Tsiampalis, Z. Frontistis, V. Binas, G. Kiriakidis, D. Mantzavinos, Degradation of Sulfamethoxazole Using Iron-Doped Titania and Simulated Solar Radiation, Catalysts 9 (2019) 16.

[217] H. Měšťánková, J. Krýsa, J. Jirkovský, G. Mailhot, M. Bolte, The influence of Fe(III) speciation on supported TiO2 efficiency: example of monuron photocatalytic degradation, Appl. Catal. B, Environ. 58 (2005) 185-191.

[218] M.M. Mohamed, W.A. Bayoumy, M.E. Goher, M.H. Abdo, T.Y. Mansour El-Ashkar, Optimization of α-Fe2O3@Fe3O4 incorporated N-TiO2 as super effective photocatalysts under visible light irradiation, Appl. Surf. Sci. 412 (2017) 668-682.

[219] X. Li, J. Wang, A.I. Rykov, V.K. Sharma, H. Wei, C. Jin, X. Liu, M. Li, S. Yu, C. Sun, D.D. Dionysiou, Prussian blue/TiO2 nanocomposites as a heterogeneous photo-Fenton catalyst for degradation of organic pollutants in water, Catal. Sci. Technol. 5 (2015) 504-514.

[220] F. Mazille, T. Schoettl, C. Pulgarin, Synergistic effect of TiO2 and iron oxide supported on fluorocarbon films. Part 1: Effect of preparation parameters on photocatalytic degradation of organic pollutant at neutral pH, Appl. Catal. B, Environ. 89 (2009) 635-644.

[221] D.M. Yun, H.H. Cho, J.W. Jang, J.W. Park, Nano zero-valent iron impregnated on titanium dioxide nanotube array film for both oxidation and reduction of methyl orange, Water Res. 47 (2013) 1858-1866.

[222] N. Banić, B. Abramović, J. Krstić, D. Šojić, D. Lončarević, Z. Cherkezova-Zheleva, V. Guzsvány, Photodegradation of thiacloprid using Fe/TiO2 as a heterogeneous photo-Fenton catalyst, Appl. Catal. B, Environ. 107 (2011) 363-371.

[223] C.M. Baerlocher, L. B., http://www.iza-structure.org/databases/.

[224] J. Yu, R. Xu, Rational Approaches toward the Design and Synthesis of Zeolitic Inorganic Open-Framework Materials, Acc. Chem. Res. 43 (2010) 1195-1204.

[225] J. Grand, S.N. Talapaneni, A. Vicente, C. Fernandez, E. Dib, H.A. Aleksandrov, G.N. Vayssilov, R. Retoux, P. Boullay, J.-P. Gilson, V. Valtchev, S. Mintova, One-pot synthesis of silanol-free nanosized MFI zeolite, Nature Materials 16 (2017) 1010.

[226] M. Choi, K. Na, J. Kim, Y. Sakamoto, O. Terasaki, R. Ryoo, Stable single-unit-cell nanosheets of zeolite MFI as active and long-lived catalysts, 2009.

[227] Y. Zhao, B. Yuan, Z. Zheng, R. Hao, Removal of multi-pollutant from flue gas utilizing ammonium persulfate solution catalyzed by Fe/ZSM-5, J. Hazard. Mater. 362 (2019) 266-274.

[228] A. Vinu, D.P. Sawant, K. Ariga, K.Z. Hossain, S.B. Halligudi, M. Hartmann, M. Nomura, Direct Synthesis of Well-Ordered and Unusually Reactive FeSBA-15 Mesoporous Molecular Sieves, Chem. Mater. 17 (2005) 5339-5345.

[229] C.T. Kresge, M.E. Leonowicz, W.J. Roth, J.C. Vartuli, J.S. Beck, Ordered mesoporous molecular sieves synthesized by a liquid-crystal template mechanism, Nature 359 (1992) 710-712.

[230] L.X. Hu, X.P. Yang, S.T. Dang, An easily recyclable Co/SBA-15 catalyst: Heterogeneous activation of peroxymonosulfate for the degradation of phenol in water, Appl. Catal. B-Environ. 102 (2011) 19-26.

[231] A.R. Martins, A.B. Salviano, A.A.S. Oliveira, R.V. Mambrini, F.C.C. Moura, Synthesis and characterization of catalysts based on mesoporous silica partially hydrophobized for technological applications, Environ. Sci. Pollut. Res. 24 (2017) 5991-6001.

[232] F. Qi, W. Chu, B.B. Xu, Catalytic degradation of caffeine in aqueous solutions by cobalt-MCM41 activation of peroxymonosulfate, Appl. Catal. B-Environ. 134 (2013) 324-332.

[233] C. Cai, Z.Y. Zhang, H. Zhang, Electro-assisted heterogeneous activation of persulfate by Fe/SBA-15 for the degradation of Orange II, J. Hazard. Mater. 313 (2016) 209-218.

[234] A. Sayari, Catalysis by crystalline mesoporous molecular sieves, Chem. Mater. 8 (1996) 1840-1852.

[235] I. Ursachi, A. Stancu, A. Vasile, Magnetic alpha-Fe2O3/MCM-41 nanocomposites: Preparation, characterization, and catalytic activity for methylene blue degradation, J. Colloid Interface Sci. 377 (2012) 184-190.

[236] C. Cai, H. Zhang, X. Zhong, L. Hou, Electrochemical enhanced heterogeneous activation of peroxydisulfate by Fe–Co/SBA-15 catalyst for the degradation of Orange II in water, Water Res. 66 (2014) 473-485.

[237] I. Mazilu, C. Ciotonea, A. Chirieac, B. Dragoi, C. Catrinescu, A. Ungureanu, S. Petit, S. Royer, E. Dumitriu, Synthesis of highly dispersed iron species within mesoporous (Al-) SBA-15 silica as efficient heterogeneous Fenton-type catalysts, Microporous Mesoporous Mater. 241 (2017) 326-337.

[238] A. Vinu, K.U. Nandhini, V. Murugesan, W. Bohlmann, V. Umamaheswari, A. Poppl, M. Hartmann,

Mesoporous FeAlMCM-41: an improved catalyst for the vapor phase tert-butylation of phenol, Appl. Catal. A-Gen. 265 (2004) 1-10.

[239] V.R. Elias, M.I. Oliva, S.E. Urreta, S.P. Silvetti, K. Sapag, A.M.M. Navarro, S.G. Casuscelli, G.A. Eimer, Magnetic properties and catalytic performance of iron-containing mesoporous molecular sieves, Appl. Catal. A-Gen. 381 (2010) 92-100.

[240] S.V. Sirotin, I.F. Moskovskaya, B.V. Romanovsky, Synthetic strategy for Fe-MCM-41 catalyst: a key factor for homogeneous or heterogeneous phenol oxidation, Catal. Sci. Technol. 1 (2011) 971-980.

[241] X.H. Zhao, Z.P. Sun, Z.Q. Zhu, A. Li, G.X. Li, X.L. Wang, Evaluation of Iron-Containing Aluminophosphate Molecular Sieve Catalysts Prepared by Different Methods for Phenol Hydroxylation, Catal. Lett. 143 (2013) 657-665.

[242] A.C. Oliveira, N. Essayem, A. Tuel, J.M. Clacens, Y. Taarit, Structural, acidic and catalytic features of transition metal-containing molecular sieves in the transformation of C-4 hydrocarbon, Appl. Catal. A-Gen. 382 (2010) 10-20.

[243] H. Lin, X. Zhong, C. Ciotonea, X.H. Fan, X.Y. Mao, Y.T. Li, B. Deng, H. Zhang, S. Royer, Efficient degradation of clofibric acid by electro-enhanced peroxydisulfate activation with Fe-Cu/SBA-15 catalyst, Appl. Catal. B-Environ. 230 (2018) 1-10.

[244] J.Y. Huang, S.P. Yi, C.M. Zheng, I.M.C. Lo, Persulfate activation by natural zeolite supported nanoscale zero-valent iron for trichloroethylene degradation in groundwater, Sci. Total Environ. 684 (2019) 351-359.

[245] R. Kohn, D. Paneva, M. Dimitrov, T. Tsoncheva, I. Mitov, C. Minchev, M. Froba, Studies on the state of iron oxide nanoparticles in MCM-41 and MCM-48 silica materials, Microporous Mesoporous Mater. 63 (2003) 125-137.

[246] Y.M. Liu, J. Xu, L. He, Y. Cao, H.Y. He, D.Y. Zhao, J.H. Zhuang, K.N. Fan, Facile Synthesis of Fe-Loaded Mesoporous Silica by a Combined Detemplation-Incorporation Process through Fenton's Chemistry, Journal of Physical Chemistry C 112 (2008) 16575-16583.

[247] B. Shao, Z. Liu, G. Zeng, Y. Liu, X. Yang, C. Zhou, M. Chen, Y. Liu, Y. Jiang, M. Yan, Immobilization of laccase on hollow mesoporous carbon nanospheres: Noteworthy immobilization, excellent stability and efficacious for antibiotic contaminants removal, J. Hazard. Mater. 362 (2019) 318-326.

[248] B. Shao, X. Liu, Z. Liu, G. Zeng, W. Zhang, Q. Liang, Y. Liu, Q. He, X. Yuan, D. Wang, S. Luo, S. Gong, Synthesis and characterization of 2D/0D g-C3N4/CdS-nitrogen doped hollow carbon spheres (NHCs) composites with enhanced visible light photodegradation activity for antibiotic, Chem. Eng. J. 374 (2019) 479-493.

[249] R.Y. Xiao, Z.H. Luo, Z.S. Wei, S. Luo, R. Spinney, W.C. Yang, D.D. Dionysiou, Activation of peroxymonosulfate/persulfate by nanomaterials for sulfate radical-based advanced oxidation technologies, Curr. Opin. Chem. Eng. 19 (2018) 51-58.

[250] R. Khaghani, B. Kakavandi, K. Ghadirinejad, E.D. Fard, A. Asadi, Preparation, characterization

and catalytic potential of gamma-Fe2O3@AC mesoporous heterojunction for activation of peroxymonosulfate into degradation of cyfluthrin insecticide, Microporous Mesoporous Mater. 284 (2019) 111-121.

[251] J.J. Wang, Y.L. Ding, S.P. Tong, Fe-Ag/GAC catalytic persulfate to degrade Acid Red 73, Sep. Purif. Technol. 184 (2017) 365-373.

[252] M.C.F. Soares, M.M. Viana, Z.L. Schaefer, V.S. Gangoli, Y. Cheng, V. Caliman, M.S. Wong, G.G. Silva, Surface modification of carbon black nanoparticles by dodecylamine: Thermal stability and phase transfer in brine medium, Carbon 72 (2014) 287-295.

[253] C.D. Dong, M.L. Tsai, C.W. Chen, C.M. Hung, Heterogeneous persulfate oxidation of BTEX and MTBE using Fe3O4-CB magnetite composites and the cytotoxicity of degradation products, Int. Biodeterior. Biodegrad. 124 (2017) 109-118.

[254] Z. Wan, J.L. Wang, Degradation of sulfamethazine using Fe3O4-Mn3O4/reduced graphene oxide hybrid as Fenton-like catalyst, J. Hazard. Mater. 324 (2017) 653-664.

[255] U. Farooq, M. Danish, S.G. Lyu, M.L. Brusseau, M.B. Gu, W.Q. Zaman, Z.F. Qiu, Q. Sui, The impact of surface properties and dominant ions on the effectiveness of G-nZVI heterogeneous catalyst for environmental remediation, Sci. Total Environ. 651 (2019) 1182-1188.

[256] S.H. Wu, H.J. He, X. Li, C.P. Yang, G.M. Zeng, B. Wu, S.Y. He, L. Lu, Insights into atrazine degradation by persulfate activation using composite of nanoscale zero-valent iron and graphene: Performances and mechanisms, Chem. Eng. J. 341 (2018) 126-136.

[257] U. Farooq, M. Danish, S. Lu, M. Naqvi, Z.F. Qiu, Q. Sui, A step forward towards synthesizing a stable and regeneratable nanocomposite for remediation of trichloroethene, Chem. Eng. J. 347 (2018) 660-668.

[258] M.B. Gu, U. Farooq, S.G. Lu, X. Zhang, Z.F. Qiu, Q. Sui, Degradation of trichloroethylene in aqueous solution by rGO supported nZVI catalyst under several oxic environments, J. Hazard. Mater. 349 (2018) 35-44.

[259] C.M. Park, J. Heo, D.J. Wang, C.M. Su, Y. Yoon, Heterogeneous activation of persulfate by reduced graphene oxide-elemental silver/magnetite nanohybrids for the oxidative degradation of pharmaceuticals and endocrine disrupting compounds in water, Appl. Catal. B-Environ. 225 (2018) 91-99.

[260] C.D. Dong, C.W. Chen, C.M. Hung, Synthesis of magnetic biochar from bamboo biomass to activate persulfate for the removal of polycyclic aromatic hydrocarbons in marine sediments, Bioresour. Technol. 245 (2017) 188-195.

[261] J.C. Yan, L. Han, W.G. Gao, S. Xue, M.F. Chen, Biochar supported nanoscale zerovalent iron composite used as persulfate activator for removing trichloroethylene, Bioresour. Technol. 175 (2015) 269-274.

[262] D. Ouyang, J.C. Yan, L.B. Qian, Y. Chen, L. Han, A.Q. Su, W.Y. Zhang, H. Ni, M.F. Chen, Degradation of 1,4-dioxane by biochar supported nano magnetite particles activating persulfate,

Chemosphere 184 (2017) 609-617.

[263] H.Y. Luo, Q.T. Lin, X.F. Zhang, Z.F. Huang, S.S. Liu, J.R. Jiang, R.B. Xiao, X.Y. Liao, New insights into the formation and transformation of active species in nZVI/BC activated persulfate in alkaline solutions, Chem. Eng. J. 359 (2019) 1215-1223.

[264] M. Cheng, Y. Liu, D. Huang, C. Lai, G. Zeng, J. Huang, Z. Liu, C. Zhang, C. Zhou, L. Qin, W. Xiong, H. Yi, Y. Yang, Prussian blue analogue derived magnetic Cu-Fe oxide as a recyclable photo-Fenton catalyst for the efficient removal of sulfamethazine at near neutral pH values, Chem. Eng. J. 362 (2019) 865-876.

[265] Y. Liu, Z. Liu, D. Huang, M. Cheng, G. Zeng, C. Lai, C. Zhang, C. Zhou, W. Wang, D. Jiang, H. Wang, B. Shao, Metal or metal-containing nanoparticle@MOF nanocomposites as a promising type of photocatalyst, Coord. Chem. Rev. 388 (2019) 63-78.

[266] B. Van de Voorde, B. Bueken, J. Denayer, D. De Vos, Adsorptive separation on metal–organic frameworks in the liquid phase, Chem. Soc. Rev. 43 (2014) 5766-5788.

[267] Y. Bai, G.-j. He, Y.-g. Zhao, C.-y. Duan, D.-b. Dang, Q.-j. Meng, Porous material for absorption and luminescent detection of aromatic molecules in water, Chem. Commun. (2006) 1530-1532.

[268] N.L. Rosi, J. Eckert, M. Eddaoudi, D.T. Vodak, J. Kim, M. Keeffe, O.M. Yaghi, Hydrogen Storage in Microporous Metal-Organic Frameworks, Science 300 (2003) 1127.

[269] T. Zhang, W. Lin, Metal–organic frameworks for artificial photosynthesis and photocatalysis, Chem. Soc. Rev. 43 (2014) 5982-5993.

[270] M.J. Pu, Z.Y. Guan, Y.W. Ma, J.Q. Wan, Y. Wang, M.L. Brusseau, H.Y. Chi, Synthesis of iron-based metal-organic framework MIL-53 as an efficient catalyst to activate persulfate for the degradation of Orange G in aqueous solution, Appl. Catal. A-Gen. 549 (2018) 82-92.

[271] X.X. Yue, W.L. Guo, X.H. Li, H.H. Zhou, R.Q. Wang, Core-shell Fe3O4@MIL-101(Fe) composites as heterogeneous catalysts of persulfate activation for the removal of Acid Orange 7, Environ. Sci. Pollut. Res. 23 (2016) 15218-15226.

[272] M.-W. Zhang, M.-T. Yang, S. Tong, K.-Y.A. Lin, Ferrocene-modified iron-based metal-organic frameworks as an enhanced catalyst for activating oxone to degrade pollutants in water, Chemosphere 213 (2018) 295-304.

[273] K.Y.A. Lin, F.K. Hsu, Magnetic iron/carbon nanorods derived from a metal organic framework as an efficient heterogeneous catalyst for the chemical oxidation process in water, Rsc Advances 5 (2015) 50790-50800.

[274] C. Liu, Y.P. Wang, Y.T. Zhang, R.Y. Li, W.D. Meng, Z.L. Song, F. Qi, B.B. Xu, W. Chu, D.H. Yuan, B. Yu, Enhancement of Fe@porous carbon to be an efficient mediator for peroxymonosulfate activation for oxidation of organic contaminants: Incorporation NH2-group into structure of its MOF precursor, Chem. Eng. J. 354 (2018) 835-848.

[275] T. Zeng, M.D. Yu, H.Y. Zhang, Z.Q. He, J.M. Chen, S. Song, Fe/Fe3C@N-doped porous carbon hybrids derived from nano-scale MOFs: robust and enhanced heterogeneous catalyst for

peroxymonosulfate activation, Catal. Sci. Technol. 7 (2017) 396-404.

[276] C. Liu, L.Y. Liu, X. Tian, Y.P. Wang, R.Y. Li, Y.T. Zhang, Z.L. Song, B.B. Xu, W. Chu, F. Qi, A. Ikhlaq, Coupling metal-organic frameworks and g-C3N4 to derive Fe@N-doped graphene-like carbon for peroxymonosulfate activation: Upgrading framework stability and performance, Appl. Catal. B-Environ. 255 (2019) 11.

[277] C.H. Weng, K.L. Tsai, Ultrasound and heat enhanced persulfate oxidation activated with Fe-0 aggregate for the decolorization of CI Direct Red 23, Ultrason. Sonochem. 29 (2016) 11-18.

[278] A. Kamal, S.F. Adil, M. Arifuddin, Ultrasonic activated efficient method for the cleavage of epoxides with aromatic amines, Ultrason. Sonochem. 12 (2005) 429-431.

[279] R. Yin, W. Guo, H. Wang, J. Du, X. Zhou, Q. Wu, H. Zheng, J. Chang, N. Ren, Enhanced peroxymonosulfate activation for sulfamethazine degradation by ultrasound irradiation: Performances and mechanisms, Chem. Eng. J. 335 (2018) 145-153.

[280] X.L. Zou, T. Zhou, J. Mao, X.H. Wu, Synergistic degradation of antibiotic sulfadiazine in a heterogeneous ultrasound-enhanced Fe-0/persulfate Fenton-like system, Chem. Eng. J. 257 (2014) 36-44.

[281] A.J. Exposito, J.M. Monteagudo, I. Diaz, A. Duran, Photo-fenton degradation of a beverage industrial effluent: Intensification with persulfate and the study of radicals, Chem. Eng. J. 306 (2016) 1203-1211.

[282] S.G. Babu, P. Aparna, G. Satishkumar, M. Ashokkumar, B. Neppolian, Ultrasound-assisted mineralization of organic contaminants using a recyclable LaFeO3 and Fe3+/persulfate Fenton-like system, Ultrason. Sonochem. 34 (2017) 924-930.

[283] J. Liu, J.H. Zhou, Z.X. Ding, Z.W. Zhao, X. Xu, Z.D. Fang, Ultrasound irritation enhanced heterogeneous activation of peroxymonosulfate with Fe3O4 for degradation of azo dye, Ultrason. Sonochem. 34 (2017) 953-959.

[284] Y.X. Pang, Y. Ruan, Y. Feng, Z.H. Diao, K.M. Shih, L.A. Hou, D.Y. Chen, L.J. Kong, Ultrasound assisted zero valent iron corrosion for peroxymonosulfate activation for Rhodamine-B degradation, Chemosphere 228 (2019) 412-417.

[285] O. Hamdaoui, Intensification of the sorption of Rhodamine B from aqueous phase by loquat seeds using ultrasound, Desalination 271 (2011) 279-286.

[286] Y.Q. Gao, N.Y. Gao, W. Wang, S.F. Kang, J.H. Xu, H.M. Xiang, D.Q. Yin, Ultrasound-assisted heterogeneous activation of persulfate by nano zero-valent iron (nZVI) for the propranolol degradation in water, Ultrason. Sonochem. 49 (2018) 33-40.

[287] X. Wang, L.G. Wang, J.B. Li, J.J. Qiu, C. Cai, H. Zhang, Degradation of Acid Orange 7 by persulfate activated with zero valent iron in the presence of ultrasonic irradiation, Sep. Purif. Technol. 122 (2014) 41-46.

[288] Y.W. Pan, Y. Zhang, M.H. Zhou, J.J. Cai, X. Li, Y.S. Tian, Synergistic degradation of antibiotic sulfamethazine by novel pre-magnetized Fe-0/PS process enhanced by ultrasound, Chem. Eng. J. 354

(2018) 777-789.

[289] Y.R. Wang, W. Chu, Degradation of 2,4,5-trichlorophenoxyacetic acid by a novel Electro-Fe(II)/Oxone process using iron sheet as the sacrificial anode, Water Res. 45 (2011) 3883-3889.

[290] L.L. Zhang, H.K. Ma, X.M. Huang, Z.X. Yan, W. Ding, Z.F. Li, D.Q. Cang, Fast and efficient inactivation of antibiotic resistant Escherichia coli by iron electrode-activated sodium peroxydisulfate in a galvanic cell, Chem. Eng. J. 355 (2019) 150-158.

[291] Z. Liu, H. Ding, C. Zhao, T. Wang, P. Wang, D.D. Dionysiou, Electrochemical activation of peroxymonosulfate with ACF cathode: Kinetics, influencing factors, mechanism, and application potential, Water Res. 159 (2019) 111-121.

[292] J. Li, J.F. Yan, G. Yao, Y.H. Zhang, X. Li, B. Lai, Improving the degradation of atrazine in the three-dimensional (3D) electrochemical process using CuFe2O4 as both particle electrode and catalyst for persulfate activation, Chem. Eng. J. 361 (2019) 1317-1332.

[293] S.D. Yan, X.P. Zhang, H. Zhang, Persulfate activation by Fe(III) with bioelectricity at acidic and near-neutral pH regimes: Homogeneous versus heterogeneous mechanism, J. Hazard. Mater. 374 (2019) 92-100.

[294] M. Arellano, M.A. Sanroman, M. Pazos, Electro-assisted activation of peroxymonosulfate by iron-based minerals for the degradation of 1-butyl-1-methylpyrrolidinium chloride, Sep. Purif. Technol. 208 (2019) 34-41.

[295] J.S. Du, W.Q. Guo, D. Che, N.Q. Ren, Weak magnetic field for enhanced oxidation of sulfamethoxazole by Fe-0/ H2O2 and Fe-0/persulfate: Performance, mechanisms, and degradation pathways, Chem. Eng. J. 351 (2018) 532-539.

[296] X.M. Xiong, B. Sun, J. Zhang, N.Y. Gao, J.M. Shen, J.L. Li, X.H. Guan, Activating persulfate by Fe-0 coupling with weak magnetic field: Performance and mechanism, Water Res. 62 (2014) 53-62.

[297] Y.W. Pan, M.H. Zhou, Y. Zhang, J.J. Cai, B. Li, X.J. Sheng, Enhanced degradation of Rhodamine B by pre-magnetized Fe-0/PS process: Parameters optimization, mechanism and interferences of ions, Sep. Purif. Technol. 203 (2018) 66-74.

[298] N.S. Zaidi, J. Sohaili, K. Muda, M. Sillanpää, Magnetic Field Application and its Potential in Water and Wastewater Treatment Systems, Separation & Purification Reviews 43 (2014) 206-240.

[299] G.P. Anipsitakis, D.D. Dionysiou, Transition metal/UV-based advanced oxidation technologies for water decontamination, Appl. Catal. B-Environ. 54 (2004) 155-163.

[300] Y.F. Huang, Y.H. Huang, Identification of produced powerful radicals involved in the mineralization of bisphenol A using a novel UV-Na2S2O8/H2O2-Fe(II,III) two-stage oxidation process, J. Hazard. Mater. 162 (2009) 1211-1216.

[301] C.A.L. Graca, A.C. de Velosa, A. Teixeira, Amicarbazone degradation by UVA-activated persulfate in the presence of hydrogen peroxide or Fe2+, Catal. Today 280 (2017) 80-85.

[302] J. Rodríguez-Chueca, S. Guerra-Rodríguez, J.M. Raez, M.-J. López-Muñoz, E. Rodríguez,

Assessment of different iron species as activators of S2O82- and HSO5- for inactivation of wild bacteria strains, Appl. Catal. B, Environ. 248 (2019) 54-61.

[303] P. Avetta, A. Pensato, M. Minella, M. Malandrino, V. Maurino, C. Minero, K. Hanna, D. Vione, Activation of Persulfate by Irradiated Magnetite: Implications for the Degradation of Phenol under Heterogeneous Photo-Fenton-Like Conditions,Environ. Sci. Technol. 49 (2015) 1043-1050.

[304] X.N. Wang, W.B. Dong, M. Brigante, G. Mailhot, Hydroxyl and sulfate radicals activated by Fe(III)-EDDS/UV: Comparison of their degradation efficiencies and influence of critical parameters, Appl. Catal. B-Environ. 245 (2019) 271-278.

[305] J.M. Zhang, H.R. Song, Y.L. Liu, L. Wang, D. Li, C. Liu, M.Y. Gong, Z.X. Zhang, T. Yang, J. Ma, Remarkable enhancement of a photochemical Fenton-like system (UV-A/Fe (II)/PMS) at near-neutral pH and low Fe(II)/peroxymonosulfate ratio by three alpha hydroxy acids: Mechanisms and influencing factors, Sep. Purif. Technol. 224 (2019) 142-151.

[306] B. Kaur, L. Kuntus, P. Tikker, E. Kattel, M. Trapido, N. Dulova, Photo-induced oxidation of ceftriaxone by persulfate in the presence of iron oxides, Sci. Total Environ. 676 (2019) 165-175.

[307] A. Bianco, M.I. Polo-Lopez, P. Fernandez-Ibanez, M. Brigante, G. Mailhot, Disinfection of water inoculated with Enterococcus faecalis using solar/Fe(III)EDDS-H2O2 or S2O82- process, Water Res. 118 (2017) 249-260.

[308] Q. Liang, X. Liu, G. Zeng, Z. Liu, L. Tang, B. Shao, Z. Zeng, W. Zhang, Y. Liu, M. Cheng, W. Tang, S. Gong, Surfactant-assisted synthesis of photocatalysts: Mechanism, synthesis, recent advances and environmental application, Chem. Eng. J. 372 (2019) 429-451.

[309] W.L. Bi, Y.L. Wu, X.N. Wang, P.P. Zhai, W.B. Dong, Degradation of oxytetracycline with SO4 center dot- under simulated solar light, Chem. Eng. J. 302 (2016) 811-818.

[310] M.M. Ahmed, S. Chiron, Solar photo-Fenton like using persulphate for carbamazepine removal from domestic wastewater, Water Res. 48 (2014) 229-236.

[311] S. Miralles-Cuevas, I. Oller, A. Ruiz-Delgado, A. Cabrera-Reina, L. Cornejo-Ponce, S. Malato, EDDS as complexing agent for enhancing solar advanced oxidation processes in natural water: Effect of iron species and different oxidants, J. Hazard. Mater. 372 (2019) 129-136.

[312] J.E. Silveira, W.S. Paz, P. Garcia-Munoz, J.A. Zazo, J.A. Casas, UV-LED/ilmenite/persulfate for azo dye mineralization: The role of sulfate in the catalyst deactivation, Appl. Catal. B-Environ. 219 (2017) 314-321.

[313] B. Shao, X. Liu, Z. Liu, G. Zeng, Q. Liang, C. Liang, Y. Cheng, W. Zhang, Y. Liu, S. Gong, A novel double Z-scheme photocatalyst Ag3PO4/Bi2S3/Bi2O3 with enhanced visible-light photocatalytic performance for antibiotic degradation, Chem. Eng. J. 368 (2019) 730-745.

[314] Y.W. Gao, Z.Y. Zhang, S.M. Li, J. Liu, L.Y. Yao, Y.X. Li, H. Zhang, Insights into the mechanism of heterogeneous activation of persulfate with a clay/iron-based catalyst under visible LED light irradiation, Appl. Catal. B-Environ. 185 (2016) 22-30.

[315] Y.W. Gao, S.M. Li, Y.X. Li, L.Y. Yao, H. Zhang, Accelerated photocatalytic degradation of

organic pollutant over metal-organic framework MIL-53(Fe) under visible LED light mediated by persulfate, Appl. Catal. B-Environ. 202 (2017) 165-174.

[316] H. Hu, H.X. Zhang, Y. Chen, Y.J. Chen, L. Zhuang, H.S. Ou, Enhanced photocatalysis degradation of organophosphorus flame retardant using MIL-101(Fe)/persulfate: Effect of irradiation wavelength and real water matrixes, Chem. Eng. J. 368 (2019) 273-284.

[317] G. Zhang, Z. Wu, H.J. Liu, Q.H. Ji, J.H. Qu, J.H. Li, Photoactuation Healing of alpha-FeOOH@g-C3N4 Catalyst for Efficient and Stable Activation of Persulfate, Small 13 (2017) 8.

[318] S.D. Yan, Y. Shi, Y.F. Tao, H. Zhang, Enhanced persulfate-mediated photocatalytic oxidation of bisphenol A using bioelectricity and a g-C3N4/Fe2O3 heterojunction, Chem. Eng. J. 359 (2019) 933-943.

[319] L. Zhao, H. Hou, A. Fujii, M. Hosomi, F.S. Li, Degradation of 1,4-dioxane in water with heat- and Fe2+-activated persulfate oxidation, Environ. Sci. Pollut. Res. 21 (2014) 7457-7465.

[320] K.Y.A. Lin, B.J. Chen, Prussian blue analogue derived magnetic carbon/cobalt/iron nanocomposite as an efficient and recyclable catalyst for activation of peroxymonosulfate, Chemosphere 166 (2017) 146-156.

[321] C. Liang, Z.-S. Wang, C.J. Bruell, Influence of pH on persulfate oxidation of TCE at ambient temperatures, Chemosphere 66 (2007) 106-113.

[322] M.J. Xu, J. Li, Y. Yan, X.G. Zhao, J.F. Yan, Y.H. Zhang, B. Lai, X. Chen, L.P. Song, Catalytic degradation of sulfamethoxazole through peroxymonosulfate activated with expanded graphite loaded CoFe2O4 particles, Chem. Eng. J. 369 (2019) 403-413.

[323] A. Stefánsson, Iron(III) Hydrolysis and Solubility at 25 °C,Environ. Sci. Technol. 41 (2007) 6117-6123.

[324] H.X. Liu, J.Y. Yao, L.H. Wang, X.H. Wang, R.J. Qu, Z.Y. Wang, Effective degradation of fenitrothion by zero-valent iron powder (Fe-0) activated persulfate in aqueous solution: Kinetic study and product identification, Chem. Eng. J. 358 (2019) 1479-1488.

[325] S. Sahinkaya, E. Kalipci, S. Aras, Disintegration of waste activated sludge by different applications of Fenton process, Process Saf. Environ. Protect. 93 (2015) 274-281.

[326] M. Li, X.F. Yang, D.S. Wang, J. Yuan, Enhanced oxidation of erythromycin by persulfate activated iron powder-H2O2 system: Role of the surface Fe species and synergistic effect of hydroxyl and sulfate radicals, Chem. Eng. J. 317 (2017) 103-111.

[327] A.L. Li, Z.H. Wu, T.T. Wang, S.D. Hou, B.J. Huang, X.J. Kong, X.C. Li, Y.H. Guan, R.L. Qiu, J.Y. Fang, Kinetics and mechanisms of the degradation of PPCPs by zero-valent iron (Fe degrees) activated peroxydisulfate (PDS) system in groundwater, J. Hazard. Mater. 357 (2018) 207-216.

[328] Y.G. Kang, H.C. Vu, T.T. Le, Y.S. Chang, Activation of persulfate by a novel Fe(II)-immobilized chitosan/alginate composite for bisphenol A degradation, Chem. Eng. J. 353 (2018) 736-745.

[329] M. Kermani, F. Mohammadi, B. Kakavandi, A. Esrafili, Z. Rostamifasih, Simultaneous catalytic

degradation of 2,4-D and MCPA herbicides using sulfate radical-based heterogeneous oxidation over persulfate activated by natural hematite (alpha-Fe2O3/PS), J. Phys. Chem. Solids 117 (2018) 49-59.

[330] J. Li, Q. Liu, Q.Q. Ji, B. Lai, Degradation of p-nitrophenol (PNP) in aqueous solution by Fe-0-PM-PS system through response surface methodology (RSM), Appl. Catal. B-Environ. 200 (2017) 633-646.

[331] J. Li, M.J. Xu, G. Yao, B. Lai, Enhancement of the degradation of atrazine through CoFe2O4 activated peroxymonosulfate (PMS) process: Kinetic, degradation intermediates, and toxicity evaluation, Chem. Eng. J. 348 (2018) 1012-1024.

[332] C. Qi, X. Liu, J. Ma, C. Lin, X. Li, H. Zhang, Activation of peroxymonosulfate by base: Implications for the degradation of organic pollutants, Chemosphere 151 (2016) 280-288.

[333] X.M. Lin, Y.W. Ma, J.Q. Wan, Y. Wang, Y.T. Li, Efficient degradation of Orange G with persulfate activated by recyclable FeMoO4, Chemosphere 214 (2019) 642-650.

[334] Y.L. Wu, Y.H. Shi, H.C. Chen, J.F. Zhao, W.B. Dong, Activation of persulfate by magnetite: Implications for the degradation of low concentration sulfamethoxazole, Process Saf. Environ. Protect. 116 (2018) 468-476.

[335] J. Li, Y. Ren, F.Z. Ji, B. Lai, Heterogeneous catalytic oxidation for the degradation of p-nitrophenol in aqueous solution by persulfate activated with CuFe2O4 magnetic nano-particles, Chem. Eng. J. 324 (2017) 63-73.

[336] Y.C. Zhang, Q. Zhang, J.M. Hong, Sulfate radical degradation of acetaminophen by novel iron-copper bimetallic oxidation catalyzed by persulfate: Mechanism and degradation pathways, Appl. Surf. Sci. 422 (2017) 443-451.

[337] S.S. Yang, P.X. Wu, J.Q. Liu, M.Q. Chen, Z. Ahmed, N.W. Zhu, Efficient removal of bisphenol A by superoxide radical and singlet oxygen generated from peroxymonosulfate activated with Fe-0-montmorillonite, Chem. Eng. J. 350 (2018) 484-495.

[338] S. Popova, G. Matafonova, V. Batoev, Simultaneous atrazine degradation and E. coli inactivation by UV/S2O82-/Fe2+ process under KrCl excilamp (222 nm) irradiation, Ecotox. Environ. Safe. 169 (2019) 169-177.

[339] T. Zhou, X.L. Zou, J. Mao, X.H. Wu, Decomposition of sulfadiazine in a sonochemical Fe-catalyzed persulfate system: Parameters optimizing and interferences of wastewater matrix, Appl. Catal. B-Environ. 185 (2016) 31-41.

[340] Y.F. Rao, L. Qu, H.S. Yang, W. Chu, Degradation of carbamazepine by Fe(II)-activated persulfate process, J. Hazard. Mater. 268 (2014) 23-32.

[341] Z. Jia, J.C. Wang, S.X. Liang, W.C. Zhang, W.M. Wang, L.C. Zhang, Activation of peroxymonosulfate by Fe78Si9B13 metallic glass: The influence of crystallization, J. Alloys Compd. 728 (2017) 525-533.

[342] P.C. Xie, Y.Z. Guo, Y.Q. Chen, Z.P. Wang, R. Shang, S.L. Wang, J.Q. Ding, Y. Wan, W. Jiang, J. Ma, Application of a novel advanced oxidation process using sulfite and zero-valent iron in treatment of organic pollutants, Chem. Eng. J. 314 (2017) 240-248.

[343] A. Romero, A. Santos, F. Vicente, C. Gonzalez, Diuron abatement using activated persulphate: Effect of pH, Fe(II) and oxidant dosage, Chem. Eng. J. 162 (2010) 257-265.

[344] Z. Li, S.Q. Luo, Y. Yang, J.W. Chen, Highly efficient degradation of trichloroethylene in groundwater based on peroxymonosulfate activation by bentonite supported Fe/Ni bimetallic nanoparticle, Chemosphere 216 (2019) 499-506.

[345] P. Neta, R.E. Huie, Rate constants for reactions of nitrogen oxide (NO3) radicals in aqueous solutions, The Journal of Physical Chemistry 90 (1986) 4644-4648.

[346] H. Li, J. Liu, W. Hou, N. Du, R. Zhang, X. Tao, Synthesis and characterization of g-C3N4/Bi2MoO6 heterojunctions with enhanced visible light photocatalytic activity, Appl. Catal. B, Environ. 160-161 (2014) 89-97.

[347] Y. Nosaka, A.Y. Nosaka, Generation and Detection of Reactive Oxygen Species in Photocatalysis, Chem. Rev. 117 (2017) 11302-11336.

[348] Z.H. Diao, J.J. Liu, Y.X. Hu, L.J. Kong, D. Jiang, X.R. Xu, Comparative study of Rhodamine B degradation by the systems pyrite/H2O2 and pyrite/persulfate: Reactivity, stability, products and mechanism, Sep. Purif. Technol. 184 (2017) 374-383.

[349] Y. Lei, C.S. Chen, Y.J. Tu, Y.H. Huang, H. Zhang, Heterogeneous Degradation of Organic Pollutants by Persulfate Activated by CuO-Fe3O4: Mechanism, Stability, and Effects of pH and Bicarbonate Ions,Environ. Sci. Technol. 49 (2015) 6838-6845.

[350] C. Wang, Q.Q. Yang, Z.H. Li, K.Y.A. Lin, S.P. Tong, A novel carbon-coated Fe-C/N composite as a highly active heterogeneous catalyst for the degradation of Acid Red 73 by persulfate, Sep. Purif. Technol. 213 (2019) 447-455.

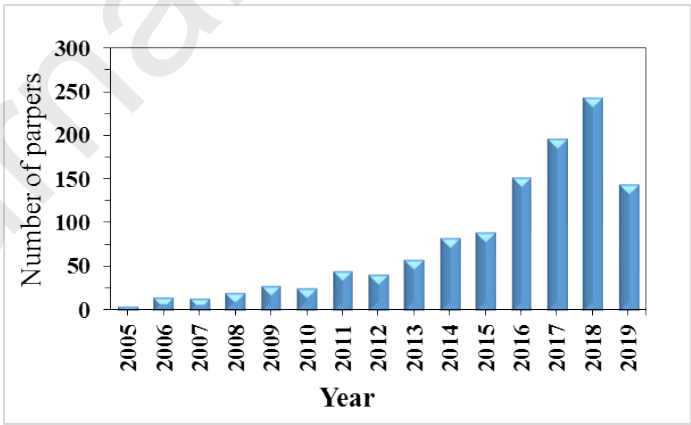

Fig. 1. The number of publications concerning the keywords of "iron + persulfate" and "iron + peroxymonosulfate" on indexed journals from 2005 to 2019. The search results are based on the database of "Web of Science".

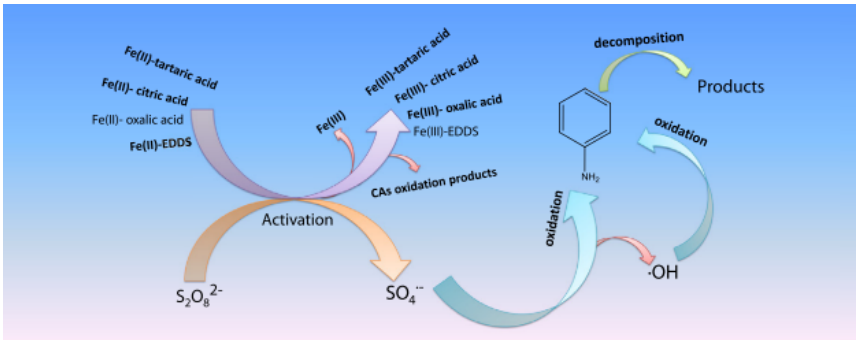

Fig. 2. The function of organic chelating agents in Fe^{2+} activated PS system. Adapted from Ref. [78].

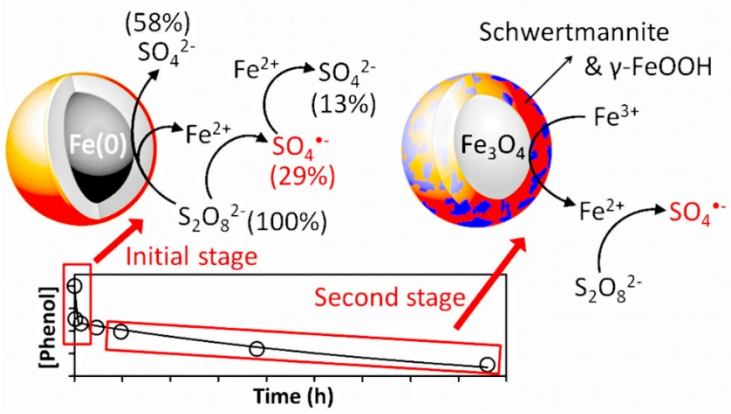

Fig. 3. Activation kinetics and mechanism of nZVI inducing PS. Adapted from Ref. [98].

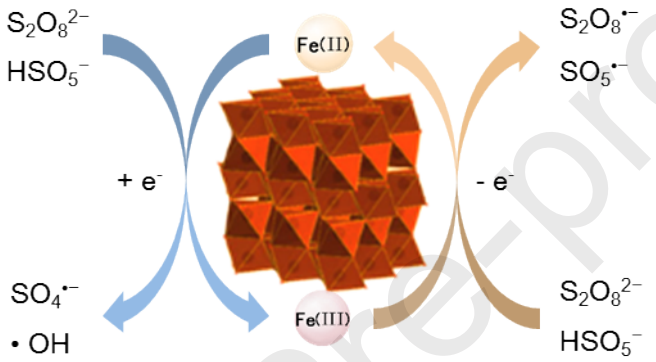

Fig. 4. Activation of PS and PMS in the presence of iron oxides and oxyhydroxides.

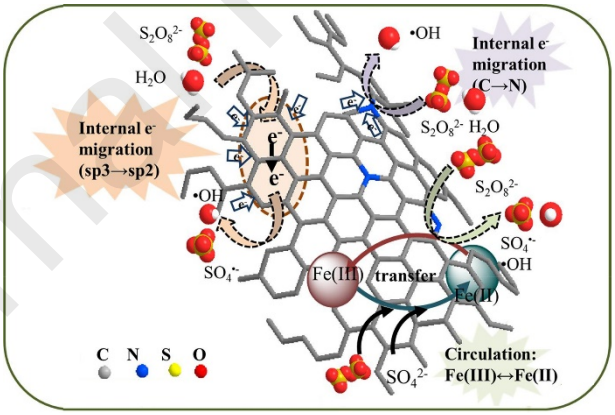

Fig. 5. Nitrogen-doped sludge-derived biochar catalysts for PS activation. Reproduced from Ref. [110].

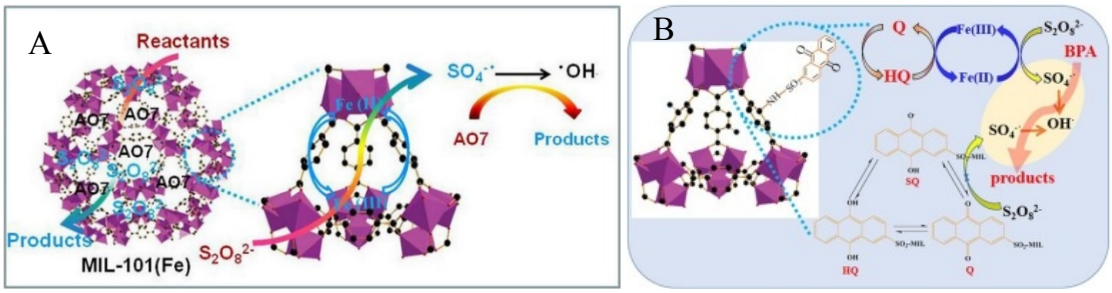

Fig. 6. (A) Proposed activation mechanism of PS by MIL-101(Fe) [108], and (B) Quinone-modified NH2-MIL-101(Fe) composite as catalysts for PS activation [109]. Reproduced from Refs. [108, 109].

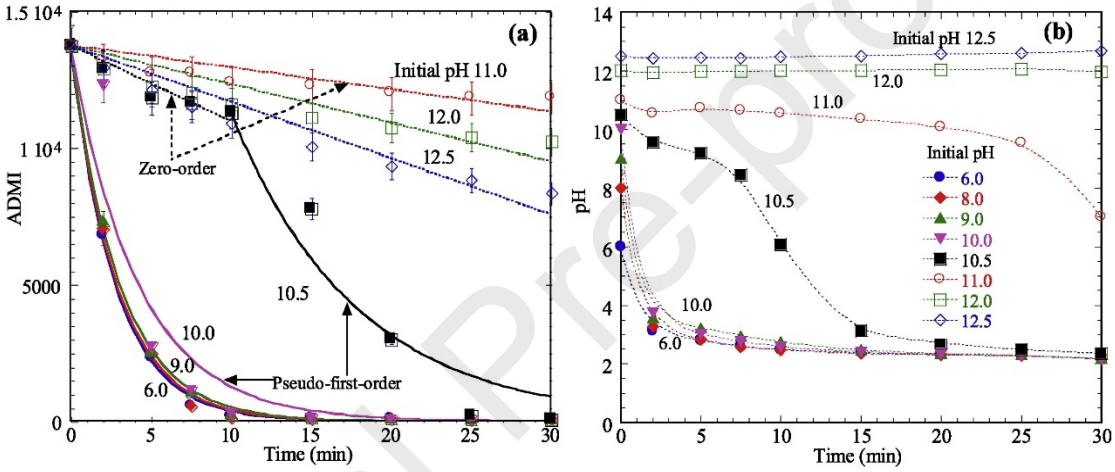

Fig. 7. Effect of initial pH on dyes degradation in PS/Fe^0 process. (Four kinds of dyes were set as the same concentration of 25 mg/L, PS=5mM, Fe^0=0.5 g/L, T=55ºC.). Adapted from Ref. [129].

Table 1. Brief summary of homogeneous activation of PS or PMS by Fe^{2+} and Fe^{3+} in the presence of absence of chelators for a series of target pollutant and their detailed reaction conditions.

Activators (assistant)	Contaminants	Optimal experiment terms	Removal rate	Highlights	Reference
Fe^{2+}	Acetaminophen	Acetaminophen= 0.05 mM, Fe^{2+}= 1.0 mM, PS=0.8 mM, pH= 3.0, T= 20 °C, reaction time= 30min.	81.4%	A kinetic model was established based on the ACT removal in the Fe^{2+}/PS system, which well predicted the degradation behavior of ACT in real water, as well as ACT, amoxicillin and pyridine mixture. Besides, it was found Cl^- played a dual role in the degradation of ACT.	[43]
Fe^{2+}	Sulfadiazine	Sulfadiazine= 100 μmol, Fe^{2+}= 1 mM, PS = 4 mM, T= 25 °C, reaction time= 120min.	About 100%	Four sulfonamides, viz., sulfadiazine, sulfamerazine, sulfadimethoxine and sulfachloropyridazine were used as model contaminants in the Fe^{2+}/PS system to elucidate the degradation pathways, where incomplete mineralization of sulfonamides could lead to higher acute toxicity.	[41]
Fe^{2+}	Trimethoprim	Trimethoprim= 1 mM, Fe^{2+} = PS= 4 mM pH=3.0, T= 25°C, reaction time = 240min.	73.4% 40.5% (TOC)	Fe^{2+}-activated PS and Fenton process could both degrade trimethoprim effectively, while Fe^{2+}/PS system was more efficient for actual	[49]

				wastewater.	
Fe^{2+}	Chlortetracycline	CTC= 1 mM, Fe^{2+}= 1000 mM, PS= 500 mM, pH= 3~4, T= 20°C, reaction time= 2h.	76%	Heterogeneous activation of PS by ZVI showed superior performance in CTC removal (94%) than homogeneous activation by Fe^{2+} under similar conditions.	[89]
Fe^{2+}	Sulfamethoxazole	SMZ= 0.05 mM, PS= Fe^{2+}=4 mM, pH= 3.0, T= 25°C, reaction time= 240 min.	100% 60% (TOC) 52.3% (in wastewater)	Less amount of oxidants and Fe^{2+} was needed in Fenton process than PS process to achieve 100% removal of SMZ in the water sample prepared with deionized water. The wastewater components negatively affected the degradation of SMZ for both Fenton and PS processes.	[50]
Fe^{2+}	Atrazine	ATZ= 20 μM, Fe^{2+}= 0.4 mM, PS= 0.4 mM, reaction time= 10 min.	About 50%	A simple kinetic model built via Matlab was capable of predicting the degradation process in Fe^{2+}/PS system and was verified by the experimental data.	[44]
Fe^{2+}	Carbamazepine	CBZ= 0.025 mM, Fe^{2+}= 0.125 mM, PS =1 mM, pH= 3.0, reaction time= 40 min.	78%	CBZ degradation process fitted a two-stage process comprising a raid initial stage followed by a slow stage. The anions NO_3^- SO_4^{2-} and $H_2PO_4^-$ had negative effect on the removal of CBZ, while	[340]

				Cl^- accelerated the degradation rate and influenced the degradation intermediates.	
Fe^{2+}	Diuron	Diuron= 20mg/L, PS= 735mg/L, Fe^{2+}= 86mg, V= 0.5 L, Q= 6.6×10−4 L/min, Fe^{2+} pumping time= 60min, T= 50 ◦C, reaction time= 180 min.	100% 64% (TOC)	Iron addition policy affected the diuron oxidation and mineralization, where higher diuron conversion and TOC decrease were obtained when iron source was continuously fed into the reactor (employing the same amount of Fe^{2+}).	[59]
Fe^{2+}	Orange G	OG= 0.1mM, PS= 4mM, Fe^{2+}= 4mM, pH = 3.5, T= 20 ◦C, reaction time= 60 min.	99%	The results demonstrated that the OG degradation could be significantly inhibited due to the existence of inorganic ions in a sequence of NO_3^- <Cl^- <$H_2PO_4^-$ <HCO_3^-.	[40]
Fe^{2+}	Diuron	Diuron= 0.09mM, PS= 2mM, Fe^{2+}= 0.72 mM, pH= 4–5, T= 50 ◦C, reaction time= 180 min.	100%	Fe^{2+}/PS system in combination with heat assistant was effective in the degradation of diuron. Bicarbonate-buffer solution rendered the degradation process slower, probably due to the existence of HCO_3^-.	[343]
Fe^{2+}/Fe^{3+} (sodium citrate)	2-chlorobiphenyl	2-CB= 0.0212 mM, PMS= 0.22 mM, Fe^{2+} = 0.22 mM, pH= 3.0, reaction time= 240 min.	100%	Fe^{2+} and Fe^{3+} were used to activate PMS or PS for the removal of 2-CB in aqueous and sediment systems, where Fe^{3+}/PMS showed relatively slower degradation compared to	[47]

		2-CB= 0.0212 mM, PMS= 0.22 mM, Fe^{2+} = 1.06 mM, pH= 3.0, reaction time= 24 h.	77.65% (TOC)	Fe^{2+}/PMS. Higher concentration of Fe^{2+} was favorable for the mineralization of recalcitrant PCBs.	
Fe^{2+} (sodium citrate)	Bisphonel A	BPA= 0.0876 mM, Fe^{2+}= 2.1925 mM, PS= 4.385 mM, initial pH= 7.0, T= 25°C, reaction time= 60min	87.71% in first 5 min 100% after 60 min	Two-stage degradation process was observed in both Fe^{2+}-PS and Fe^{0}-PS systems, and these two systems exhibited best removal efficiency of BPA at the same ratio of metal to PS.	[87]
		BPA= 0.0876 mM, Fe^{2+}= 2.1925 mM PS = 4.385 mM, sodium citrate= 2.1925 mM, initial pH= 7.0, T= 25°C, reaction time= 5min.	96.89%	Small amount of sodium citrate had positive effect on the degradation of BPA, while excessive amount could exert adversary effects.	
Fe^{2+} (citric acid)	Trichloroethylene	TCE = 0.15 mM, Fe^{2+} = 0.3 mM, PS= 2.25 mM, citric acid= 0.15 mM, T= 20 ± 0.5 °C, reaction time= 60 min.	100%	Citric acid could significantly enhance the utilization efficiency of Fe^{2+} to activate PS for the degradation of TCE, and this PS/Fe^{2+}/CA system showed two-stage degradation kinetics. The Cl^- and HCO_3^- anions had inhibitory effects on the TCE degradation.	[42]
Fe^{2+} (EDTA)	Orange G	OG = 0.1 mM, PS =4.0 mM, Fe^{2+} = 1.0 mM, EDTA= 1.0 mM, pH= 3.0, T=30 °C, reaction time= 12 h.	97.4%	Microbial fuel cell, using Fe^{2+}-EDTA catalyzed persulfate as the cathode solution, could degrade OG and harvest electricity	[67]

				simultaneously, in which EDTA addition could improve the stability of voltage output.	
Fe^{2+} (citrate, EDDS)	Sulfaquinoxaline	SQX=30 μM, Fe^{2+}= 1 mM, PS= 1.0 mM; pH= 3.0, T= 20°C, reaction time= 20 min. 0.2 mM Fe^{2+} was spiked into the reaction solution every 4 min	About 91.7% 100% after 4 times of addition	Adopting sequential Fe^{2+} addition policy to activate PMS was favorable for the degradation of SQX, while no enhancement in SQX degradation was observed when 1 mM chelating agents, like EDDS or citrate was present.	[68]
Fe^{2+} (hydroxylamine)	Benzoic acid	BA= 40 μM, PMS= 0.32 mM, Fe^{2+}= 10.8 μM, hydroxylamine= 0.40 mM , pH= 3, T= 25 °C, reaction time= 15 min.	About 80%	The introduction of hydroxylamine was considered to accelerate the transformation from Fe^{3+} to Fe^{2+}, which then favored the activation of PMS and generation of radicals for BA degradation over the wide pH range of 2.0−6.0.	[83]
Fe^{2+} (hydroxylamine)	Decabromodiphenyl ether	BDE209= 10 mg/kg, Fe^{2+}= 0.5 M, PS=1 M, hydroxylamine= 2M, pH= 3.0, T= 25°C, reaction time= 15 min.	66%	Hydroxylamine was used in the Fe^{2+}/PS system and promoted the degradation efficiency of BDE209 in spiked soil samples.	[72]
Fe^{2+} (hydroxylamine)	Sulfamethoxazole	SMX= 20 μM, Fe^{2+}= 10 μM, PMS= 0.3 mM, hydroxylamine= 0.4 mM, pH= 3.0, T= 25°C, reaction time= 15 min.	80%	Compared with Fe^{2+}/PMS process, the optimum addition dosage of hydroxylamine (HA/Fe^{2+}/PMS) could achieve 4 times higher degradation efficiency of SMX, while excess	[86]

		SMX= 31.3 μM, Fe^{2+}= 20.6 μM, PMS= 2.0 mM, hydroxylamine= 0.4 mM, pH= 5.0, T= 25°C, reaction time= 15 min (real pharmaceutical wastewater)	70% 50% (TOC)	HA could inhibit the SMX removal.	
Fe^{2+} (Quinone in products)	Orange G	Orange G= 0.2 mM, Fe^{3+}= 2 mM, PS= 6 mM, T= 20 °C, reaction time= 250 min.	100% 75% (TOC)	Quinone intermediates produced during pollutant oxidation might act as electron shuttles, allowing the reduction of Fe^{3+} into Fe^{2+} in the redox cycling of iron. Therefore, activation of PS by Fe^{3+} allowed complete OG removal.	[61]
Fe^{2+} (hydroxylamine, sodium thiosulfate, ascorbic acid, sodium ascorbate and sodium sulfite)	Trichloroethylene	TCE= 0.15 mM, PS= 2.25 mM, Fe^{2+}= 0.3 mM, hydroxylamine= 1.5 mM, T= 20°C, reaction time= 30 min.	97.9%	Different reducing agents, i.e., hydroxylamine (HA), sodium thiosulfate, ascorbic acid, sodium ascorbate and sodium sulfite, were added into PS/Fe^{2+} system and found that HA was most efficient in accelerating Fe^{2+} regeneration and then for TCE degradation. Cl^-, HCO_3^-, SO_4^{2-} and NO_3^- anions had inhibitory effects on TCE removal, and the suppressive effects could be ranked in an ascending order of NO_3^- < SO_4^{2-} < Cl^- < HCO_3^-.	[84]

Fe^{2+} (citric acid, oxalic acid, tartaric acid and EDDS)	Aniline	Aniline= 0.5mM, Fe^{2+}= 5 mM, PS= 10 mM, citric acid= 5 mM, pH = 3.0, T=25 °C, reaction time = 120 min.	69%	Among citric acid, oxalic acid, tartaric acid and EDDS, tartaric acid and citric acid with moderate chelating property could effectively coordinate the Fe^{2+} availability and proved to be the most favorable chelating agents for PS activation.	[78]
Fe^{3+} (citric acid, gallic acid, EDTA, EDDS)	Iopamidol	IPM= 20μM, PS= 0.2 mM, Fe^{3+}= 10 μM, gallic acid= 10 μM, pH= 7.0, T= 25 °C, reaction time= 150 min.	About 80%	Among the four tested chelating agents in the activation of PS/Fe^{3+}, GA was demonstrated to outperform EDTA, EDDS and CA for the activation of PS/Fe^{3+} in promoting Fe^{3+} reduction and PS decomposition to generate more radicals, thus accelerating IPM degradation.	[71]
Fe^{2+} (citric acid, EDTA and EDDS)	Ciprofloxacin and sulfamethoxazole	CIP= 30 μM, Fe^{2+}= 600 μM, PS= 600 μM, pH= 6.0, ambient temperature, reaction time= 240 min. SMX= 30 μM, Fe^{2+}= PS= EDTA = 300 μM, pH= 6.0, ambient temperature, reaction time= 240 min.	95.6% for CIP 49.7% for SMX	Citric acid, EDTA and EDDS in the Fe^{2+}/PS system showed no enhancement in CIP degradation at near neutral pH, while CA and EDTA showed some promoting effect on SMX degradation. Degradation rate was nearly the same in Milli-Q and river water.	[76]
Fe^{2+}	Orange G	OG= 1.25 mM, PS/EDDS/	98%	The simultaneous presence of EDDS and	[79]

(EDDS and hydroxylamine)		Fe^{2+}/hydroxylamine/OG= 40/10/10/16/5, pH= 3, T= 25 °C, reaction time= 180 min.		hydroxylamine in the Fe^{2+}/PS could expand the effective pH range up to 7, Moreover, hydroxylamine addition mode played a significant role in affecting oxidative ability.	
Fe^{2+} (citric acid, diethylene triamine pentaacetic acid, EDTA-Na_2, and $Na_2S_2O_3$)	Arsenic(III) and diuron	As(III)= 6.6μM, PS= 20μM, Fe^{2+}= 20μM, T= 25 °C, reaction time= 60 min. Diuron= 0.1 mM, PS= 2 mM, Fe^{2+}= 2.0 mM, citric acid= 0.5 mM, pH= 3.0, T=25 °C, reaction time= 300 min.	About 77% for As(III) 100% for diuron	Citric acid (CA), $Na_2S_2O_3$, EDTA-Na_2, diethylene triamine pentaacetic acid (DTPA) were combined with Fe^{2+} to activate PS for diuron and As(III) degradation, where CA and $Na_2S_2O_3$ showed higher efficiency and environmental friendly nature than EDTA-Na_2 and DTPA.	[74]
Fe^{2+} (citrate, EDDS, and pyrophosphate)	4-chlorophenol	4-CP= 0.396 mM, PMS= 3.96 mM, Fe^{2+} =Pyrophosphate = 0.99 mM, pH= 7.0, reaction time= 4h.	91.5%	Among citrate, EDDS, and pyrophosphate on Fe^{2+}-mediated activation of PMS, PS, and H_2O_2 at neutral pH, pyrophosphate showed effective activation of PMS in Fe^{2+}/PMS system, while very fast dissociation of PMS was recorded in the case of EDDS without any apparent 4-CP degradation. The Fe^{2+}/citrate was effective in activating all three oxidants to varying degrees, and resulted in the maximum contaminant removal through PS activation.	[38]

Table 2. Brief summary of the performance and synthesis methods of typical Fe-based heterogeneous activators.

Catalysts	Contaminants	Optimal experiment terms	Removal rate	Synthesis methods	Reference
nZVI	2,2',4,4'-tetrabromodiphenyl ether (BDE-47)	BDE-47= 3.1 μM, PS= 71.4 mM, nZVI= 1 g/L, pH= 11.48, T= 25 ± 2 °C, reaction time= 48h.	64%	Borohydride reduction	[116]
Fe_3O_4	2,4,4'-CB (PCB28)	PCB28= 2.5 μM, PS= 2.0 mM, Fe_3O_4= 1g/L, pH= 7.0, T= 25 °C, reaction time= 4h	90%	Chemical coprecipitation	[100]
Fe_2O_3	Rhodamine B (RhB)	RhB= 50 mg/L, PMS= 1 mM, Fe_2O_3= 1.5 g/L, pH = 6.2, T= 25 °C, reaction time= 1 h.	100%	Hydrothermal-calcination	[105]
S-nZVI	Trichloroethylene (TCE)	TCE=1 mM, PS=5 mM, S-nZVI= 5 mM, pH=2.32, T= 20 ± 1 °C, reaction time= 30min.	90.68%	Modified borohydride reduction method with $Na_2S_2O_4$	[90]
Iron oxide/MnO_2 composite	Carbon tetrachloride (CT) Benzene	CT= 0.26 mM, benzene=0.51 mM, PS= 3.56 mM, Catalysts= 0.25 g/L, pH= 9, T= 25 °C, reaction time= 24 h.	75% for carbon tetrachloride 50% for benzene	Impregnation	[118]
nZVI/zeolite	Trichloroethylene	TCE= 0.15mM, PS= 1.5 mM, Catalysts=	98.8%	In situ borohydride reduction	[244]

	(TCE)	84 mg/L, pH= 7, T= 22 °C, reaction time=2 h.			
Fe–Co/SBA-15 Electrolysis	Orange II	Orange II= 100 mg/L, PS= 2.0 g/L, Catalysts= 1.0 g/ L, pH= 6, T= 20 °C, reaction time=1 h, j= 8.40 mA/cm^2.	95.6%	Auto-combustion	[236]
Fe-Ag/granular activated carbon	Acid Red 73 (AR 73)	AR 73= 20 mg/L, PS= 0.5 g/L, Catalyst= 7.5 g/L, pH= 7, T= 35 °C, reaction time= 1 h.	99% 84.1 (TOC)	Two-step impregnation	[251]
Fe_3O_4/carbon black	BTEX MTBE	BTEX=MTBE= 10mg/L, PS= 15mg/L, Catalyst= 1g/L, pH=3, T= 30 °C, reaction time= 24 h.	100% for BTEX 69% for MTBE	Co-precipitation and wet-chemistry approach	[253]
nZVI/graphene	Atrazine	Atrazine=10 mg/L, PS= 0.50mM, Catalysts= 0.10 g/L, pH=6.0, T=25 °C, reaction time= 21 min.	92.1%	In situ borohydride reduction	[256]
Ag^0/Fe_3O_4-rGO	Acetaminophen 17β-estradiol (E2)	Acetaminophen=E2=10 μM, PS= 1 mM, Catalysts= 0.1 g/L, pH= 7, T= 25 °C, reaction time=3 h.	99% for acetaminophen and E2	In situ nucleation and crystallization	[259]
Fe-BC (sawdust biochar)	Bisphenol A (BPA)	BPA= 20 mg/L, PMS= 0.2 g/L, Catalysts=0.15 g/L, pH= 9, T= 25 ± 2 °C, reaction time= 5 min	100%	Pyrolysis of iron pre-impregnated sawdust	[119]

γ-Fe_2O_3@BC (banana peels biochar)	Bisphenol A (BPA)	BPA= 20 mg/L, PS= 5 Mm, Catalyst= 0.3 g/L, T=25 °C, without pH adjustment, reaction time= 20 min.	100% 90% (TOC)	Hydrothermal	[117]
MIL-53(Fe)	Orange G (OG)	OG= 0.2 mM, PS= 32 mM, Catalyst= 1 g/L, T = 25 °C, ambient pH, reaction time= 90 min.	90%	Solvothermal	[270]
NH_2-MIL-101(Fe)	Bisphenol A (BPA)	BPA= 60 mg/L, PS= 10 mM, Catalyst= 0.2 g/L, T= 25 °C, pH= 5.76, reaction time= 180 min.	97.7% (23.1% adsorption)	Solvothermal	[109]
Fe/Fe_3C@ N-doped porous carbon	4-chlorophenol (4-CP)	4-CP= 20 mg/L, PMS= 2 g/L, Catalyst= 0.2 g/L, T= 25 °C, without pH adjustment, reaction time= 90 min.	100%	Pyrolysis of Fe-MIL-88B-NH_2	[275]
Fe@N-doped graphite-like carbon	4-aminobenzoic acid ethyl ester (ABEE) Sulfamethoxazole (SMX)	ABEE=SMX= 0.06 mM, PMS= 0.65 mM, Catalyst= 50 mg/L, pH=7.0, reaction time= 60 min.	100% for ABEE 87.37% for SMX	Pyrolysis of a combination of g-C_3N_4 and NH_2-MIL-53(Fe)	[276]
CoFe CoAgFe	Sulfamethoxazole (SMX)	SMX= 39.5 mM, PS= 1.0 mM, Catalyst= 2.23 mM, room temperature, pH= 5.67, reaction time= 10 min.	63% 67%	Plating	[58]

Modified basic oxygen furnace slag	Propylparaben (PP)	PP= 0.4 mg/L, PS= 1 g/L, Catalyst= 50 mg/L, ambient temperature, pH= 6.2, reaction time= 90 min.	90%	Oxidative digestion in acid media of BOF slag	[113]
Modified drinking water treatment residuals	Sulfamethoxazole (SMX)	SMX= 50 μM, PS= 2.0 mM, Catalyst= 0.2 g/L, ambient temperature, pH= 5.3, reaction time= 60 min.	80%	Reduction calcination of WTRs	[114]

Graphical Abstract

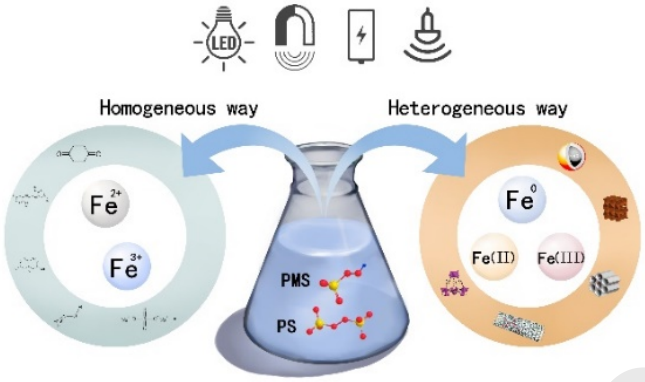

Highlights:

- The recent advances and mechanisms of homogeneous and heterogeneous iron species-based activation of PS and PMS are presented.
- Synthetic methods of heterogeneous iron-based catalysts for PS and PMS activation are overviewed.
- Influencing factors and synergistic approaches for iron/PS and iron/PMS are introduced.
- Further efforts related to iron-mediated activation of PS and PMS are proposed.